

**ASSESSMENT OF SEISMICALLY INDUCED  
ROCKFALL IN THE EMPLACEMENT DRIFTS OF THE  
PROPOSED REPOSITORY AT YUCCA  
MOUNTAIN—PROGRESS REPORT**

*Prepared for*

**Nuclear Regulatory Commission  
Contract NRC-02-97-009**

*Prepared by*

**Sui-Min Hsiung  
Gen-Hua Shi  
Asadul H. Chowdhury**

**Center for Nuclear Waste Regulatory Analyses  
San Antonio, Texas**

**April 2000**

# CONTENTS

Section	Page
ACRONYMS .....	iv
FIGURES .....	v
TABLES .....	vii
ACKNOWLEDGMENTS .....	viii
EXECUTIVE SUMMARY .....	ix
1 INTRODUCTION .....	1-1
1.1 Background .....	1-1
1.2 Objective and Scope .....	1-3
2 ANALYSIS OF EXCAVATION-INDUCED ROCKFALL .....	2-1
2.1 Key Block Theory .....	2-1
2.2 Joint Data Input .....	2-2
2.3 Identification of Key Blocks .....	2-3
3 ANALYSIS OF ROCKFALL DUE TO EARTHQUAKES .....	3-1
3.1 Discontinuous Deformation Analysis .....	3-1
3.2 Data Input and Model Geometry .....	3-4
3.3 Modeling Results and Discussion .....	3-5
3.3.1 DDA Block Model 1 .....	3-5
3.3.2 DDA Block Model 2 .....	3-6
3.3.3 DDA Block Model 3 .....	3-6
3.3.4 Discussion .....	3-7
4 SUMMARY .....	4-1
5 FUTURE WORK .....	5-1
6 REFERENCES .....	6-1

## ACRONYMS

2D	2-Dimensional
3D	3-Dimensional
CNWRA	Center for Nuclear Waste Regulatory Analyses
CRWMS M&O	Civilian Radioactive Waste Management System Management & Operating Contractor
DDA	Discontinuous Deformation Analysis
DOE	Department of Energy
ESF	Exploratory Studies Facility
EBS	Engineered Barrier System
EDA	Enhanced Design Alternatives
FEM	Finite Element Method
JP	Joint Pyramid
Key Block Code	KB
NRC	Nuclear Regulatory Commission
QA	Quality Assurance
RSS	Repository Safety Strategy
TM	Thermal-Mechanical
TPA	Total-System Performance Assessment
TSw2	Topopah Springs Welded Unit 2
VA	Viability Assessment
WP	Waste Package
YM	Yucca Mountain

## FIGURES

Figure	Page	
2-1	Types of blocks: I key blocks; II potential key blocks; III safe removable block; IV tapered block; V infinite block; VI joint block . . . . .	2-2
2-2	Stereographic projection of joint set for TSw2 upper lithophysal unit . . . . .	2-8
2-3	Stereographic projection of joint sets for TSw2 lower lithophysal unit . . . . .	2-9
2-4	Key block zones of all joint side combinations for TSw2 lower lithophysal unit . . . . .	2-10
2-5	Key block zones of all joint side combinations for TSw2 upper lithophysal unit . . . . .	2-11
2-6	Sliding planes of the key block zones for TSw2 lower lithophysal unit . . . . .	2-12
2-7	Sliding planes of the key block zones for TSw2 upper lithophysal unit . . . . .	2-13
2-8	Maximum key block in JP=011 for TSw2 lower lithophysal unit . . . . .	2-14
2-9	Maximum key block in JP=011 for TSw2 upper lithophysal unit . . . . .	2-15
2-10	Maximum key block in JP=101 for TSw2 lower lithophysal unit . . . . .	2-16
2-11	Maximum key block in JP=101 for TSw2 upper lithophysal unit . . . . .	2-17
2-12	Three-dimensional joint trace map on the surface of emplacement drift for the TSw2 lower lithophysal unit . . . . .	2-18
2-13	Three-dimensional joint trace map on the surface of emplacement drift for the TSw2 upper lithophysal unit . . . . .	2-19
2-14a	Traces of key blocks in JP=011 on emplacement drift surface for TSw2 lower lithophysal unit (one KB run) . . . . .	2-20
2-14b	Traces of key blocks in JP=011 on emplacement drift surface for TSw2 lower lithophysal unit (second KB run) . . . . .	2-21
2-15a	Traces of key blocks in JP=101 on emplacement drift surface for TSw2 lower lithophysal unit (one KB run) . . . . .	2-22
2-15b	Traces of key blocks in JP=101 on emplacement drift surface for TSw2 lower lithophysal unit (second KB run) . . . . .	2-23
2-16a	Traces of key blocks in JP=011 on emplacement drift surface for TSw2 upper lithophysal unit (one KB run) . . . . .	2-24
2-16b	Traces of key blocks in JP=011 on emplacement drift surface for TSw2 upper lithophysal unit (second KB run) . . . . .	2-25
2-17a	Traces of key blocks in JP=011 on emplacement drift surface for TSw2 upper lithophysal unit (one KB run) . . . . .	2-26
2-17b	Traces of key blocks in JP=011 on emplacement drift surface for TSw2 upper lithophysal unit (second KB run) . . . . .	2-27
3-1	Joint distribution for block mesh model 1 . . . . .	3-9
3-2	Joint distribution for block mesh model 2 . . . . .	3-10
3-3	Joint distribution for block mesh model 3. . . . .	3-11
3-4	DDA block model 1 . . . . .	3-12
3-5	DDA block model 2 . . . . .	3-13
3-6	DDA block model 3 . . . . .	3-14
3-7a	Components X and Y of earthquake accelerations . . . . .	3-15
3-7b	Components X and Y of earthquake accelerations (cont'd) . . . . .	3-16
3-8a	Z component and resultant of earthquake accelerations . . . . .	3-17
3-8b	Z component and resultant of earthquake accelerations (cont'd) . . . . .	3-18

## FIGURES (Cont'd)

Figure		Page
3-9	Effects of ground motion on rockfall after 1 s of shaking for DDA block model 1 .....	3-19
3-10	Effects of ground motion on rockfall after 2 s of shaking for DDA block model 1 .....	3-20
3-11	Effects of ground motion on rockfall after 5 s of shaking for DDA block model 1 .....	3-21
3-12	Effects of ground motion on rockfall after 6 s of shaking for DDA block model 1 .....	3-22
3-13	Effects of ground motion on rockfall after 7 s of shaking for DDA block model 1 .....	3-23
3-14	Effects of ground motion on rockfall after 16 s of shaking for DDA block model 1 .....	3-24
3-15	Effects of ground motion on rockfall after 1 s of shaking for DDA block model 2 .....	3-25
3-16	Effects of ground motion on rockfall after 4 s of shaking for DDA block model 2 .....	3-26
3-17	Effects of ground motion on rockfall after 5 s of shaking for DDA block model 2 .....	3-27
3-18	Emplacement drift condition after ground motion for DDA model 2 .....	3-28
3-19	Effects of ground motion on rockfall after 1 s of shaking for DDA block model 3 .....	3-29
3-20	Effects of ground motion on rockfall after 2 s of shaking for DDA block model 3 .....	3-30
3-21	Effects of ground motion on rockfall after 3 s of shaking for DDA block model 3 .....	3-31
3-22	Effects of ground motion on rockfall after 6 s of shaking for DDA block model 3 .....	3-32
3-23	Effects of ground motion on rockfall after 4 s of shaking for DDA block model 3 .....	3-33

## TABLES

Table		Page
2-1	Orientations and strength properties of joint sets for TSw2 lower lithophysal unit .....	2-3
2-2	Orientations and strength properties of joint sets for TSw2 upper lithophysal unit .....	2-3
2-3	Calculated volume and area of exposure of the maximum possible key blocks .....	2-5
2-4	Joint set data for TSw2 lower lithophysal unit .....	2-6
2-5	Joint set data for TSw2 upper lithophysal unit .....	2-6
2-6	Calculated percentage of key block trace area to the emplacement drift surface area .....	2-7
3-1	Rock block material properties for TSw2 lower lithophysal unit .....	3-5

## ACKNOWLEDGMENTS

This report was prepared to document work performed by the Center for Nuclear Waste Regulatory Analyses (CNWRA) for the Nuclear Regulatory Commission (NRC) under Contract No. NRC-02-97-009. The activities reported here were performed on behalf of the NRC Office of Nuclear Material Safety and Safeguards, Division of Waste Management. The report is an independent product of the CNWRA and does not necessarily reflect the views or regulatory position of the NRC.

The authors thank A. Ghosh and B. Sagar for their review of the report. The authors are thankful to C. Patton for assisting with the word processing and preparation of the report and to C. Gray and C. Cudd for the editorial review.

## QUALITY OF DATA, ANALYSES, AND CODE DEVELOPMENT

**DATA:** All CNWRA-generated original data contained in this report meet quality assurance (QA) requirements described in the CNWRA QA Manual. Sources of other data should be consulted for determining the level of quality for those data.

**ANALYSES AND CODES:** Analyses in this report were conducted by a CNWRA consultant using computer codes Keyblock and Discontinuous Deformation Analysis. These two computer codes are proprietary codes and are not controlled under the CNWRA software QA procedure (QAP) (TOP-018, Development and Control of Scientific and Engineering Software). The executables of the two computer codes and the input files used in the report are placed in the QA record related to this report.

## EXECUTIVE SUMMARY

Seismicity is a potential disruptive event that needs adequate consideration in assessing performance of the proposed geologic repository. Rockfall induced by seismicity could damage drip shields and waste packages (WPs) effecting their performance. The potential effects on the performance of the drip shields and WPs are twofold. The first potential effect of rockfall is to rupture WPs and drip shields by the impact produced by the falling rock. The second aspect is that rockfall may cause damage to the drip shields and WPs leading to accelerated corrosion that may reduce their intended service life.

The proposed repository design employs an engineered barrier system (EBS) in concert with the desert environment and geologic features of Yucca Mountain (YM) with the intent of keeping water away from the high-level radioactive waste for thousands of years. The primary component of the proposed EBS is a WP. The U.S. Department of Energy (DOE) Repository Safety Strategy (RSS) has identified several principal factors that would be addressed in its performance assessment. Water seepage into drifts is one of the principal factors that could affect the long-term performance of the repository. Other factors identified in the DOE RSS that may be affected by rockfall and consequent alteration of drift geometry include (i) coupled thermal-mechanical-hydrological-chemical processes, (ii) environment on the drip shields, (iii) environments on and within the WP.

The new Enhanced Design Alternative II has been adopted recently by the DOE as its Site Recommendation reference design. This new design includes design features (e.g. drip shields) that reduce the effects of dripping water and rockfall on the performance of WPs.

The impact load caused by a seismically induced rockfall can affect the confinement capabilities of the WP and drip shield. The current Nuclear Regulatory Commission Total-System Performance Assessment computer code includes a SEISMO module (Mohanty et al., 2000) that evaluates the potential for only direct rupture of WPs from rockfall induced by seismicity based on several simplifying assumptions and without consideration of the possible accelerated degradation of the WPs. The effect of rockfall on drip shield performance is not currently included in the SEISMO module. An effort is under way to re-evaluate the assumptions made for the SEISMO module so that the assessment of seismically induced rockfall impacts on WP and drip shield performance can be done in a more reasonable manner.

This report documents progress on determining the size and areal coverage of rockfalls under various ground motions that may occur in the repository. The work will continue in the future to establish relationships between the ground motions and rockfall potential and sizes, and assess how such rockfall may affect the emplacement drift geometry. The effects of thermal load and long-term degradation of rock-mass including joint strength reduction and joint length growth on rockfall are not included in the study presented in this progress report and will be addressed later.

The key block analysis was used to quantify unstable zones immediately after excavation. The study focused on the Topopah Springs Welded Tuff, Unit 2 (TSw2) lower and upper lithophysal units. Three major joint sets were used in the key block analysis for both the TSw2 lower and upper lithophysal units. The joint orientations, frictional properties, spacings, and lengths used in key block analysis for the TSw2 lower and upper lithophysal units were derived from a Civilian Radioactive Waste Management System Management & Operating Contractor (CRWMS M&O) report on drift degradation analysis (Civilian Radioactive Waste Management System Management & Operating Contractor, 1999).

In the stereographic projection, the three major joint planes cut a sphere into eight zones (called Joint Pyramid, JP). The result of the key block analysis identified two zones of key blocks that were located in

Joint Pyramid (JP)=011 and JP=101, and are liable to fall for both the TSw2 lower and upper lithophysal units. Based on the assumptions that the joint length for each joint set is sufficiently long (i.e., joints are persistent) and the joint spacing for each joint set is sufficiently small, the maximum possible sizes of key blocks for JP=011 and JP=101 were 0.76 m<sup>3</sup> and 0.92 m<sup>3</sup> for the TSw2 lower lithophysal unit, and 1.06 m<sup>3</sup> and 0.61 m<sup>3</sup> for the upper lithophysal unit. Any of the actual key blocks in any JP cannot be bigger than the maximum possible key block of that JP.

The sliding surfaces for the four JPs that are liable to fall are either along joint set 1 or 2. Joint sets 1 and 2 are near vertical for both rock units. Therefore, relatively small resistance is available between joint interfaces to prevent rockfall. The combined key block trace areas for JP=011 and JP=101 on the emplacement drift wall is about 2.94 percent and 4.45 percent of the entire drift surface for the TSw2 lower and upper lithophysal units, respectively. From the perspective of drift length affected, however, key blocks appear quite frequently on the top walls of both sides of the emplacement drift. Most of these key blocks are expected to be very small in size.

In analyzing seismically induced rockfall in the emplacement drifts located in the TSw2 lower lithophysal unit, the two-dimensional Discontinuous Deformation Analysis computer code was used. Since the site-specific time history of earthquakes from YM was not available, the three-dimensional acceleration time history developed by the California Department of Transportation for the Yeba Buena Island Tunnel seismic retrofit program was used for input loads.

The three DDA block models constructed using the same joint information with a slight variation in joint spacing exhibited different rockfall patterns. The first rockfall took place at an early stage of the ground acceleration for all three models. It was before 1 s of shaking for DDA block models 1 and 2 and between 1 s and 2 s for DDA model 3. The rockfall associated with DDA block model 3 was much more massive than the other two models. DDA block models 1 and 2 experienced a second rockfall several seconds after the first rockfall while no further rockfall was observed for DDA block model 3. No additional rockfalls were experienced for DDA block models 1 and 2 for the rest of the ground acceleration time history, even through some large local peak ground accelerations were encountered later. The reason for no further rockfall may be attributed to the geometry of the remaining rock blocks that prevented rockfall from taking place. Further rockfall may still be possible if long-term deterioration of the associated joint and rock strength takes place.

The phenomenon of multiple rock blocks falling in unison appears to be possible although it may not be a frequent event. One limiting factor is the constraints associated with the block geometry that cause rock blocks to rotate and bump into each other while falling. These situations tend to eliminate the potential for multiple rock blocks to fall in unison.

The final shapes of the emplacement drifts after collapse appear to be quite different and complex for the three models. These shapes are compared to the final shapes reported by CRWMS M&O (Civilian Radioactive Waste Management System Management & Operating Contractor, 1999). However, it is not clear how these complex geometries will affect water dripping into the emplacement drifts. Investigations on this aspect may be needed.

# 1 INTRODUCTION

## 1.1 BACKGROUND

The U.S. Department of Energy (DOE) has been studying the Yucca Mountain (YM) site in Nevada for more than 15 yr to determine whether it is a suitable site for building a geologic repository for the nation's high-level radioactive waste (U.S. Department of Energy, 1998a). The proposed repository design employs an engineered barrier system (EBS) in concert with the desert environment and geologic features of YM with the intent of keeping water away from the waste for thousands of years. The primary component of the proposed EBS is a waste package (WP). Other potential components of the EBS include drip shields, backfills, and emplacement drift seals. The basic concept of geologic disposal at YM is to place carefully prepared and packaged waste in excavated drifts in tuff about 300 m below the surface and 225 m above the water table in what is called the unsaturated zone. In this condition, the engineered barriers are intended to work with the natural barriers—the geology of YM—to contain and isolate waste for thousands of years.

The design of the repository, including engineered barriers and the underground facility, is an evolving process. It changes often as more information and knowledge become available. Since the DOE submitted its Viability Assessment (VA) (U.S. Department of Energy, 1998a,b) to the U.S. Congress, the reference design that used to support the VA was replaced in early 2000 with the Enhanced Design Alternative (EDA II). The EDA II is a result of an extensive process—License Application Design Selection, and will be used as the reference design for its Site Recommendation Consideration report (Barrett, 1999) to be completed in 2001. The new EDA II (Civilian Radioactive Waste Management System Management & Operating Contractor, 2000a) includes the following essential features:

- WPs with 2-cm-thick corrosion resistance material as the outer barrier and 5-cm-thick corrosion allowance material as the inner barrier to extend their service life,
- Drip shields intended to limit the amount of water to be in contact with WPs from dripping and to mitigate rockfall effects on WPs, and
- An option of placing backfill before permanent closure.

Water seepage into drifts has been identified as one of the principal factors in the DOE Repository Safety Strategy (RSS) (Civilian Radioactive Waste Management System Management & Operating Contractor, 2000b) that affect the long-term performance of the repository. A study (Hughson and Dodge, 1999) indicated that change of drift geometry as a result of rock deformation (in the form of joint displacement) and rockfall, that might cause the geometry of an emplacement drift to become irregular or rugged, could potentially reduce the percolation threshold necessary for water to start dripping into emplacement drifts by more than one order of magnitude. Other factors identified in the DOE RSS that may be affected by rockfall and consequent alteration of drift geometry include (i) coupled processes-effects on seepage, (ii) environment on the drip shield, (iii) environments on and within the WP.

In a jointed rock mass, rockfall may be induced by three possibilities:

- Existence of unstable rock blocks, after excavation and before placement of support. The rockfall related to this situation is primarily controlled/determined by the joint pattern and orientation of the openings relative to the orientation of the joint sets in which these openings are located. The rock blocks that are inherently unstable and tend to fall immediately or a short period of time after the excavation due to gravity loads are called key blocks. The fall of the key blocks may trigger

subsequent fall of other rock blocks above the key blocks due to the loss of support.

- The long-term deterioration of rock-mass under prolonged thermal load. The deterioration of rock-mass could come from three sources. The first possible condition is reduction of joint shear strength due to a long-term creeping effect under a high state of shear stresses. The second possible condition is failure of intact rock block under a high state of stresses. Extensive failure could be possible, and has been identified through numerical modeling (Ahola et al., 1996) for the VA reference design. For the EDA II design, the magnitude of thermal load has been reduced and further controlled through preclosure ventilation to remove decay heat. However, after permanent closure, the emplacement drift temperature could still go beyond 100 °C. The state of stresses induced by temperature of this magnitude could still cause rock block to fail. Another important factor that has not been considered in the DOE program is the long-term deterioration of rock strength due to a creep effect. Observations indicate that creep effect could reduce rock strength (Griggs, 1939; Hardy, 1969; Scholz, 1968; Wawersik, 1972); rock strength reduction of 30 to 50 percent has been reported (Cruden, 1970; Wawersik, 1972). All of these situations could substantially increase rockfall potential. As the rock-mass surrounding the repository begins to cool down, the relaxation of stresses tends to loosen the rock and thus creates further rockfall conditions (Wilder and Yow, 1987).
- Seismically induced ground motion. Seismicity at YM is one of the major sources that could potentially damage rock-mass surrounding underground excavations and subsequently induce rockfall. Studies indicate that rock-mass may be damaged by a single ground motion or through repeated ground motions. The fundamental mechanics that weaken rock-mass surrounding underground excavations involve accumulation of joint shear displacements and temporary reduction of joint normal stresses, which in turn reduce joint resistances (Hsiung et al., 1992, 1999; Brown and Hudson, 1974; Barton and Hansteen, 1979). There are also numerous studies on the effects of stress waves that cause damage to underground excavations in certain mines where rockbursts are major concerns that cost the mine operator millions of dollars for excavation rehabilitation (e.g., Hsiung et al., 1992; Kaiser et al., 1992). The DOE has conducted a study on drift degradation subjected to seismic ground motion using the key block theory (Civilian Radioactive Waste Management System Management & Operating Contractor, 1999). In the study, the fundamental mechanics mentioned above were accounted for by the reduction of joint friction angle.

The Nuclear Regulatory Commission (NRC) consideration in its Total-System Performance Assessment (TPA) Version 4.0 of the effects of seismicity, faulting, and igneous activity for the assessment of the performance of WPs has been discussed by Mohanty et al. (2000), Ghosh et al. (1998), and Hill and Trapp (1997). Ongoing and future NRC activities on the effects of faulting and volcanism on WP performance have been discussed in the appropriate NRC issue resolution status reports (Center for Nuclear Waste Regulatory Analyses, 1999a,b).

Seismicity can affect the WP and drip shield performance by causing rockfall onto the drip shield and WP, and shaking of the WP. The impact load caused by a seismically induced rockfall can affect the confinement capabilities of the WP and drip shield in two ways. The first is a catastrophic rupture of the WP and drip shield, which may be weakened by corrosion in the latter stage of their design lives. The second is that rockfall may cause damage to WPs and drip shields in a manner that will accelerate the WP and drip shield corrosion process. The current NRC TPA code includes a SEISMO module (Mohanty et al., 2000) that evaluates only the potential for direct rupture of WPs from rockfall induced by seismicity based on several simplifying assumptions and without consideration of the degradation of the WPs with time. The performance of the new design feature, drip shields, has not been considered in the NRC performance assessment and will need to be evaluated as well. An effort is under way to re-evaluate the assumptions made in the SEISMO module so that the assessment of seismically induced rockfall impacts on the performance of WPs and drip

shields can be done in a more reasonable manner. This effort focuses on two areas: (i) mechanical response of WPs and drip shields due to rockfall impact, and (ii) size and areal coverage of rockfalls due to various ground motions that may occur in the repository. This report focuses mainly on the study of the second item. The study of the first item will be addressed in a separate report.

## 1.2 OBJECTIVE AND SCOPE

This study focuses on analyzing seismically induced rockfall. The objectives of the study are twofold: (i) development of relationships between the magnitude of ground motions and size of rockfall, and ground motions and areal coverage of rockfall in the emplacement drifts; and (ii) assessment of the potential change in drift geometry. As discussed earlier, the results from the first item will be used as input to the SEISMO module for the NRC future version of the TPA code to estimate the effects of seismically induced rockfall on WP integrity. The results from the second item will be provided as input to investigate its effects on water seepage into emplacement drifts. The latter study will be performed under the Thermal Effects on Flow Key Technical Issue. To meet the objectives, specific activities include:

- Quantify sizes and areal coverage of key blocks in the emplacement drifts,
- Determine size distribution of rockfalls subjected to various levels of ground motions,
- Estimate the potential for multiple rock blocks to fall in unison,
- Determine areal coverage of rockfalls subjected to various levels of ground motions, and
- Estimate changes in geometry under various levels of ground motions.

This report documents the progress made to date. The primary focus of the analysis is the Topopah Springs Welded Tuff Unit 2 (TSw2) lower lithophysal unit since about 75 to 80 percent of the emplacement drifts will be in this unit. Analyses on the TSw2 middle non-lithophysal and upper lithophysal zones in which the rest of 20 to 25 percent of waste will be emplaced may be conducted in the future. The key block theory was used in analysis of sizes and areal coverage of key blocks in the emplacement drifts. The results provide information regarding the rock blocks that are potentially unstable and liable to fall without appropriate supports. The key block analysis for the TSw2 upper lithophysal unit is also reported in this progress report. The rockfall analysis on emplacement drifts subjected to earthquake ground motion was performed using a two-dimensional (2D) discontinuous deformation analysis approach. In this progress report, no thermal loading is considered. The effects of thermal stress will be evaluated in a subsequent report.

## 2 ANALYSIS OF EXCAVATION INDUCED ROCKFALL

Although underground excavations are more stable compared to surface excavations, all underground excavations undergo localized "overbreak" as the dimensions of the opening readjust to geological realities (Goodman and Shi, 1985). It is the tangential stress around the underground opening that makes the excavations stable. In very deep mines, or excavations into weak rock, these tangential stresses may themselves initiate new cracking, or even violent rock bursts. More often, however, the tangential stress around the opening tends to hold the potentially moving rock blocks in place, thereby acting as a stabilizing factor. In fact, it is usually the absence of continuous compression around the opening, rather than its presence in elevated magnitudes, that permits failure.

Various possible modes of failure of rock excavations have been discussed by Goodman and Shi (1985). In many cases, failures of underground excavations in fractured rock develop from the movement of a single rock block from the surface of the excavation. The movement of this block creates a space into which previously restrained blocks may then advance. Thus a serious failure can occur retrogressively, sometimes very quickly. This first rock block is a critical block that is formed by the intersection of pre-existing joint planes and the excavation surfaces and is called a key block. Goodman and Shi (1985) have developed techniques to identify key blocks intersecting an excavation surface. The theory of key blocks and their identification using those techniques is presented in this chapter.

### 2.1 KEY BLOCK THEORY

Excavations made in a rock-mass with several sets of discontinuities may liberate rock blocks of various sizes (Goodman, 1989). The potential movements of the most critically located rock blocks may then undermine neighboring blocks, and the ensuing block falls and slides can menace the integrity of the engineering scheme. A block of rock is formed by the intersection of joints and isolated by excavation surfaces. No matter how many faces it has, a rock block can move initially in only a few ways: by falling, by sliding on one face, by sliding on two faces, or by combined sliding and rotation. All of these motions require that joint faces are open or that the rock block is intersected by an excavation that provides space for the rock block to move. Thus the first warning of block movement is the widening of particular joints. This is the principle of key block theory (Goodman and Shi, 1985). In a stereographic projection, depending on the number of joint sets available, several zones can be formed in a stereographic sphere by the intersection of the joint planes. These zones are called Joint Pyramid (JP). Key blocks in the same JP are in the same side of joints of each joint set. All key blocks of a JP can form a maximum key block.

There are many finite-sized blocks around an excavation. The key blocks are the first to fall. Other blocks can fall only after key blocks fall which creates more moving space. Key block theory is a convenient way to determine the most critical blocks that may fall or slide into an excavation, given the excavation direction, shape, and dimensions. The information required to describe the rock-mass consists simply of the orientations of the joint planes and their friction angles.

Figure 2-1 identifies six types of blocks around an excavation, some of which are key blocks. Type VI is a rock block, having no faces on the excavation perimeter, that is, no free faces. Therefore, type VI cannot fall into the excavation. Type V has a free face but the block is infinite. Unless there are new cracks formed around the excavation, neither of these two block types can be key blocks. The same is true for block IV, which has a tapered shape; this tapered block cannot move without pushing into its neighbors. Block types I, II, and III are finite and removable. Whether they will move depends not only on geometry but on the direction of the resultant force and the magnitudes of the friction angles between the block interfaces. Block type III is safe under the action of gravity. Type II blocks are also safe by virtue of friction. The one in the roof has parallel sides so the block can move only in one direction, namely parallel to these sides; this restriction on the freedom to displace greatly increases the shear resistance on its faces (Goodman and

Boyle, 1986). The type II block in the wall has a flat base on it so it is unlikely to move if the friction angle is any reasonable value. These type II blocks are potential key blocks. Type I blocks will probably move unless supported as soon as the excavation succeeds in isolating them as individual blocks. The type I block in the roof will fall out and the one in the wall will slide. These are the key blocks.

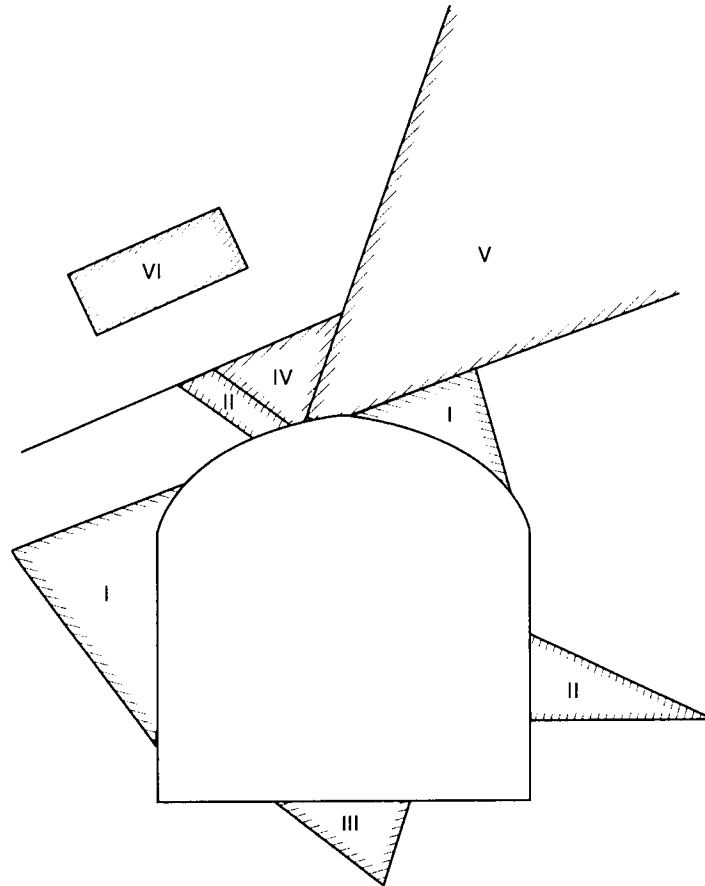


**Figure 2-1. Types of Blocks: I key blocks; II potential key blocks; III safe removable block; IV tapered block; V infinite block; VI joint block**

Key block theory provides a system for dividing all the blocks into these groupings. The first decision separates the nonremovable blocks (types IV, V, and VI) from the removable blocks (types I, II, and III) by means of Shi's theorem that establishes a criterion to determine if a block is finite [see Goodman and Shi (1985) for detail]. A mode analysis, taking into account the direction of the sliding and falling tendencies, given the direction of the resultant force, then distinguishes types III blocks from types II and I blocks. Finally a limit equilibrium analysis, invoking friction on the block faces, establishes the key blocks.

## **2.2 JOINT DATA INPUT**

The joint orientations and joint frictional properties used in key block analysis for the TSw2 lower and upper lithophysal units are given in tables 2-1 and 2-2. These data are derived from a 1999 Civilian Radioactive Waste Management System Management & Operating Contractor ( CRWMS M&O) report on

drift degradation analysis (Civilian Radioactive Waste Management System Management & Operating Contractor, 1999). The TSw2 upper lithophysal unit contains six regular joint sets and one random joint set. The six regular joint sets were simplified (combined) to three joint sets for use in this study due to a limitation with the currently available keyblock code. The problem lies in the difficulty of forming or cutting rock blocks in three dimensions (3D). A new 3D block-cutting technique is under development. In combining the joint sets, joint sets with similar dip direction and dip angle were grouped together. Averaged joint dip direction and angle were used in the study. The random joint sets for both units were not included in this analysis. Figures 2-2 and 2-3 show the upper hemisphere equal angle stereographic projections of joint sets for both TSw2 lower and upper lithophysal units. The joint sets for both units are similar, two nearly vertical joint sets and one nearly horizontal joint set. The difference between the dip directions of joint set 1 for the lower and upper lithophysal units is about 18°.

The cohesion used for both TSw2 units in the 1999 CRWMS M&O report was 0.1 MPa which was scaled down from the value of 0.86 MPa reported in the 1997 CRWMS M&O YM site geotechnical report (Civilian Radioactive Waste Management System Management & Operating Contractor, 1997). In this analysis, a zero value was assumed. The friction angles listed in tables 2-1 and 2-2 are slightly smaller than the ones used by CRWMS M&O in its 1999 report. The value of 41° was used in that report. This value is considered relatively high as compared to the average value obtained by an early Center for Nuclear Waste Regulatory Analyses study sponsored by the NRC Office of Research (Hsiung et al., 1994) which is 38.6°. A 39° value was used in this analysis.

**Table 2-1. Orientations and strength properties of joint sets for TSw2 lower lithophysal unit**

Joint Set No.	Dip Angle, degrees	Dip Direction, degrees	Friction Angle, degrees	Cohesion
1	79	270	39	0
2	81	230	39	0
3	5	45	39	0

**Table 2-2. Orientations and strength properties of joint sets for TSw2 upper lithophysal unit**

Joint Set No.	Dip Angle, degrees	Dip Direction, degrees	Friction Angle, degrees	Cohesion
1	82	288	39	0
2	82	228	39	0
3	14	39	39	0

### 2.3 IDENTIFICATION OF KEY BLOCKS

The primary excavation in this analysis was a horizontal emplacement drift. The drift is 5.5 m in diameter and has an azimuth angle of 105° for the emplacement drift axis. Figures 2-4 and 2-5 show the zones of maximum key blocks for each JP for TSw2 lower and upper lithophysal units, respectively. The key block computer code (KB) (Shi, 1998a), was used in generating 3D blocks. The maximum key block zones are the projections of the maximum 3D key blocks on the tunnel section plane. Also, all the key blocks of the same

JP are in the same key block zone. The reference circle (the equatorial plane of the reference sphere projected as a circle in a stereographic projection), shown as a dashed circle on the figure, is for clarity. The center of the circle represents the arbitrary origin (0, 0, 0) in space. The greater solid curved lines or the great circles are stereographic projections of joint planes. Since the focal point adopted for the stereographic projection is at the bottom of the sphere, the projection of the half space (upper side) about a joint plane is in the circle. The stereographic projection of the lower half space (lower side) of the joint plane is located outside the circle. The system of three joint planes cuts the whole sphere into eight JPs all having their apex at (0, 0, 0). Each of these joint planes is represented by a great circle on the reference sphere and, therefore, by a great circle in the stereographic projection.

The zone labeled 011 in figures 2-4 and 2-5 means JP=011, where 0 denotes the upper side (upper half space) of a joint set and 1 denotes the lower side of a joint set. The first digit represents location information of the JP relative to joint set 1 (lower or upper side of the joint plane), the second digit is for joint set 2, and the third digit is for joint set 3. All the key blocks in JP=011 are on the upper side of joint set 1, lower side of joint set 2, and lower side of joint set 3. Refer to figures 2-2 and 2-3 for joint set orientation for TSw2 lower and upper lithophysal unit, respectively. The solid line circles in figures 2-2 and 2-3 are the reference circles in figures 2-4 and 2-5. In figures 2-4 and 2-5, the solid line circles denote joint set 3; the near north-south trending curve in each of the figures denotes joint set 1 and the other curve represents joint set 2.

Figures 2-6 and 2-7 show the sliding planes (joint sets) of the related maximum key blocks for TSw2 lower and upper lithophysal units. The zone labeled 1 indicates that all the key blocks of this JP slide on the plane of joint set 1. The zone labeled 13 means that all the key blocks of this JP slide along the intersection line (common edge) of joint sets 1 and 3.

If the joints have limited lengths and wide spacing, the key blocks can occupy only a portion of the maximum key block zone. Thus, most of the real key blocks will be located near the emplacement drift surface and only a relatively smaller region needs to be considered in the stability analysis. For both TSw2 lower and upper lithophysal units, only those key blocks located in JP=011 and JP=101 are liable to fall (refer to figures 2-4 and 2-5 for locations of the JPs). Key blocks in JP=101 mean the key blocks that are on the lower side of joint set 1, upper side of joint set 2, and lower side of joint set 3. As indicated in figures 2-5 and 2-7, the key blocks in JP=101 slide on the planes of the joints belonging to joint set 2. Key blocks of JP=011 means the blocks that are on the upper side of joint set 1, lower side of joint set 2, and lower side of joint set 3. Key blocks in JP=011 slide on the planes of the joints belonging to joint set 1.

Figures 2-8 and 2-9 provide a 3D view of the maximum possible key block in JP=011 for TSw2 lower and upper lithophysal units, respectively, and figures 2-10 and 2-11 show a 3D view of the maximum possible key blocks in JP=101 for TSw2 lower and upper lithophysal units, respectively. The maximum possible key blocks shown in figures 2-8 to 2-11 are produced with the assumptions that the joint length for each joint set is sufficiently long and the joint spacing for each joint set is sufficiently small. In this case, many rock blocks may be formed and combined to form the maximum key block. Any of the actual key blocks in a JP cannot be bigger than the maximum possible key block for that JP. In fact, the actual key blocks could be much smaller due to the limited length and substantial spacing of the joints such that the chances for rock blocks to form is reduced.

The calculated volume and area of exposure on the surface of the emplacement drift for the maximum possible key blocks identified are given in table 2-3. As can be observed, the maximum possible key blocks for both the lower and upper lithophysal units are relatively small. These key blocks are first to fall. Other rock blocks may fall only after the fall of key blocks that create more space for other blocks to move. Therefore, if all the maximum key blocks are well supported, other rock blocks will remain stable. Also as can be observed in table 2-3, the sliding surfaces for the JPs that are liable to fall are either along joint set 1 or 2. Given that joint sets 1 and 2 are near vertical for both rock units, relatively small resistance is available

between joint interfaces to prevent rockfall.

Further key block analysis was conducted to determine the percentage of areas that are occupied by key blocks around the excavation surface of the emplacement drift. This analysis was conducted with the following assumptions:

- No long-term degradation induced growth on joint length was considered,
- No long-term degradation of joint strength was considered, and
- The key blocks only lie on one side of each joint set.

If rock blocks are confined by the joint planes of the same joint set, the problem becomes statically indeterminate. Key block theory deals with only the determinate problems. Normally, key blocks located on both sides of a joint set can be relatively bigger than the key blocks that lie on one side of each joint. Discontinuous deformation analysis will need to be used to assess the potential of rockfall under this type of condition.

**Table 2-3. Calculated volume and area of exposure of the maximum possible key blocks**

	TSw2 Lower Lithophysal Unit		TSw2 Upper Lithophysal Unit	
Key Block JP Code	011	101	011	101
Volume, m <sup>3</sup>	0.76	0.92	1.06	0.61
Area on Surface of Drift, m <sup>2</sup>	2.83	3.09	3.39	2.53
Sliding Plane	Joint Set 1	Joint Set 2	Joint Set 1	Joint Set 2

Due to practical limitations, the joint data are often developed based on joint trace mappings directly from the surface of an excavation. It is difficult to estimate whether, or how far, a joint can actually extend beyond the excavation surface; that is, the persistency of a set is also uncertain. In conducting the key block analysis, the assumption was made that the joints having traces on the surface of an excavation possess sufficient persistence such that rock blocks can form by the intersections of these joints. If this assumption is true, the 3D key blocks around an excavation can be delimited by using the joint traces exposed on the excavation surface and the key block zones are defined from the curved polygons of the unrolled joint trace map.

Tables 2-4 and 2-5 listed joint spacings, joint lengths, and bridge lengths used in the key block analysis for the joint sets of TSw2 lower and upper lithophysal units, respectively. Since the joint data for both rock units are not readily available, the joint spacing and length were estimated from the joint mapping data of the Exploratory Studies Facility (ESF) Main Drift and Alcove 6a and 6b. The Main Drift has 875 mapped joints, Alcove 6a has 133 mapped joints, and Alcove 6b has 830 mapped joints. It is recognized that the joint spacing and joint length determined from the ESF data described above are not strictly representative of the TSw2 lower and upper lithophysal units. More representative values will be used in the future when they become available. The bridge length is the gap between the end points of two adjacent collinear joint lines and was also assumed since no data are currently available. Bridge length is normally a smaller value relative to the joint length. Without bridge length, a joint becomes a persistent one. A negative joint bridge length is available in both key block and Discontinuous Deformation Analysis (DDA).

In generating 3D rock blocks for identification of key blocks using the KB code, the joint spacing,

length, and bridge length were varied  $\pm 35$  percent about the mean values for the parameters listed in tables 2-4 and 2-5 according to a uniform distribution. The variation was determined using a random number generator with a seed based on the computer clock time; a different seed was used for each different parameter. Consequently, the variation was completely random. Figures 2-12 and 2-13 show a joint trace map on the surface of emplacement drift generated using data from tables 2-1, 2-2, 2-4, and 2-5 for the TSw2 lower and upper lithophysal units.

Figures 2-14 and 2-15 show the surface traces of zones of key blocks in JP=011 and JP=101, respectively, on the emplacement drift for the TSw2 lower lithophysal unit. Figures 2-16 and 2-17 show the surface traces of zones of key blocks in JP=011 and JP=101 on the emplacement drift for TSw2 upper lithophysal unit. Figures 2-14(a) and 2-14(b) illustrate two runs using the KB code. It can be observed that the traced areas of the key blocks and their relative locations on the emplacement drift are different because of use of the random number generator. Similar observations can be made for figures 2-15(a) and 2-15(b). Table 2-6 lists the range of percentage of key block trace area to the emplacement drift surface area for both rock units using the results of six KB runs. The key block area on the emplacement drift wall (the sum of the trace areas for JP=011 and JP=101) is about 2.94 percent to 4.45 percent of the entire drift surface. Bear in mind that the percentage is calculated based on the entire drift surface area. If one were to evaluate from the perspective of drift length affected instead of emplacement drift surface area, one can observe from figures 2-16 and 2-17 that the key blocks appear quite frequently along the top walls on both sides of the emplacement drift, indicating that rockfall from key blocks could be frequent events throughout the entire emplacement drift, if the emplacement drift is not properly supported. Most of these key blocks are expected to be small in size.

**Table 2-4. Joint set data for TSw2 lower lithophysal unit**

Joint Set No.	Mean Spacing, m	Mean Length, m	Mean Bridge Length, m
1	0.3	1.8	0.1
2	0.3	2.4	0.1
3	0.5	1.8	0.1

**Table 2-5. Joint set data for TSw2 upper lithophysal unit**

Joint Set No.	Mean Spacing, m	Mean Length, m	Mean Bridge Length, m
1	0.3	1.8	0.1
2	0.3	2.4	0.1
3	0.5	1.8	0.1

**Table 2-6. Calculated percentage of key block trace area to the emplacement drift surface area**

	<b>TSw2 Lower Lithophysal Unit</b>		<b>TSw2 Upper Lithophysal Unit</b>	
Key Block JP Code	011	101	011	101
Trace Area, percent	1.37 to 2.23	1.57 to 1.64	2.25 to 2.41	1.75 to 2.04

2-8

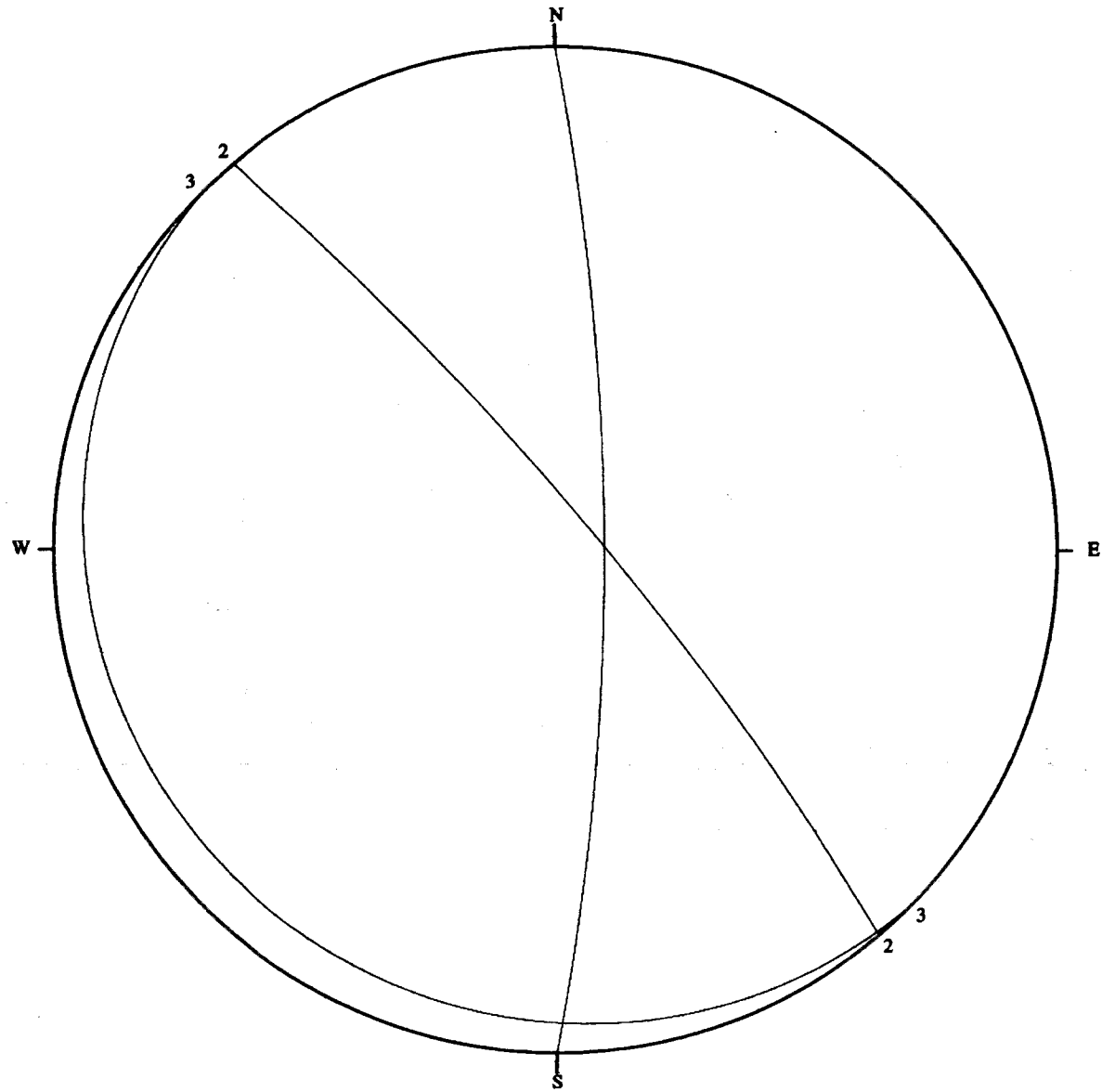


**Figure 2-2. Stereographic projection of joint sets for TSw2 lower lithophysal unit**

2-9

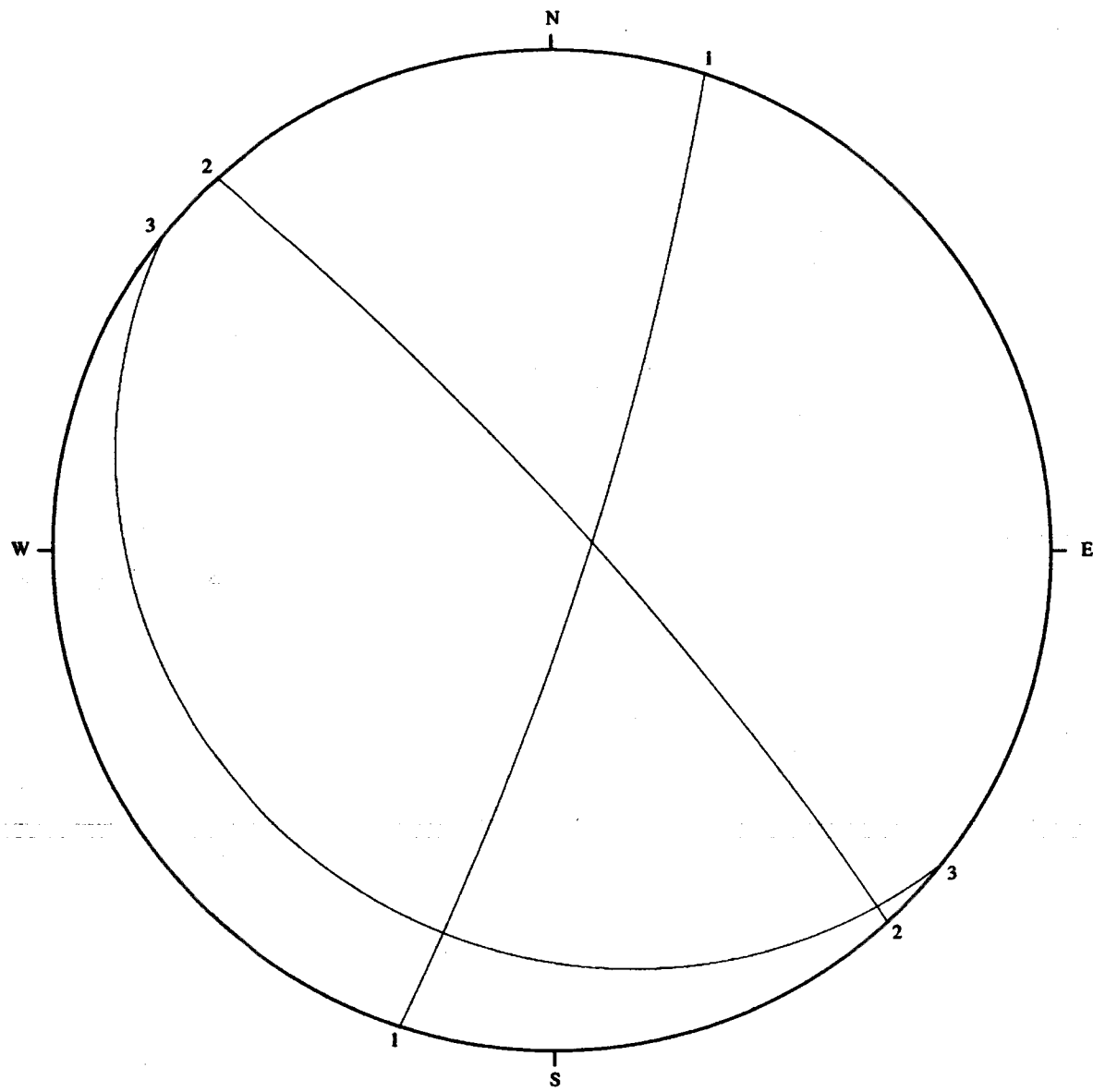
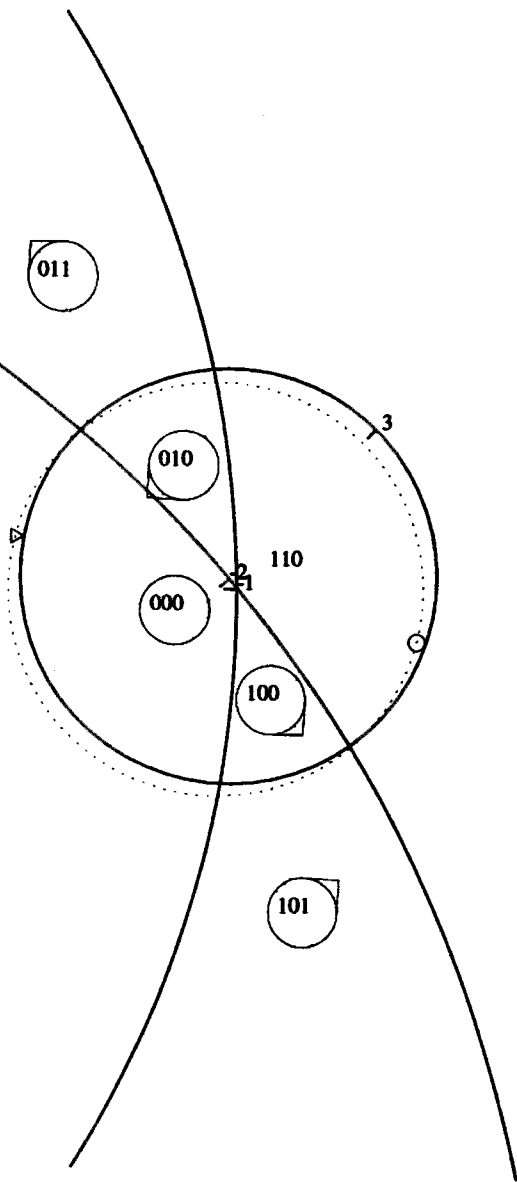


**Figure 2-3. Stereographic projection of joint sets for TSw2 upper lithophysal unit**

resultant  
0.00e+00 0.00e+00 -1.00e+00  
dip & dip d.  
79.0 270.0  
81.0 230.0  
5.0 45.0  
focus  
0.0 0.0 1.0  
tunnel axis  
105.0 0.0

111



2-10

001

Figure 2-4. Key block zones of all joint side combinations for TSw2 lower lithophysal unit

resultant  
 0.00e+00 0.00e+00 -1.00e+00  
 dip & dip d.  
 82.0 288.0  
 82.0 228.0  
 14.0 39.0  
 focus  
 0.0 0.0 1.0  
 tunnel axis  
 105.0 0.0

2-11

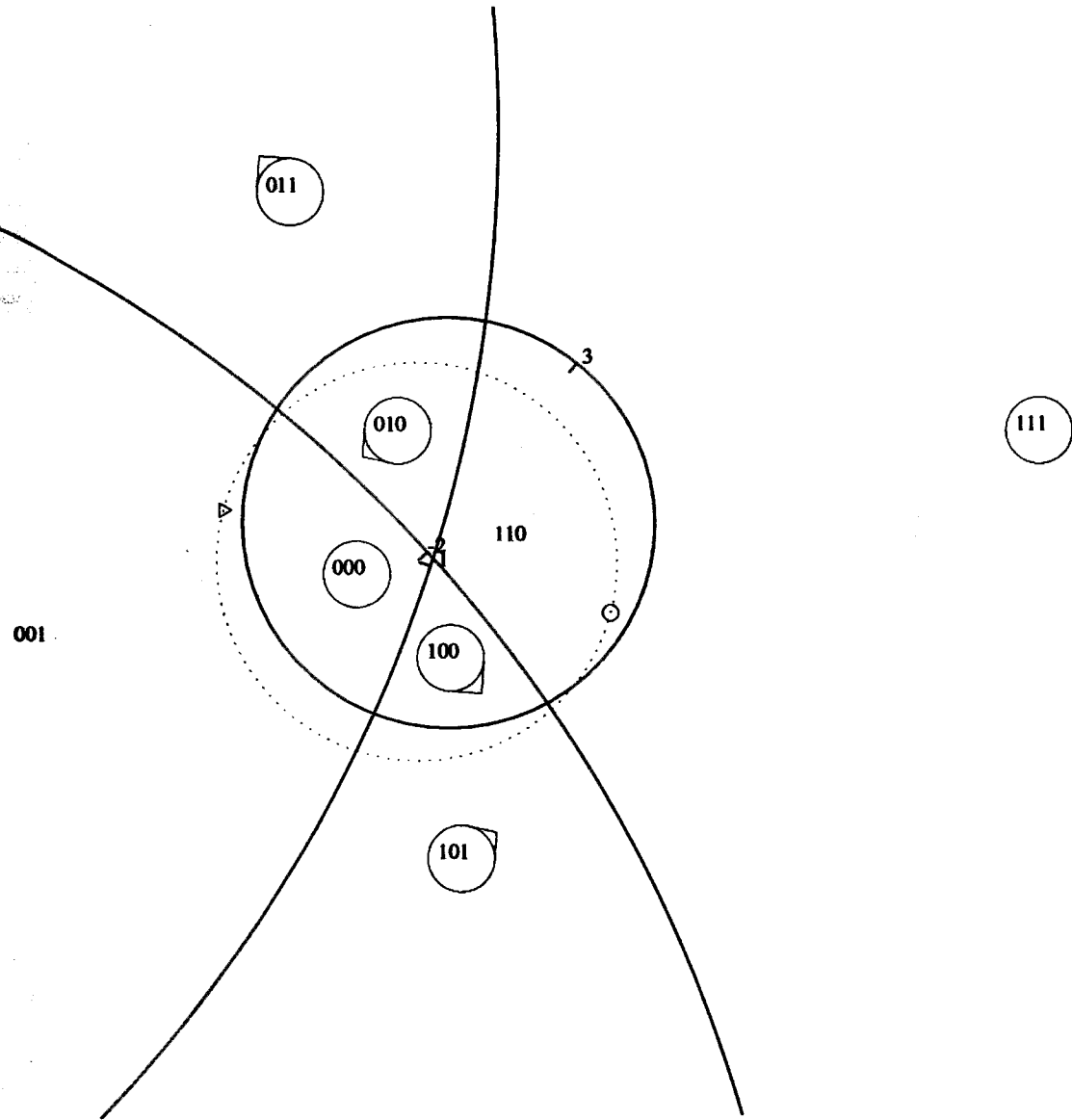


Figure 2-5. Key block zones of all joint side combinations for TSw2 upper lithophysal unit

resultant  
0.00e+00 0.00e+00 -1.00e+00  
dip & dip d.  
79.0 270.0  
81.0 230.0  
5.0 45.0  
focus  
0.0 0.0 1.0  
tunnel axis  
105.0 0.0

2-12

12

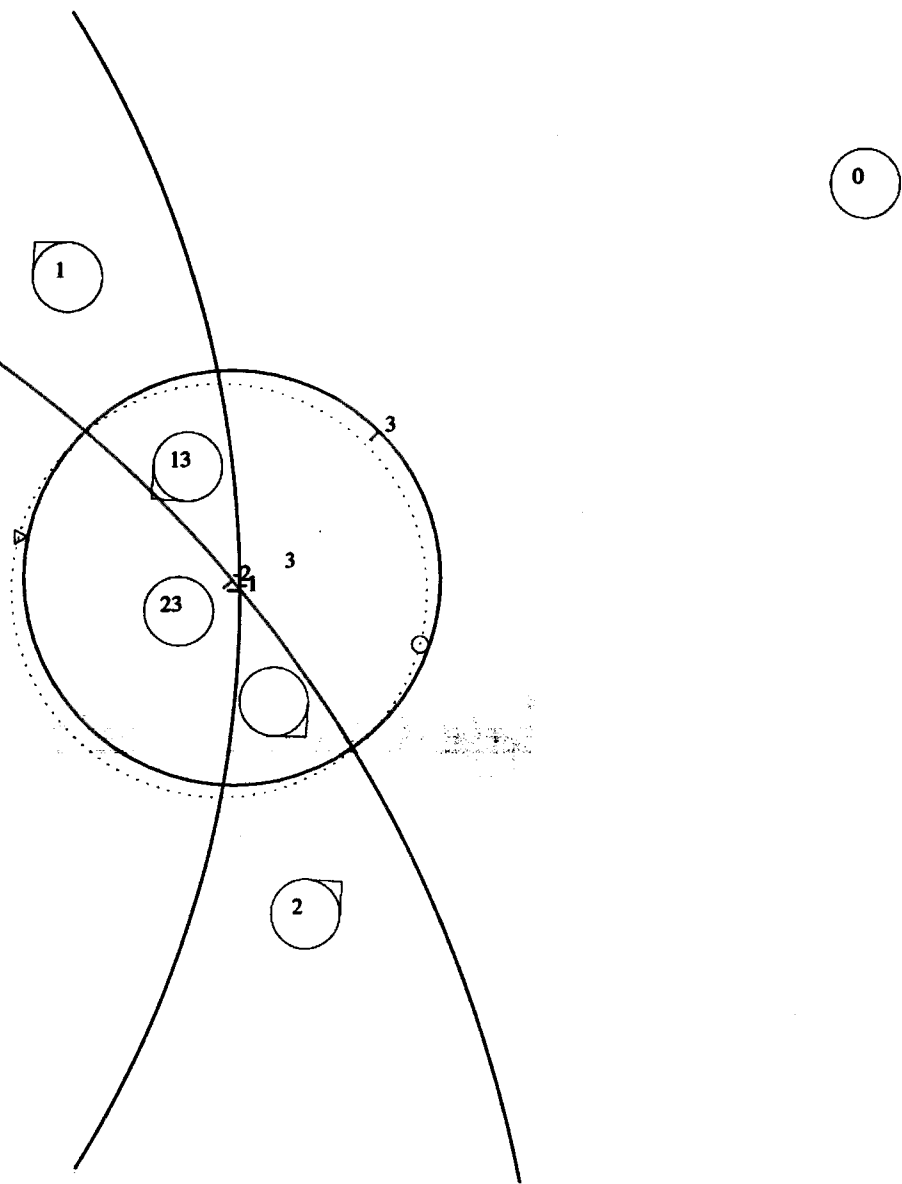


Figure 2-6. Sliding planes of the key block zones for TSw2 lower lithophysal unit

resultant  
0.00e+00 0.00e+00 -1.00e+00  
dip & dip d.  
82.0 288.0  
82.0 228.0  
14.0 39.0  
focus  
0.0 0.0 1.0  
tunnel axis  
105.0 0.0

2-13

12

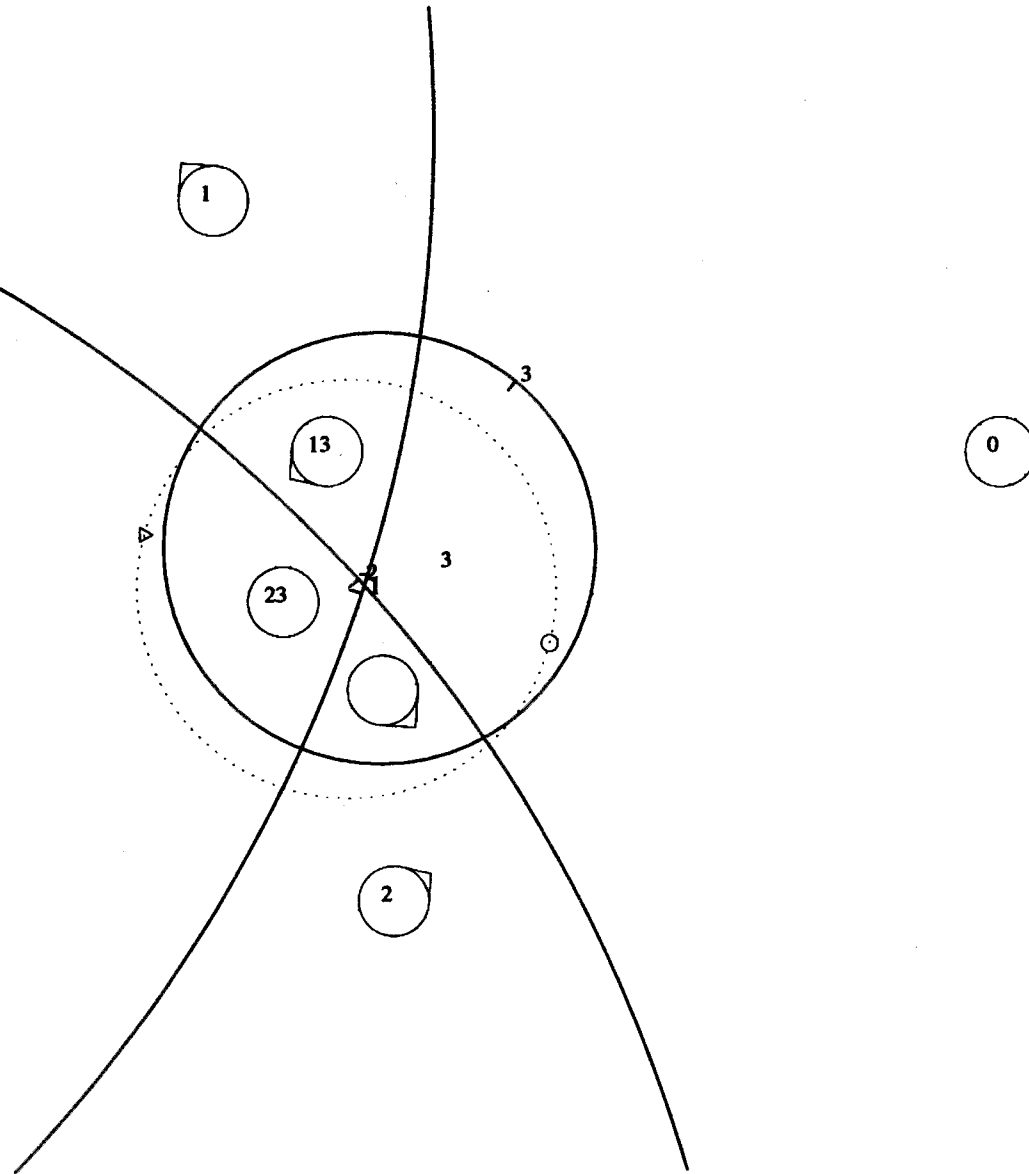
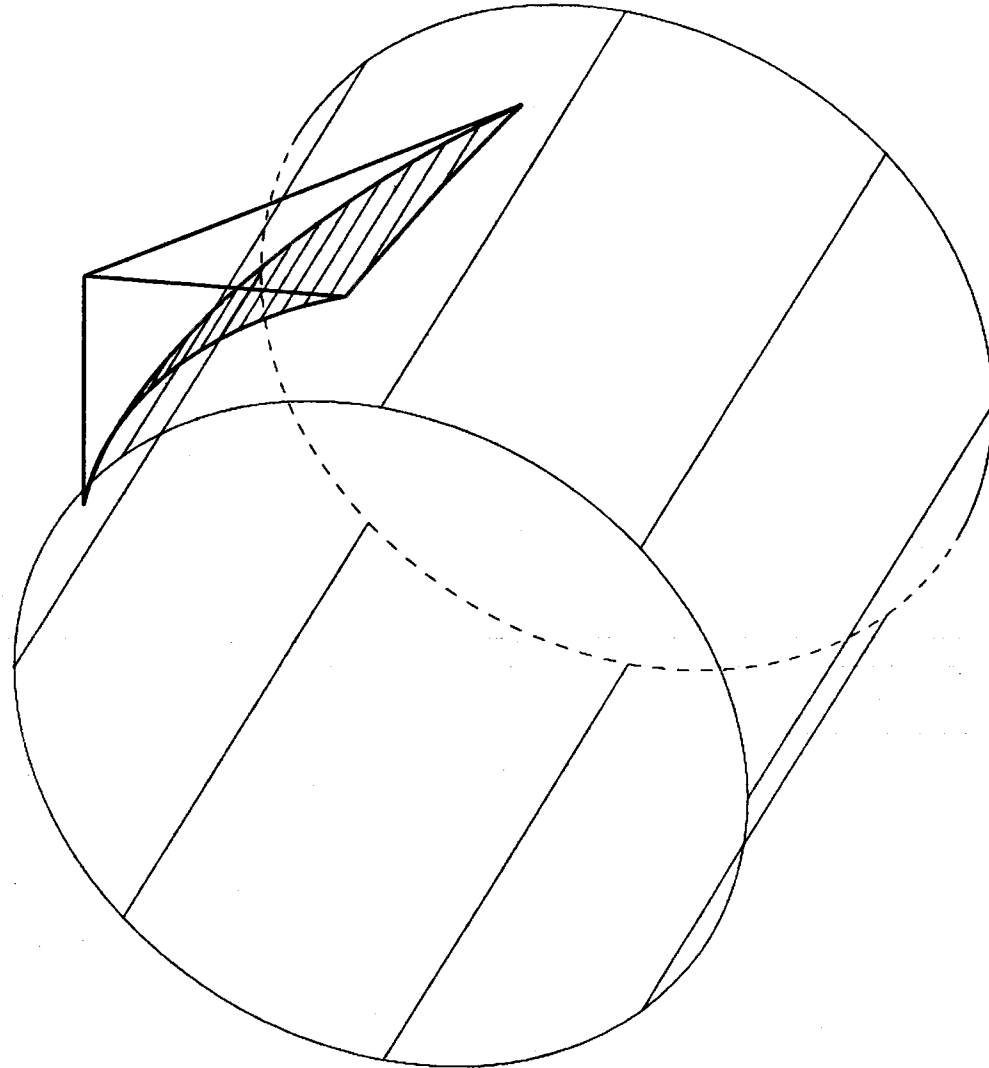


Figure 2-7. Sliding planes of the key block zones for TSw2 upper lithophysal unit

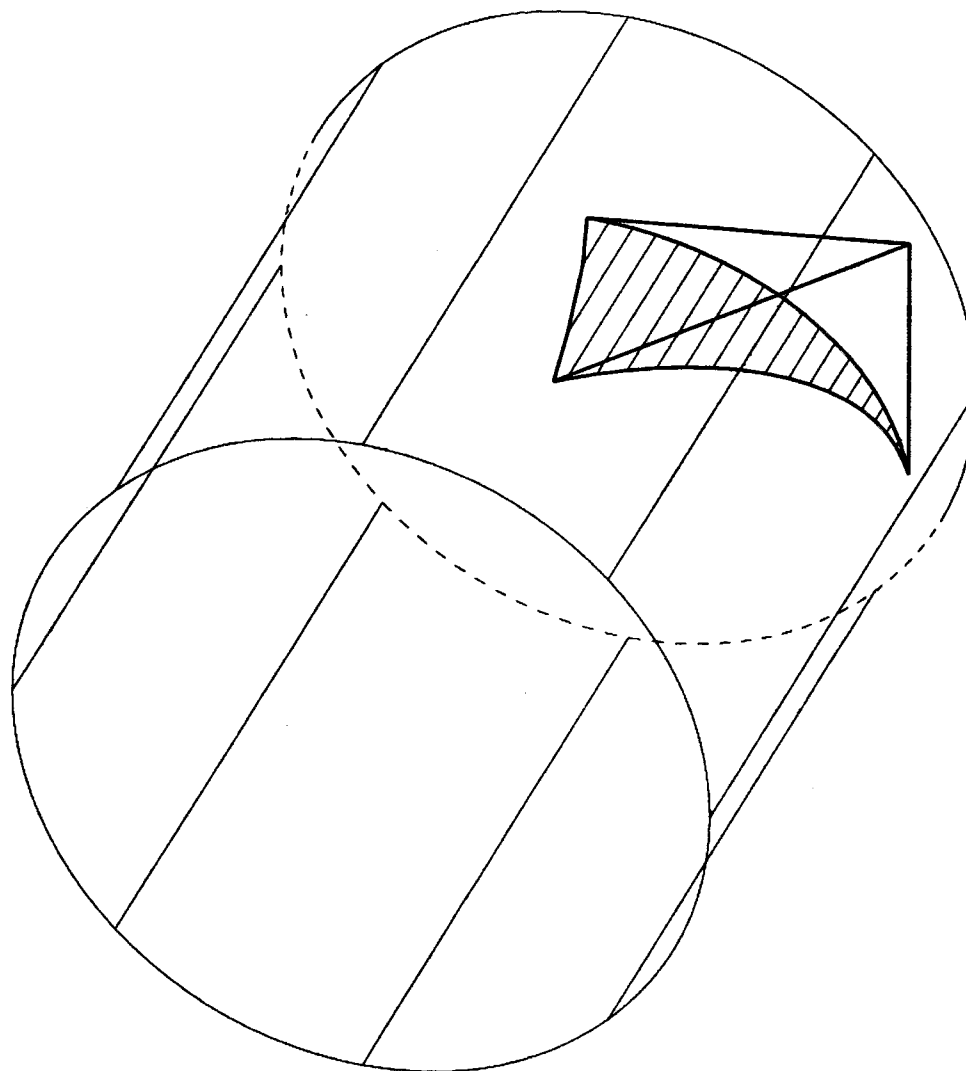
tunnel shape  
2.75e+00 2.75e+00 0.00e+00  
projective dir.  
1.00e+00 2.00e+00 3.00e+00  
top vertex dis.  
0.00e+00  
0.00e+00  
0.00e+00  
top distance  
0.00e+00  
011



2-14

Figure 2-8. Maximum key block in JP=011 for TSw2 lower lithophysal unit

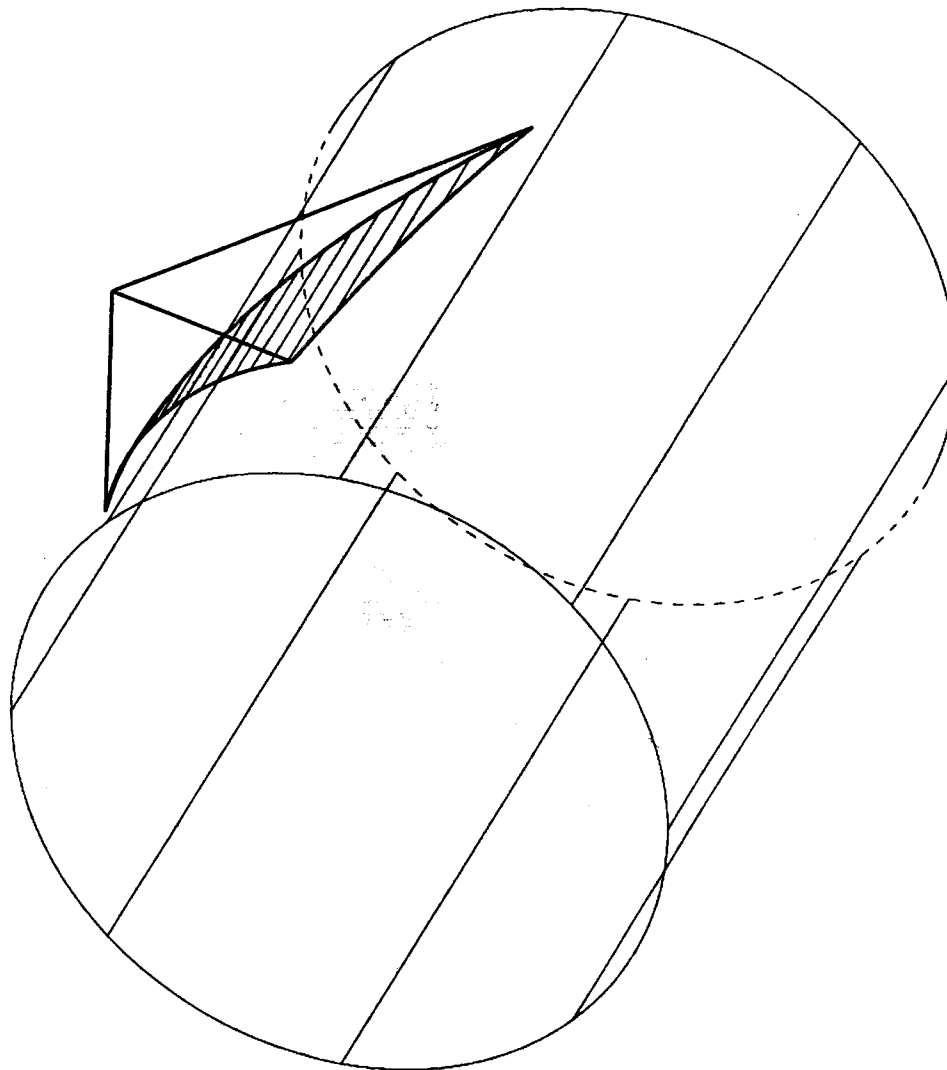
tunnel shape  
2.75e+00 2.75e+00 0.00e+00  
projective dir.  
1.00e+00 2.00e+00 3.00e+00  
top vertex dis.  
0.00e+00  
0.00e+00  
0.00e+00  
top distance  
0.00e+00  
101



2-15

Figure 2-9. Maximum key block in JP=011 for TSw2 upper lithophysal unit

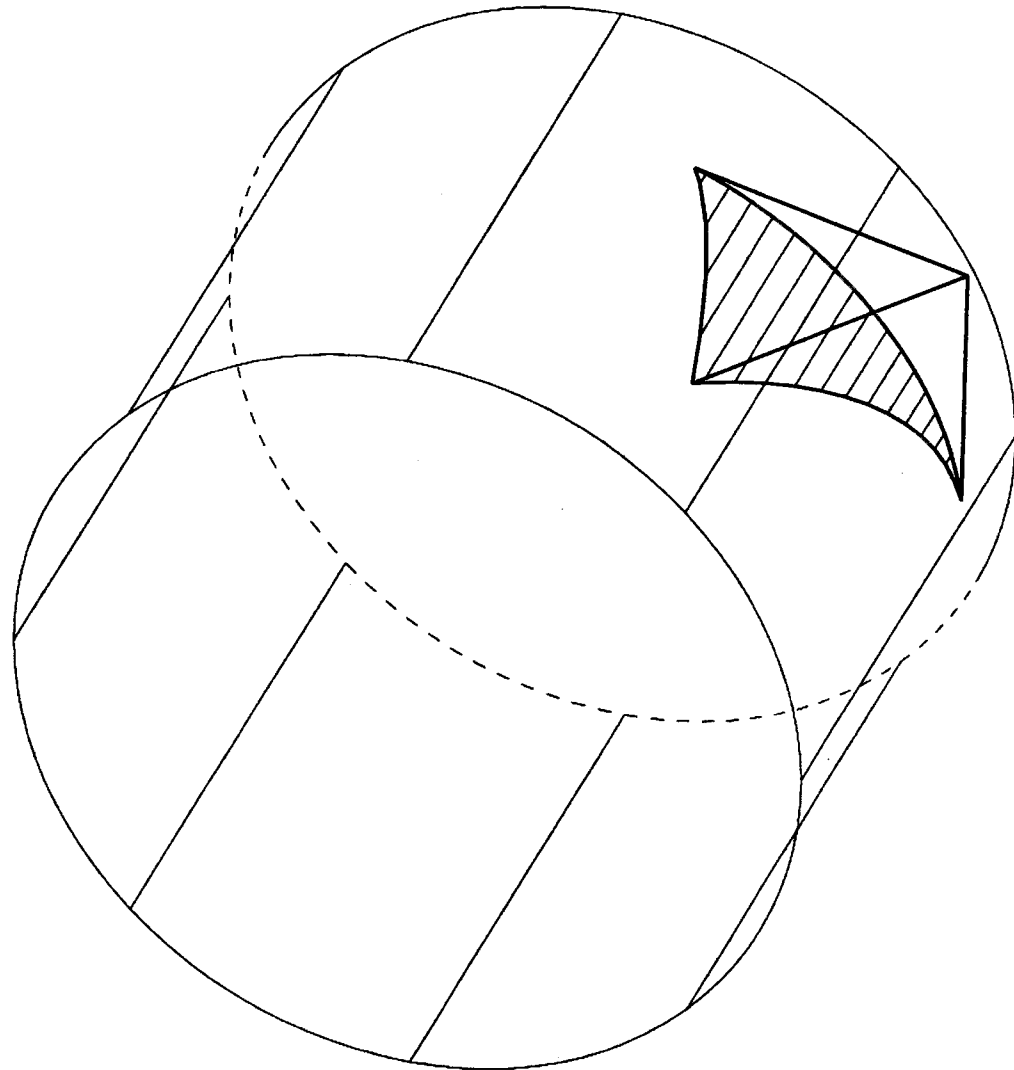
tunnel shape  
2.75e+00 2.75e+00 0.00e+00  
projective dir.  
1.00e+00 2.00e+00 3.00e+00  
top vertex dis.  
0.00e+00  
0.00e+00  
0.00e+00  
top distance  
0.00e+00  
011



2-16

**Figure 2-10. Maximum key block in JP=011 for TSw2 lower lithophysal unit**

tunnel shape  
2.75e+00 2.75e+00 0.00e+00  
projective dir.  
1.00e+00 2.00e+00 3.00e+00  
top vertex dis.  
0.00e+00  
0.00e+00  
0.00e+00  
top distance  
0.00e+00  
101



2-17

**Figure 2-11. Maximum key block in JP=101 for TSw2 upper lithophysal unit**

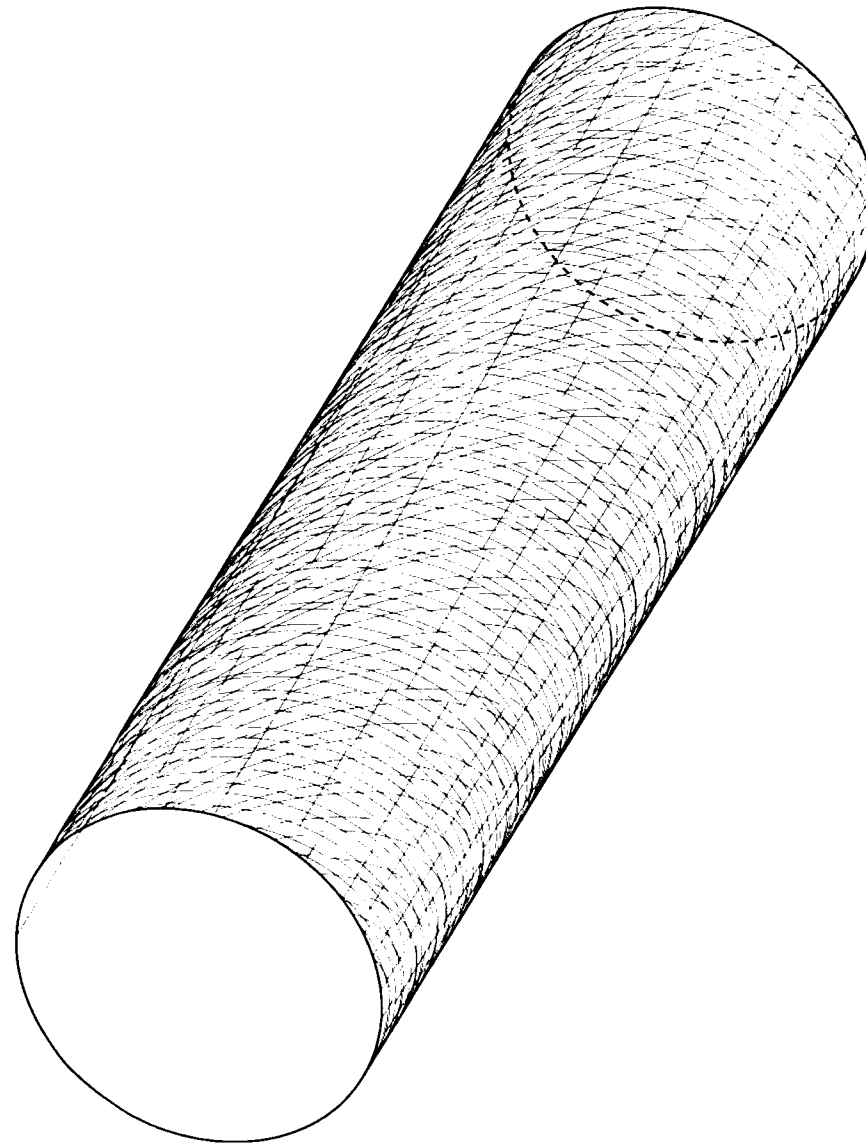


**Figure 2-12. Three-dimensional joint trace map on the surface of emplacement drift for the TSw2 lower lithophysal unit**

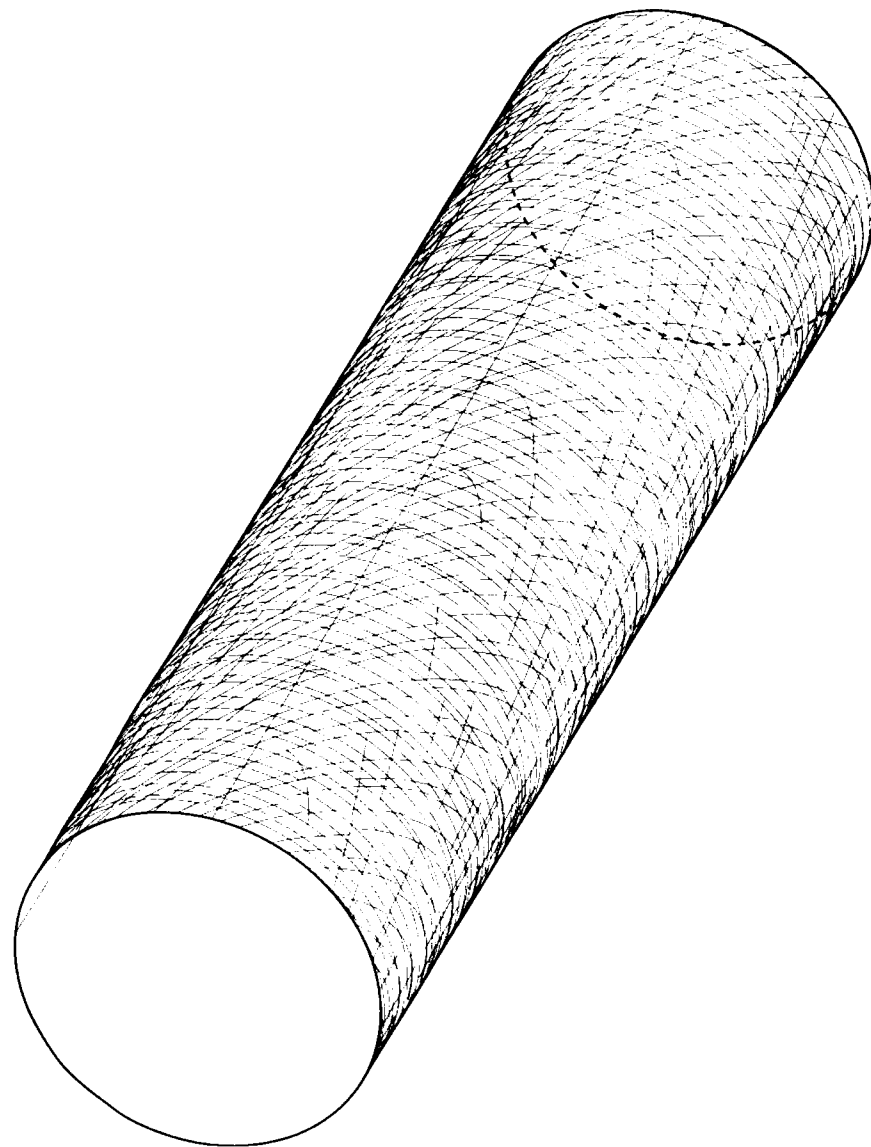


**Figure 2-13. Three-dimensional joint trace map on the surface of emplacement drift for the TSw2 upper lithophysal unit**

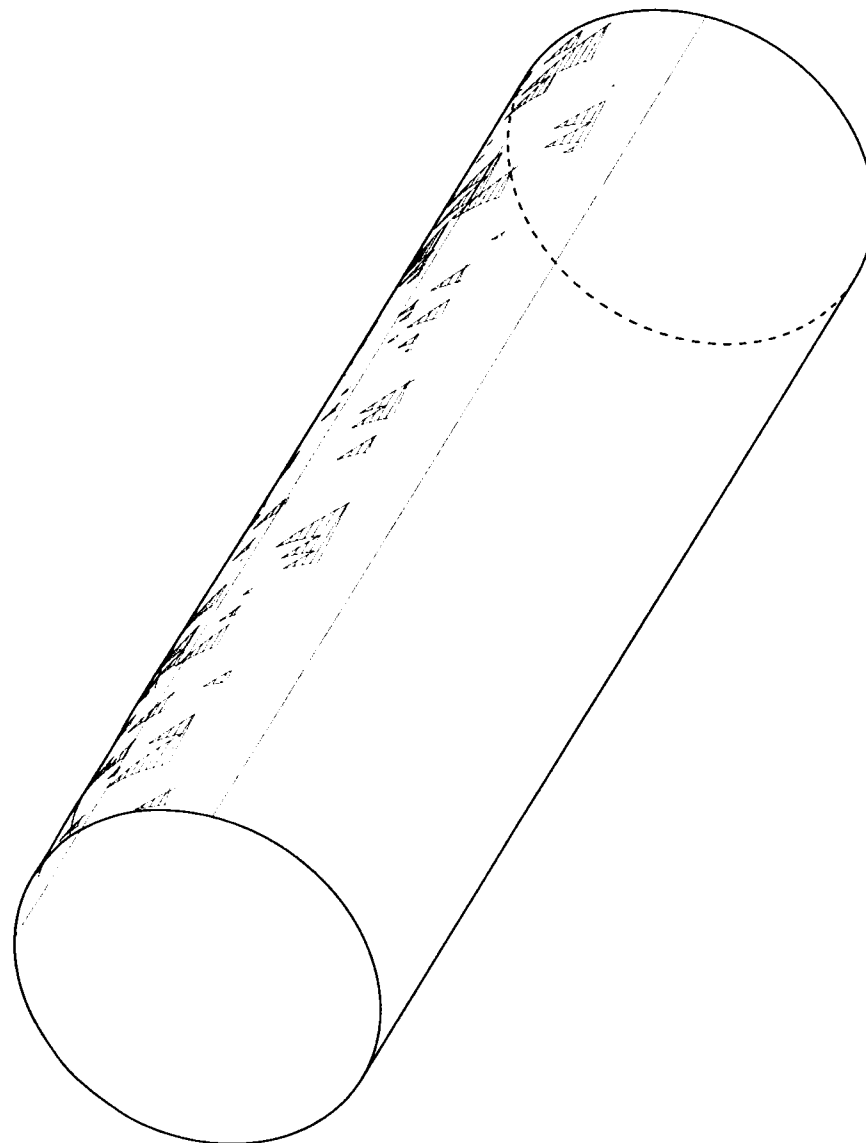


**Figure 2-14a. Traces of key blocks in JP=011 on emplacement drift surface for TSw2 lower lithophysal unit (one KB run)**

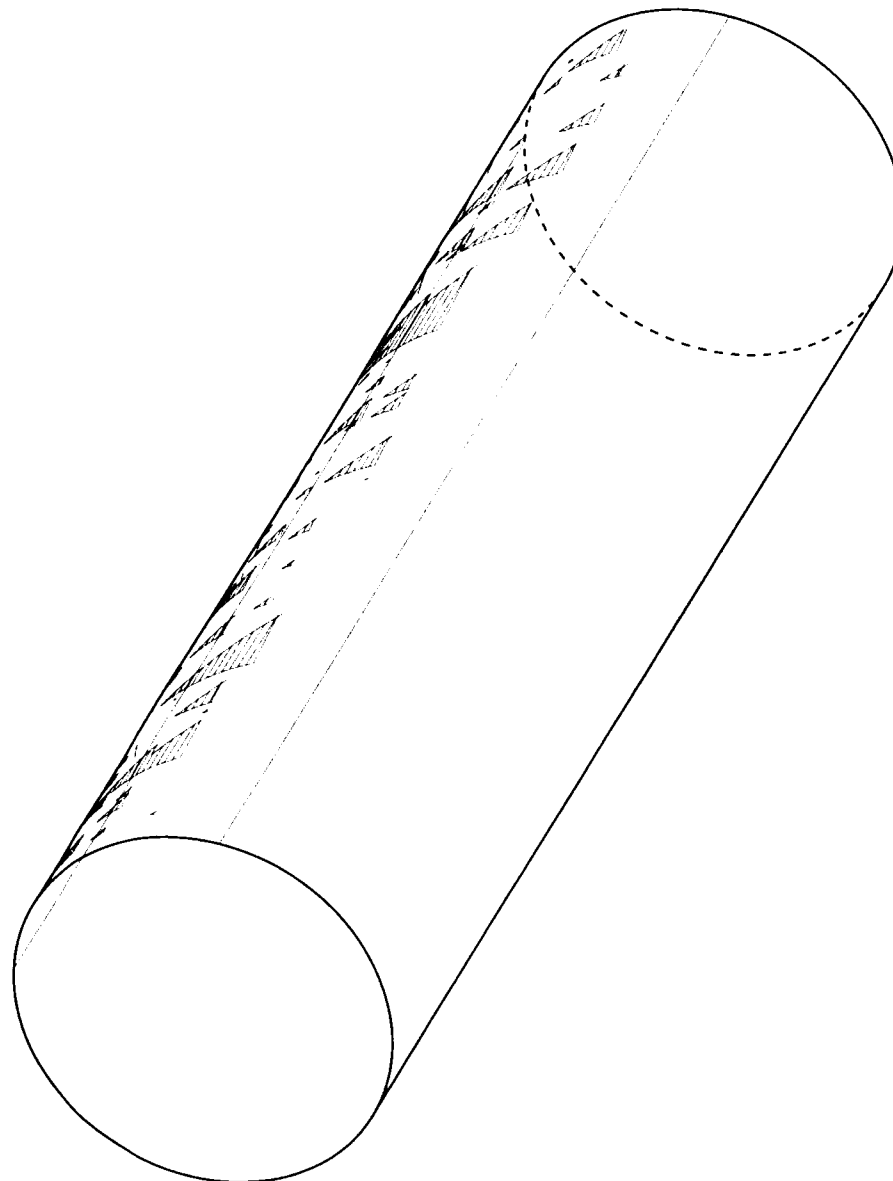


**Figure 2-14b. Traces of key blocks in JP=011 on emplacement surface for TSw2 lower lithophysal unit (second KB run)**

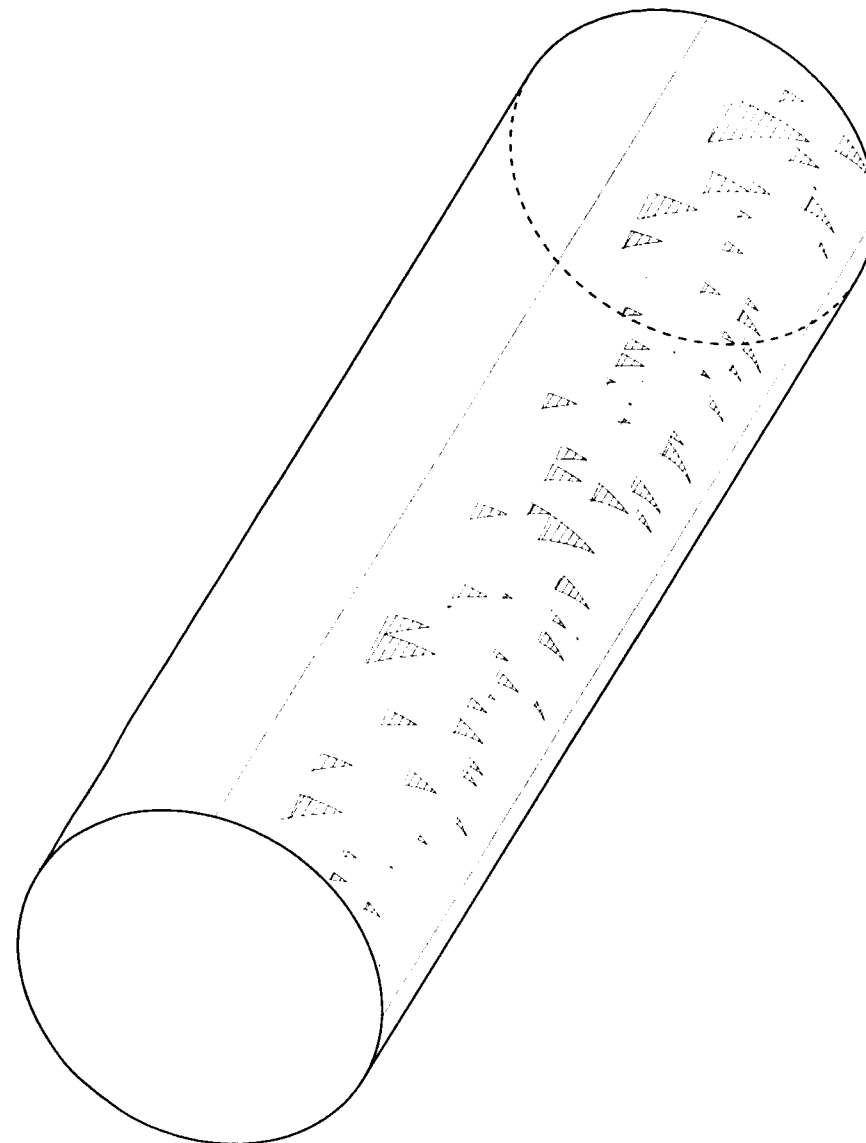


**Figure 2-15a. Traces of key blocks in JP=101 on emplacement drift surface for TSw2 lower lithophysal unit (one KB run)**

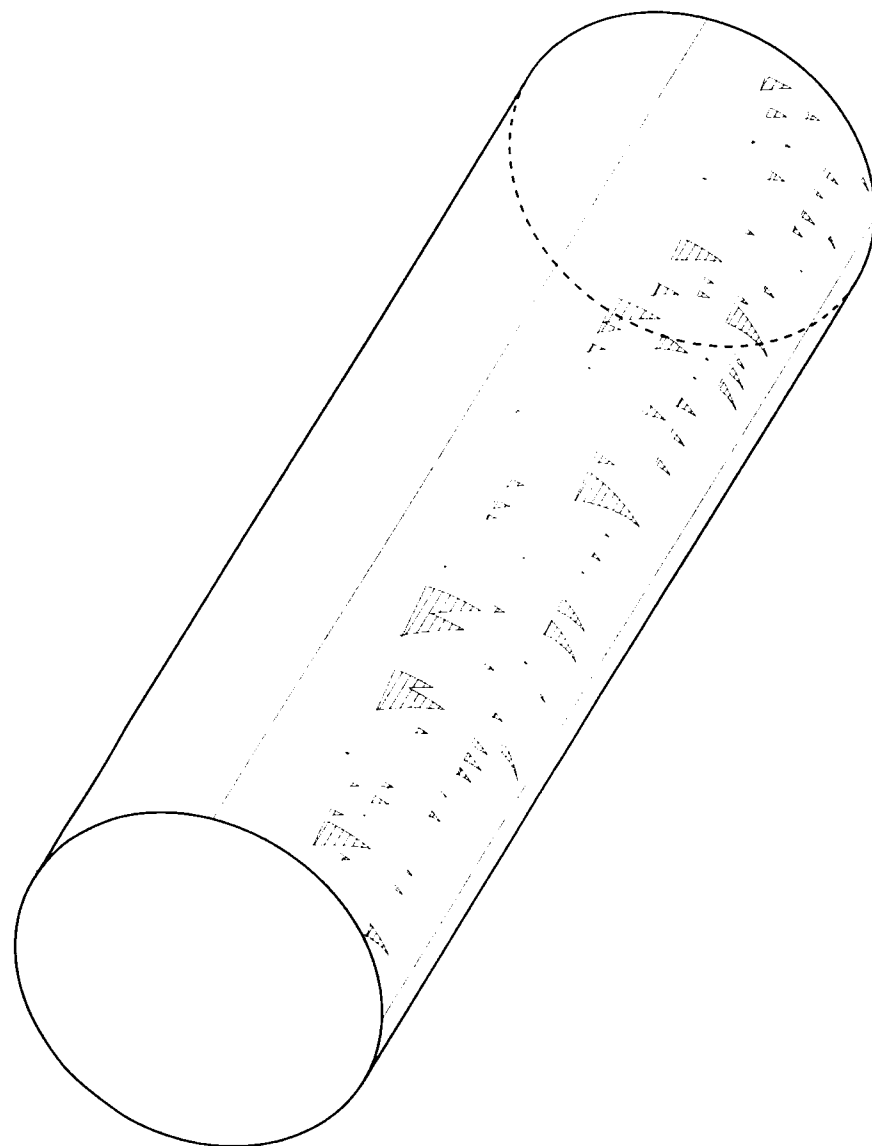


**Figure 2-15b. Traces of key blocks in JP=101 on emplacement drift surface for TSw2 lower lithophysal unit (second KB run)**

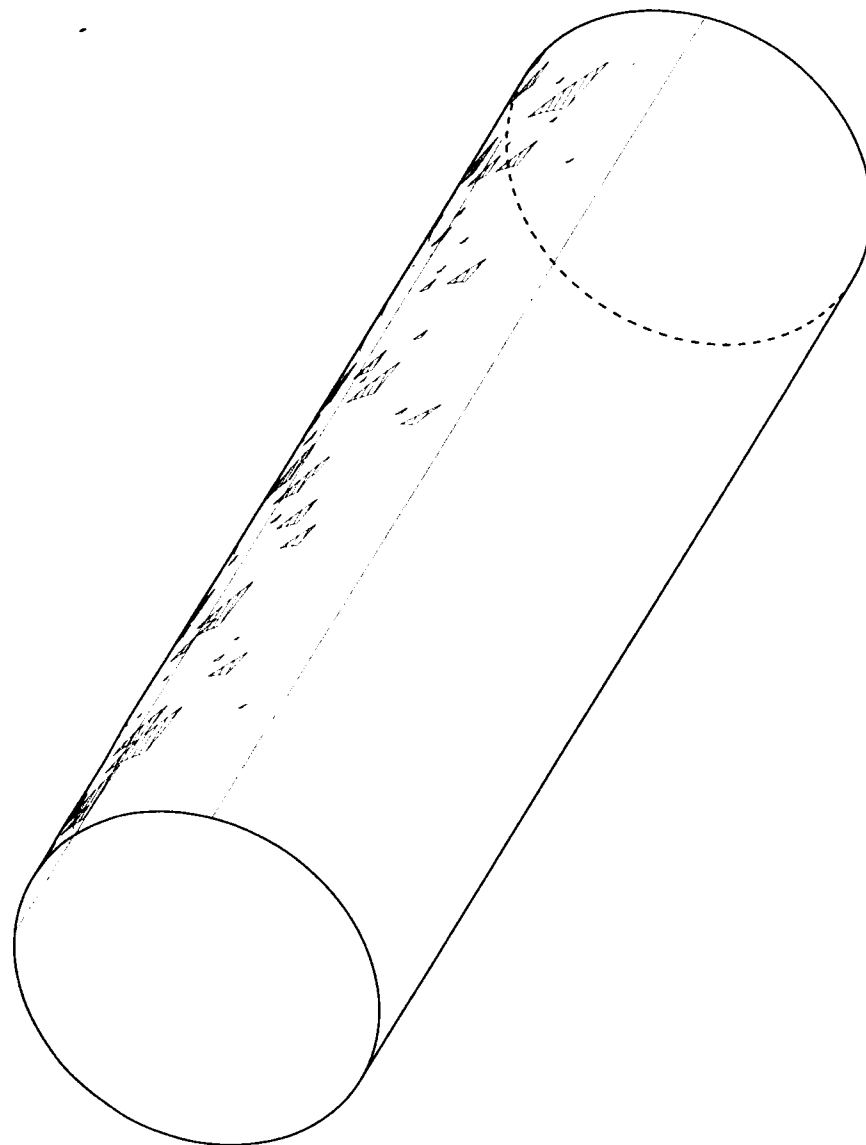


**Figure 2-16a. Traces of key blocks in JP=011 on emplacement drift surface for TSw2 upper lithophysal unit (one KB run)**

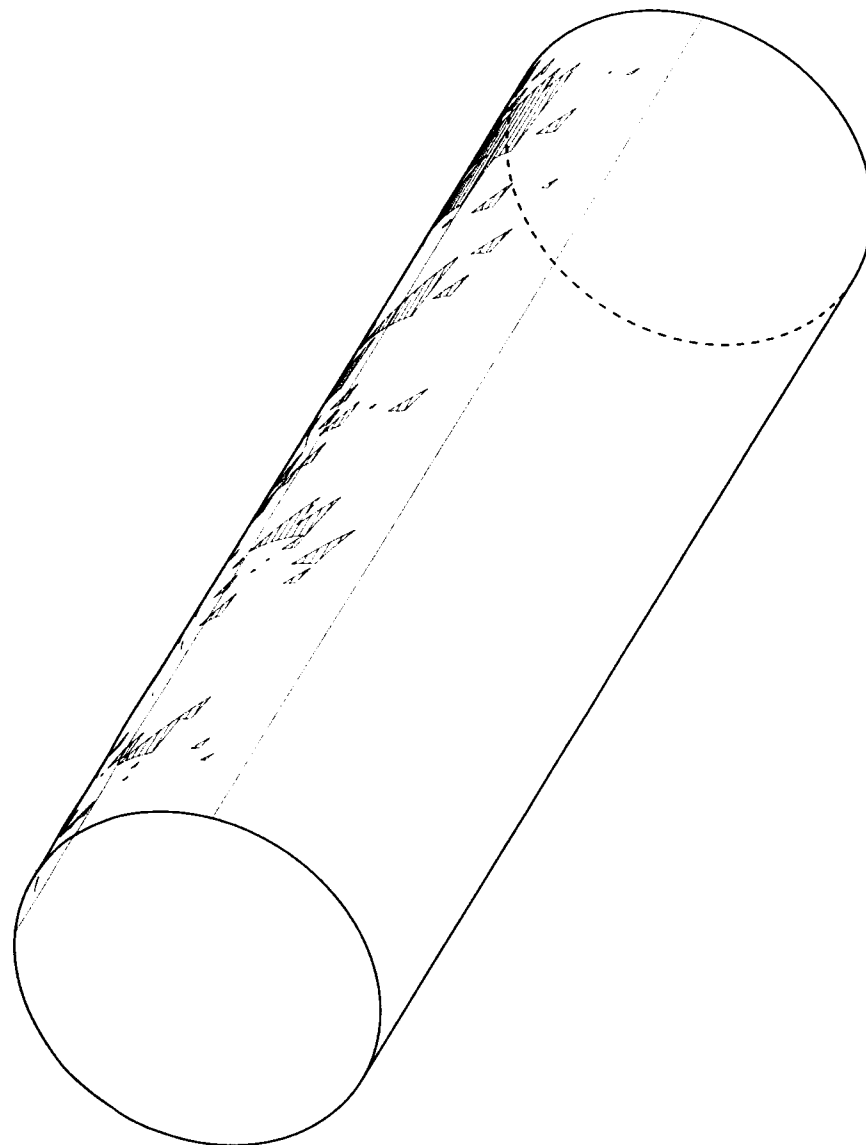


**Figure 2-16b. Traces of key blocks in JP=011 on emplacement drift surface for TSw2 upper lithophysal unit (second KB run)**

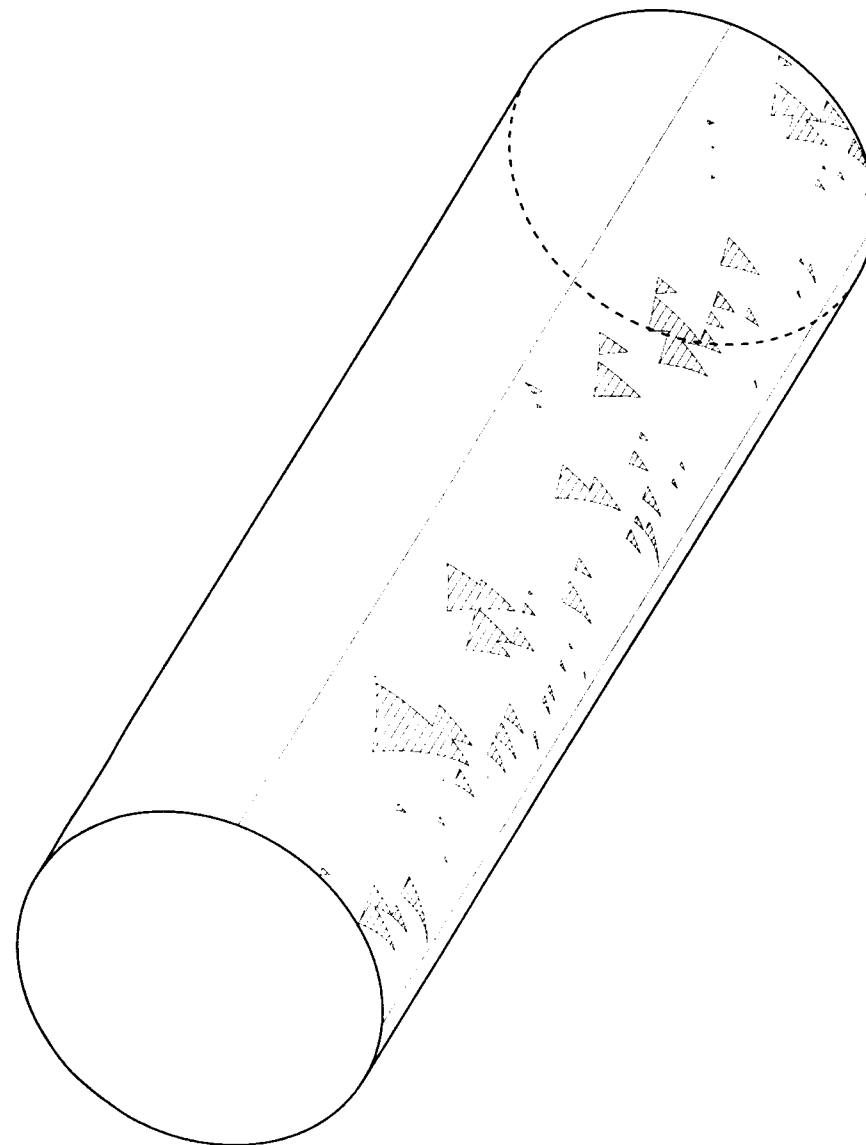


**Figure 2-17a. Traces of key blocks in JP=101 on emplacement drift surface for TSw2 upper lithophysal unit (one KB run)**

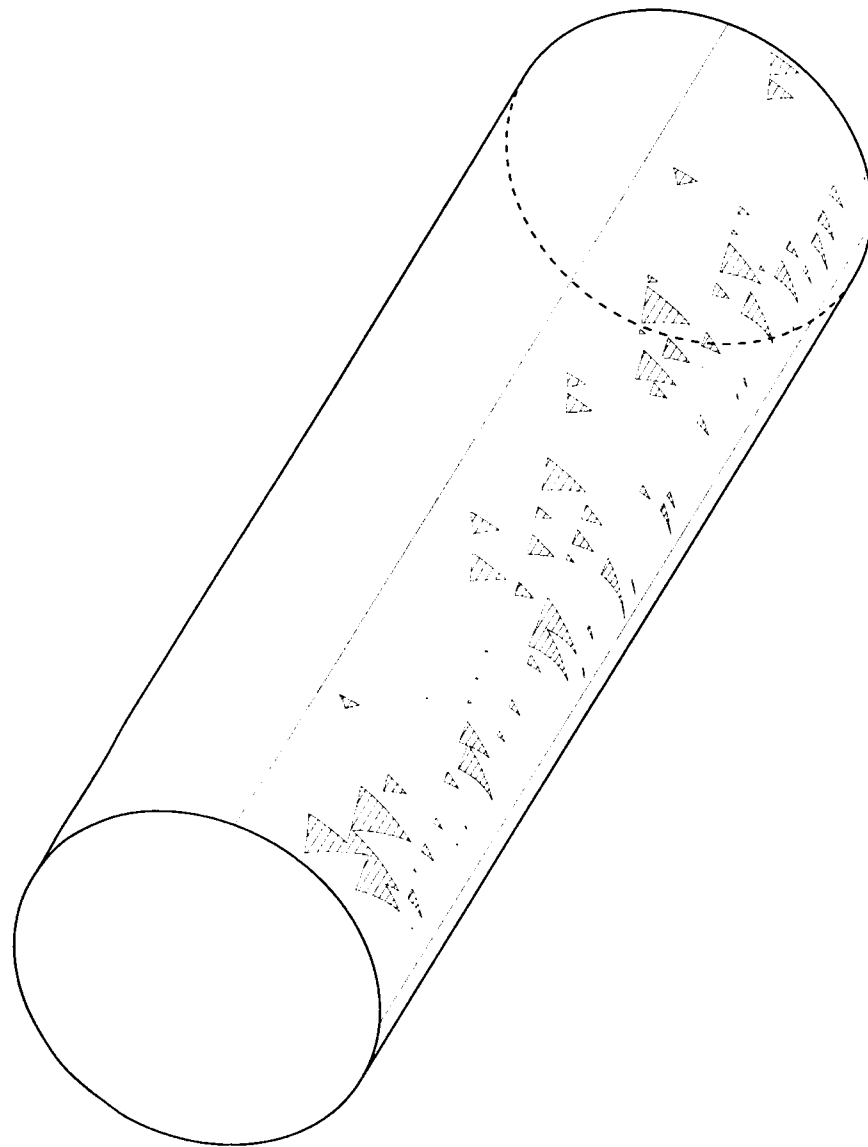


**Figure 2-17b. Traces of key blocks in JP=101 on emplacement drift surface for TSw2 upper lithophysal unit (second KB run)**

### 3 ANALYSIS OF ROCKFALL DUE TO EARTHQUAKES

Long-term stability of emplacement drifts at YM will primarily depend on time-dependent thermal-mechanical (TM) effects. The TM effects are caused by *in situ* and excavation-induced stresses, thermally induced stresses, and dynamic motions. Because the preclosure operations period (up to 300 yr) and postclosure compliance period (thousands of years) are long, the repository openings are expected to be subjected to repeated episodes of seismic events of various magnitudes.

One of the major consequences of the instability of emplacement drifts in a jointed rock-mass is rockfall. The key block analysis discussed in the previous section provides a means for estimating unstable rock blocks that could have the potential to fall within a short time after excavation without considering the effects of seismic ground motion. Seismic ground motions could possibly cause additional rockfall conditions that will require direct modeling.

The most intuitive way to assess rockfall potential and extent of rockfall due to seismicity is using the discontinuum approach. In this progress report, the 2D DDA computer code (Shi, 1998b) is adopted for the analysis. The intent of DDA is to allow for direct modeling of fractures/joints that are common in rock media. The unique scheme of tracking nodal (vertex) points of blocks makes DDA attractive for structural analysis involving complex and fractured geologic media.

#### 3.1 DISCONTINUOUS DEFORMATION ANALYSIS

DDA is the block system version of finite element method (FEM). It involves a finite element type of mesh where all elements are real isolated blocks, bounded by pre-existing discontinuities (or joints). Although DDA seems to resemble the distinct element method in that it accounts for joint contact behavior, mathematically it parallels FEM in the following aspects (Shi, 1996)

- DDA establishes its equilibrium equations by minimizing the total potential energy of the system;
- DDA uses displacements as unknowns for the simultaneous equations; and
- Stiffness, mass, and loading matrices of individual blocks are calculated independently and added to the global matrix of the entire system.

The blocks simulated in DDA can be of any shape (both convex and concave). An implicit solution algorithm is adopted in the DDA. The large displacements of the blocks are accounted for by the use of a time step scheme; at the end of each time step, the equilibrium is reached by minimizing the total potential energy, and block geometry is updated. The deformed block geometry and resulting state of stresses from the previous time step is used as the initial condition for the next time step.

As discussed earlier, in DDA, the large displacements and large deformations are the accumulation of the small displacements and deformations of each small time step. Within each time step, assuming the stresses and strains within a block are constant, the  $x$ - and  $y$ -direction displacements,  $(u, v)$ , at any point  $(x, y)$  of a block, are small and the displacement function can be represented using the first order approximation by six displacement variables (Shi, 1996):

$$\begin{pmatrix} u \\ v \end{pmatrix} = \begin{pmatrix} 1 & 0 & -(y - y_0) & x - x_0 & 0 & \frac{y - y_0}{2} \\ 0 & 1 & x - x_0 & 0 & y - y_0 & \frac{x - x_0}{2} \end{pmatrix} \begin{pmatrix} u_0 \\ v_0 \\ r_0 \\ \varepsilon_x \\ \varepsilon_y \\ \gamma_{xy} \end{pmatrix} \quad (3-1)$$

where

- $(x_0, y_0)$  — reference point in the block (for convenience, centroid of the block in normally used)
- $(u_0, v_0)$  — rigid body translation of point  $(x_0, y_0)$
- $r_0$  — rotation angle of the block with respect to point  $(x_0, y_0)$  and
- $\varepsilon_x, \varepsilon_y,$  and  $\gamma_{xy}$  — normal and shear strains of the block.

Eq. (3-1) can be generalized as

$$\begin{pmatrix} u_i \\ v_i \end{pmatrix} = [A_i][D_i] = \begin{pmatrix} t_{11}^i & t_{12}^i & t_{13}^i & t_{14}^i & t_{15}^i & t_{16}^i \\ t_{21}^i & t_{22}^i & t_{23}^i & t_{24}^i & t_{25}^i & t_{26}^i \end{pmatrix} \begin{pmatrix} d_{1i} \\ d_{2i} \\ d_{3i} \\ d_{4i} \\ d_{5i} \\ d_{6i} \end{pmatrix} \quad (3-2)$$

where the subscript  $i$  denotes the  $i$ th block,  $[A_i]$  is the transformation function, and  $[D_i]$  contains the variables mentioned earlier.

Determination of block deformation involves solving for the variables  $[D_i]$ . The simultaneous equation for the system for solving  $[D_i]$  is

$$[K]_G [D]_G = [F]_G \quad (3-3)$$

where  $[K]_G$  is the system stiffness matrix and  $[F]_G$  is the force or loading matrix. The contribution to  $[K]_G$  and  $[F]_G$  is calculated from stresses and strains, initial stresses, body forces, inertia force, loading conditions, and displacement constraints of individual blocks. To give an example, assuming that a point load  $(F_x, F_y)$  is applied to point  $(x, y)$  of block  $i$ . The displacement of point  $(x, y)$  is determined using Eq. (3-2). The potential energy due to the applied point load  $(F_x, F_y)$  is (Shi, 1996):

$$\Pi_p = -(F_x u + F_y v) \quad (3-4)$$

Eq.(3-4) can also be expressed in the matrix form

$$\Pi_p = -(u \quad v) \begin{pmatrix} F_x \\ F_y \end{pmatrix} \quad (3-5)$$

Replacing  $(u, v)$  with Eq. (3-2), Eq. (3-5) becomes

$$\Pi_p = -[D_i]^T [A_i(x, y)]^T \begin{pmatrix} F_x \\ F_y \end{pmatrix} \quad (3-6)$$

To minimize  $\Pi_p$  with respect to  $[D_i]$ , the contribution of point load at point  $(x, y)$  of block  $i$  to the system matrix  $[F]_G$  for block  $i$  can be obtained as

$$[A_i(x, y)]^T \begin{pmatrix} F_x \\ F_y \end{pmatrix} \rightarrow [F_i]_G \quad (3-7)$$

where  $[A_i(x, y)]$  is the transformation function at point  $(x, y)$ . The left portion of Eq. (3-7) is a  $6 \times 1$  matrix.

To numerically model a blocky system, a complete solution has to satisfy both equilibrium and compatibility conditions (Ma, 1999). DDA uses an open-close iteration criterion to fulfill the compatibility conditions between blocks by solving a set of algebraic inequalities through iterations within a given time step. The open-close iteration process continues until no tension nor penetration occurs at all conditions of contact modes before the calculation proceeds to the next time step. Based on natural contact phenomena, three basic contact modes can be identified: open, sliding, and locking.

Assume that a point  $P_1$  has the coordinate of  $(x_1, y_1)$  and line  $P_2P_3$  has the coordinates  $(x_2, y_2)$  and  $(x_3, y_3)$  at the two end points, respectively. After deformation, the open-close condition of  $P_1$  versus line  $P_2P_3$  can be described by the inequality (Shi, 1996)

$$\Delta = \begin{vmatrix} 1 & x_1 + u_1 & y_1 + v_1 \\ 1 & x_2 + u_2 & y_2 + v_2 \\ 1 & x_3 + u_3 & y_3 + v_3 \end{vmatrix} < 0 \quad (3-8)$$

where  $\Delta$  is the determinant and  $(u_i, v_i)$  is the displacement of the three points and  $i = 1, 2, \text{ and } 3$ . When  $\Delta$  is positive, an open condition is satisfied; that is,  $P_1$  has no contact with line  $P_2P_3$ . Otherwise,  $P_1$  is in contact with line  $P_2P_3$ . The distance  $d$  between  $P_1$  and line  $P_2P_3$  after deformation can be approximated assuming small deformation using

$$d = \frac{\Delta}{\sqrt{(x_2 - x_3)^2 + (y_2 - y_3)^2}} \quad (3-9)$$

In DDA, Coulomb's Law is applied to assess the contact condition to ensure that compatibility is satisfied. At each iteration for a given time step, each contact is evaluated to determine if

- the normal contact force at the contact is greater than or equal to the contact tensile strength;
- the shear contact force is smaller than the contact shear strength multiplied by the half length of the block edge where this contact is located, when the normal contact force is compressive; or
- the shear contact force is greater than or equal to the contact shear strength multiplied by the half length of the block edge where this contact is located, when the normal contact force is compressive.

If the first condition is satisfied, no normal spring is applied. The contact is judged as open. When the second condition is satisfied, the contact is essentially locked such that no sliding between point  $P_1$  and line  $P_2P_3$  has occurred. At this condition, both normal and shear stiffnesses are simulated using normal and shear springs at contact. If the third condition is satisfied,  $P_1$  slides along line  $P_2P_3$ ; a normal spring is added to allow sliding and a pair of friction forces at the contact are added to the system force matrix  $[F]_G$ . The contribution of the added contact springs should be included in the system stiffness matrix  $[K]_G$  to account for the block kinematics in the system.

### 3.2 DATA INPUT AND MODEL GEOMETRY

In this progress report, the rockfall analysis focuses on the TSw2 lower lithophysal unit. The properties of the joint sets used in the 2D DDA analysis are the same as those listed in tables 2-1 and 2-4 except for the mean bridge length. The mean bridge lengths used in the 2D DDA analysis were 0.4 m, 0.3 m, and 0.5 m for joint sets 1, 2, and 3, respectively. The use of larger values than those listed in table 2-4 is necessary to account for the conservatism associated with the 2D DDA models as opposed to the 3D models. Most rock blocks in 3D may be constrained by the neighboring blocks in all three dimensions while the rock blocks analyzed in 2D are only constrained in two dimensions. Consequently, the results from 2D analysis are more conservative than those from 3D analysis. Using relatively larger bridge lengths in 2D analysis may reduce some conservatism. Statistically, a bridge length cannot be much larger than joint spacing. Otherwise, joint spacing may need to be redefined. The bridge length values used in this analysis were about the same as the corresponding joint spacings. Figures 3-1 to 3-3 show three types of joint distributions generated stochastically for constructing DDA block models.

As with the key block analysis, in generating DDA meshes, joint spacing, length, and bridge length in table 2-4 were varied  $\pm 35$  percent about the mean values of the respective parameters according to a uniform distribution. A random number generator was used to define the variation. Different seeds were used for different joint parameters. In the future analysis, these parameters can be made to follow normal or log-normal distribution, as appropriate.

No variation on dip angles of the joint sets are considered in the current analysis. A study on the effects of dip angle variation may be evaluated in the future. The joint lines in the figures are bounded by the inner edges of the boundary frame on four sides. In the cases studied in this progress report, no displacement is allowed in the direction perpendicular to the boundaries. The circular spaces in the figures represent emplacement drifts. The diameter of the emplacement drift is 5.5 m. The dimensions for all DDA block

models are 18 m wide and 16 m high. The emplacement drift is assumed to be 307.25 m beneath the ground surface. The distance from the top of the model to the top of the emplacement drift is 7.25 m. The additional overburden is accounted for in the DDA block models as initial stresses for both vertical and horizontal directions. The horizontal initial stress is estimated based on Poisson's effect.

The joint mesh models in figures 3-1 to 3-3 were further processed to form blocks. A tree cutting procedure was used to remove joints or portions of joints that were not used to form block boundaries. DDA deals with only blocks. Behavior of independent joints cannot be modeled in the DDA without some code modification. In this regard, removing independent joints or portions of joints that are not used by block boundaries is necessary. Figures 3-4 to 3-6 show the DDA numerical models after blocks are formed and non-intersecting joints are removed. The rock blocks in contact with the inner edges of the boundary frame were allowed to slide along the contacted edge. The boundary frame was used to provide horizontal and vertical displacement constraints for the DDA block models. Notice that the rock blocks formed for the three models contain many different shapes with any number of vertices. Many of them are concave in nature. It can also be observed that the block sizes associated with the three models vary. The block size immediately above the emplacement drift for the DDA model shown in figure 3-4 is the largest, followed by that in figures 3-6 and 3-5, in that order.

The material properties used for the DDA computations are given in table 3-1 from Civilian Radioactive Waste Management System Management & Operating Contractor (1999). A total of 20,000 time steps were used for the analysis and the duration of each time step was 0.002 s. The input earthquake data were used in the form of acceleration.

**Table 3-1. Rock block material properties for TSw2 lower lithophysal unit**

Unit Weight, tons/m <sup>3</sup>	2.27
Young's Modulus, tons/m <sup>2</sup>	3,000,000
Poisson's Ratio	0.21

At the time of this analysis, the site-specific time history of earthquakes from YM was not available; the 3D acceleration time history developed by the California Department of Transportation for the Yeba Buena Island Tunnel seismic retrofit program were used for input loads. The original data are for 50 s. In this analysis, the data from 10 to 30 s were used. The acceleration signals in this duration encompass the major part of the strong ground motion. Figures 3-7 and 3-8 show the acceleration time histories along x, y, and z directions and the resultant acceleration for 10 to 30 s. The time in the figures has been adjusted to begin at 0 s to facilitate modeling. The horizontal and vertical accelerations applied to the models were the x, y, and z accelerations shown in figures 3-7 and 3-8 projected to the model cross-section. In DDA, the Newmark method for assessing sliding of a single block was extended to multi-blocks and the earthquake accelerations were applied to the DDA models as body forces.

### 3.3 MODELING RESULTS AND DISCUSSION

#### 3.3.1 DDA Block Model 1

By examining DDA block model 1 (figure 3-4), one can immediately identify an area that is inherently less stable. In the inherently unstable regions, the rock blocks are constrained only by the frictions along joint interfaces. No geometrical constraints exist to physically eliminate the possibility for rock to fall. These rock blocks are the key blocks, in the sense discussed in section 2, if the frictions along joint interfaces are not sufficient to hold the rock blocks in place. For DDA block model 1, the potential rockfall initiation

area is located at the top left corner above the spring line. A few blocks in that region are kinematically controlled by joint frictions. When ground motion hits, this region is most likely to initiate rockfall and produce a domino effect to other areas.

Figure 3-9 shows the ground motion effects on rockfall after 1 s of shaking for DDA block model 1 using the acceleration time histories along the x and z direction as shown in figures 3-7 and 3-8. The maximum resultant acceleration is about 0.85 g between 1 and 2 s. There are another three occasions when the accelerations exceed 0.7 g. They occurred between 8 and 9 s, 10 and 11 s, and 16 and 17 s. As can be seen in figure 3-9, 11 rock blocks in the weakest zone identified above fell during the first second of shaking. The maximum resultant acceleration experienced was slightly over 0.4 g (figure 3-8). Studies are ongoing using the scaled down ground acceleration to determine how much ground acceleration, in terms of g value, that the rock blocks at the top left wall of the emplacement drift in figure 3-4 can sustain without falling.

As the ground acceleration continued, two rock blocks located at the top right corner of the emplacement drift were shaken loose and fell between 1 and 2 s (figure 3-10). Comparing figure 3-10 with figure 3-9, one can observe that the gaps between the rock blocks at the top of the emplacement drift continued to widen as these rock blocks progressively moved downwards during ground acceleration. This phenomenon is consistent with the results from the dynamic small-scale physical model experiment conducted at the CNWRA (Hsiung, et al., 1999). In that experiment, the rock-mass was found to become weaker (or less stable) as the displacements of joints continued to accumulate in the form of both joint normal and shear displacements.

The widening of the gaps continued as the shaking proceeded for the rock blocks (11 of them) at the top of the emplacement drift (figure 3-11). These 11 rock blocks fell eventually between 5 and 6 s of shaking. Figures 3-11 and 3-12 show the rock conditions after 5 and 6 s of ground acceleration, respectively. Figure 3-13 shows that the falling rock blocks began to settle down on the floor of the emplacement drift. Notice the two rock blocks at the top of the emplacement drift; one is triangular in shape. These two blocks did not fall until an additional 8 to 9 s of shaking (figure 3-14).

### **3.3.2 DDA Block Model 2**

Examining DDA block model 2 (figure 3-5), one can identify that the potentially unstable region is located at the top and top left side of the emplacement drift. Figure 3-15 shows that this potentially unstable region is the first to fall during the first second of ground motion. As compared to DDA block model 1, the rock block sizes for DDA block model 2 are relatively smaller for the first run of seismically induced rockfall. Additional rock blocks were eventually shaken loose from the top right side of the emplacement drift at a time between 4 and 5 s. Figures 3-16 and 3-17 give a snapshot of rock movements at the end of 4 and 5 s of ground motion, respectively. This run of rockfall involved 22 blocks; one of them was a size greater than any of the rock blocks that fell for DDA block model 1. It took these 22 blocks more than 3 s to eventually settle down on the emplacement drift floor. No additional rockfall was observed for the rest of the ground motion. Figure 3-18 shows the rock condition after ground motion stopped.

### **3.3.3 DDA Block Model 3**

DDA block model 3, shown in figure 3-6, indicates that a large region mainly at the top and top right side of the emplacement drift appears to be susceptible to ground motion. During the first second of the ground motion only nine small rock blocks fell out (figure 3-19). However, one can observe from figure 3-19 that the fall of a large number of rock blocks at the top and top right side was imminent. There seems to be a small geometrical resistance provided by the rectangular rock block located at the top left side, but this resistance was soon overcome by ground motion. The large collapse seems to begin at the end of 2 s shaking and took about 2 to 3 s to settle. Figures 3-20 to 3-22 illustrate the movements of falling rocks at 2, 3, and

6 s, respectively.

### 3.3.4 Discussion

The three DDA block models were developed using the same joint information with a  $\pm 35$  percent variation about the mean values in joint spacing, length, and bridge length. This variation produced different responses to seismicity. Rockfall patterns for DDA block models 1 and 2 can be divided into two groups. The first group of rock blocks fall early on during the ground motion. This group involves rock blocks that are maintained in place by the frictional strength of the block interfaces. When the shear stresses along the interfaces are sufficiently large to overcome the interface friction, block movements begin. The shear stresses along joint interfaces surrounding underground excavation are, in general, generated from the gravity of the blocks and *in situ* stresses. These shear stresses can be perturbed by seismic ground motion. The shear stress between the two neighboring rock blocks can be increased or decreased depending on the block movements relative to the direction of the shear stress. The frictional resistance of block movements can be perturbed by increasing or decreasing the joint normal stress because of ground motion. When the shear stress is increased and normal stress is decreased, it creates a favorable condition for rock blocks to slide downwards and, in some situations, for rockfall.

The second group of rockfall occurred several seconds into the ground motion. The rock blocks in this group appear to have some geometrical resistance to rockfall and, therefore, are relatively more stable than the rock blocks in the first group. Consequently, relatively longer time and a larger magnitude of shaking appears necessary to create the rockfall condition. As shown from figure 3-8, several local peak ground accelerations with magnitude greater than 0.6 g between 1 and 5 s can be identified, with the maximum value of 0.85 g occurring between 1 and 2 s. These large accelerations may be the main trigger of rockfall. It should be noted that the maximum acceleration of 0.85 g between 1 and 2 s was not the direct cause of the second group of rockfall.

The rockfall condition for DDA block model 3 appears to be different from that of DDA block models 1 and 2. There is only one major group of rockfall that involves a total of 22 rock blocks at an earlier stage of ground motion than the other models.

After the second group of rockfall for DDA block models 1 and 2 and the major group of rockfall for DDA block model 3, no further major rockfall occurred throughout the rest of the ground motion for all DDA block models, even if the models experienced several additional local maximum ground accelerations of 0.6 and 0.7 g.

As can be observed in DDA block model 1 in figure 3-14, three relatively large geometrically complex rock blocks at the top of the emplacement drift remained in place after the completion of ground motion simulation, even though the gaps between these blocks and other surrounding blocks are obvious. This condition is because of the slight geometric constraint applied to the smaller block at right. This constraint prevented the three blocks from falling down. These blocks could eventually fall, perhaps, because of a long-term deterioration of the associated joint and rock strength, repeated ground motions of similar magnitude to the one simulated in this analysis, or from a ground motion with a maximum acceleration greater than 0.85 g. One thing that can be certain is that once these three blocks start to fall, they will trigger at least 13 rock blocks located at the top left region to fall as well.

Similar situations can also be observed for DDA block model 2 (figure 3-18); the rock blocks at the top of the emplacement drift appear to be geometrically stable and may be even more so compared to those for DDA block model 1 (figure 3-14). Consequently, it may require a much longer time for the rock to deteriorate to an extent that produces a favorable condition for rockfall, or a much larger ground acceleration is needed to cause rockfall. After the massive rockfall, the remaining rock blocks surrounding the

emplacement drift for DDA block model 3 appear to be quite stable and it may be the most stable model among the three.

Observing the movements of the falling rock blocks in DDA modeling indicates a complex pattern. Depending on the relative locations of the rock blocks before they fall and the relative conditions for which the rockfall is initiated, a falling rock involves most likely a combination of downward and lateral displacements and rotation, all of which were observed during the analysis. As a result, the effects of rockfall on drip shields or WPs could vary. A falling rock with rotation could have less effect on drip shields or WPs than one without rotation (difference between direct hit and glancing hit) because the energy available for impact is smaller. The rockfall coming directly from the top and without involving rotation could potentially impose the most damage to the engineered barrier components as compared to rock falling from the side or wall, provided that the size of the rock involved is the same. The reason may be intuitive because the fall height (distance between the rock and the engineered barrier component in question) is smaller for the rockfall from the side than that from the top. Furthermore, rock blocks falling from the side are likely to also rotate during the process. The damping of the kinetic energy associated with a rockfall could also take place when two falling rocks collide with each other. All the situations mentioned above could have reduced the energy available for impact of the engineered barrier components.

Falling of multiple rock blocks in unison is an important topic in assessing performance of engineered barrier components. This condition potentially could increase the effective size of rockfall during impact. Consequently, the effect will be greater than that of the individual rock blocks. The phenomenon of multiple rock blocks falling in unison is observed in the analysis (figure 3-23). As can be seen, a big rock block at the right side of the emplacement drift and a small block sitting on the left corner on the big block are falling in unison. For the three models analyzed, the graphical representations were output with a time interval of 1 s. This time interval provides a coarse snapshot of the rock movements and is not sufficient to capture the interaction activities among falling rock blocks. However, preliminary observation indicates that multiple rock blocks falling in unison would not appear to be frequent events since, due to the constraints (geometrical conditions) discussed earlier, falling rock blocks may involve rotation and bumping or they may not be able to fall at the same time. These conditions tend to eliminate the potential for multiple rock blocks to fall in unison.

Although the three DDA block models use the same joint data for the TSw2 lower lithophysal unit, the final geometry of the emplacement drift after collapse appear to be quite different (figures 3-14, 3-18, and 3-22). The final shapes of the emplacement drift cross sections in some ways resemble the results presented in a CRWMS M&O report (Civilian Radioactive Waste Management System Management & Operating Contractor, 1999), but are not quite the same. It is not clear how these complex geometries will affect water dripping into the emplacement drifts. Investigations on this aspect should be conducted in the future.

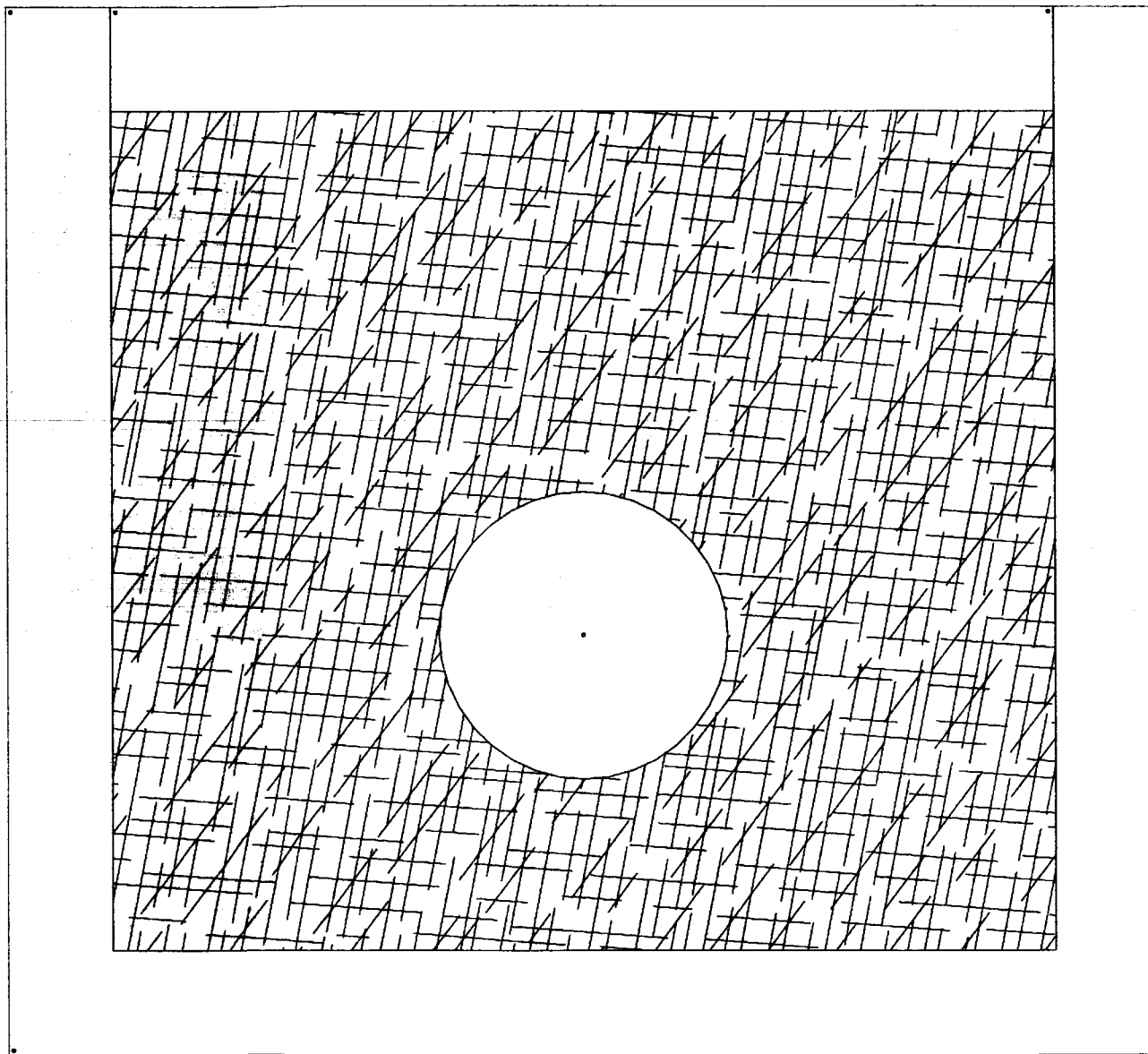


**Figure 3-1. Joint distribution for block mesh model 1**

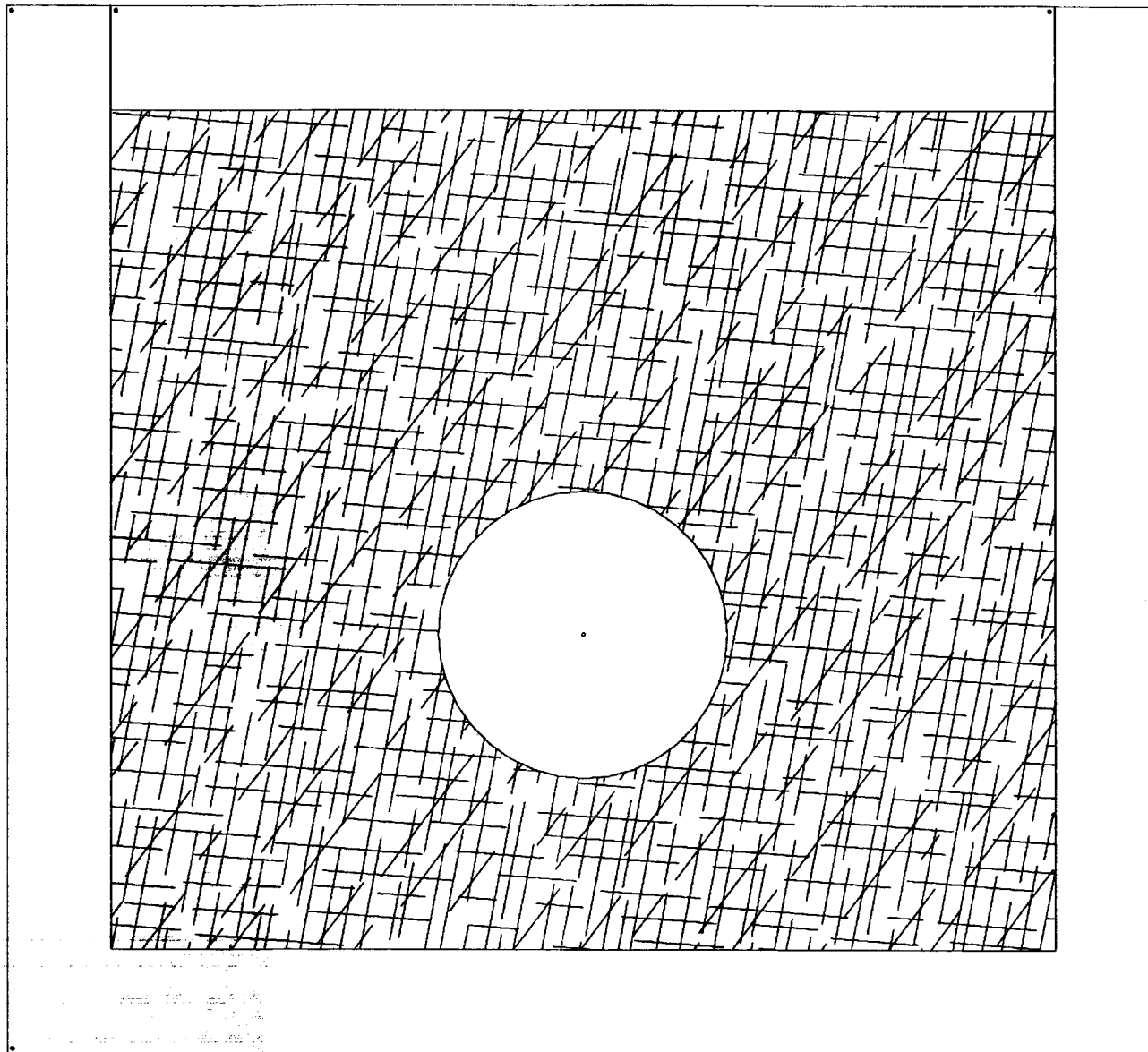


**Figure 3-2. Joint distribution for block mesh model 2**

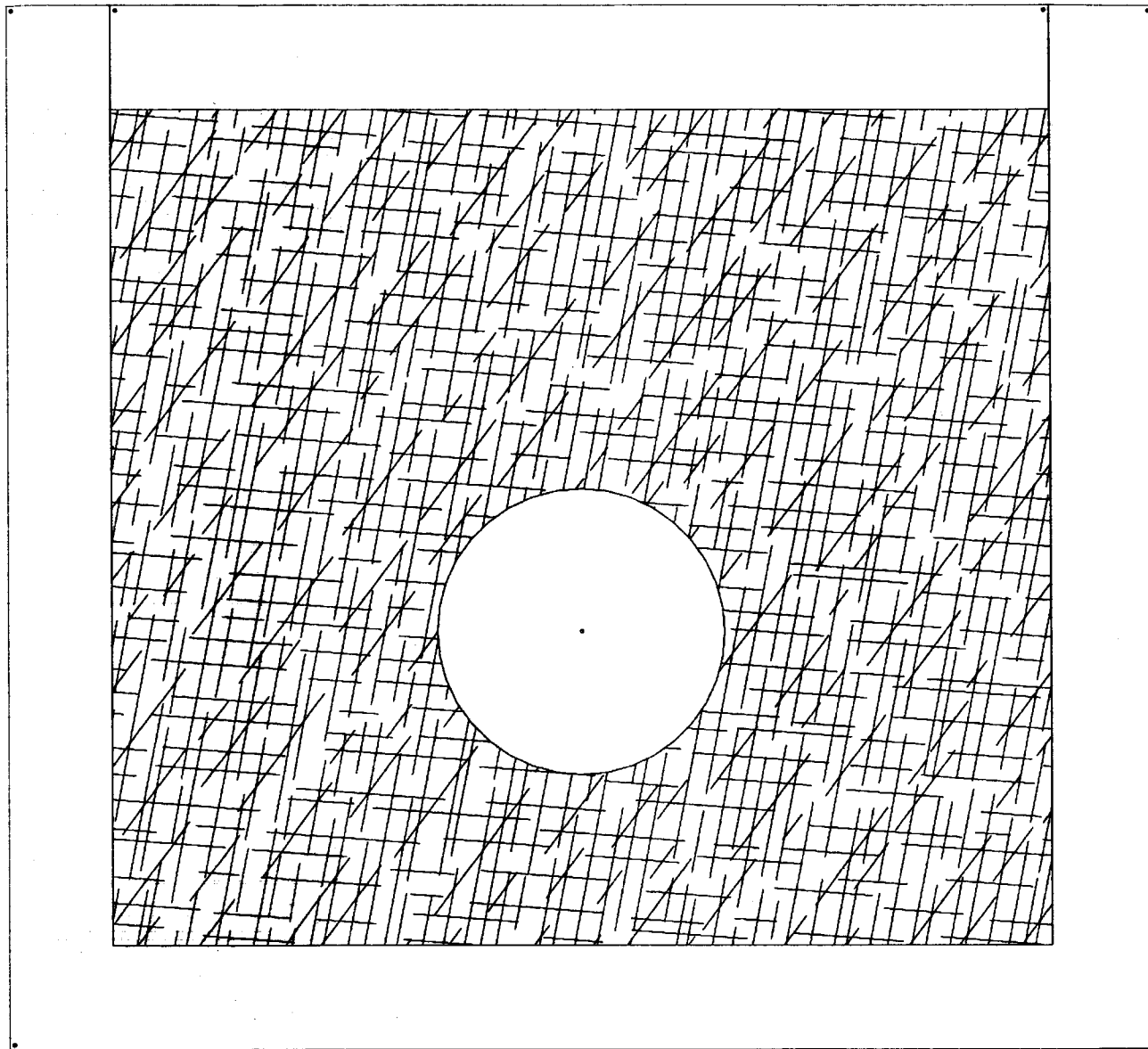


**Figure 3-3. Joint distribution for block mesh model 3**

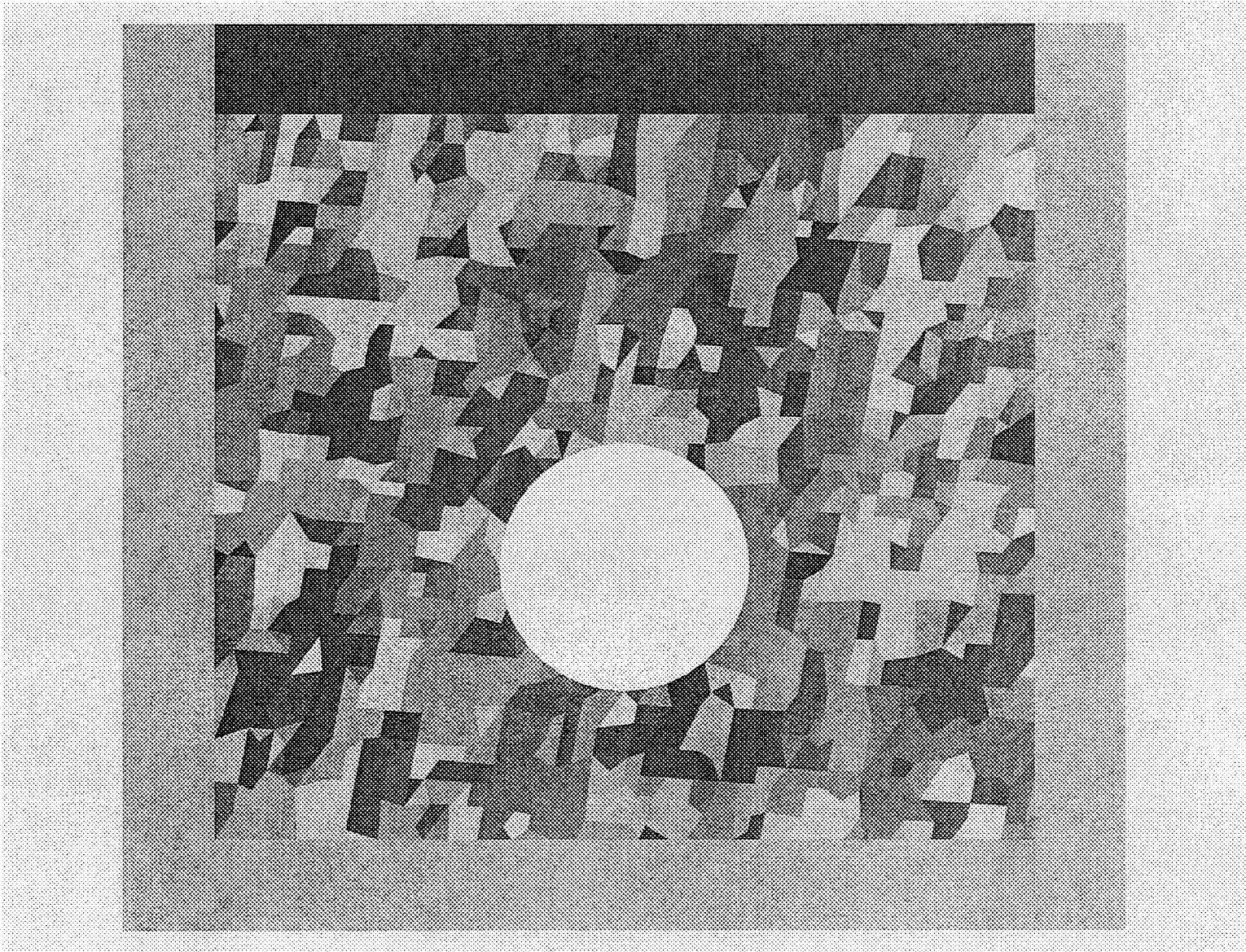


Figure 3-4. DDA block model 1

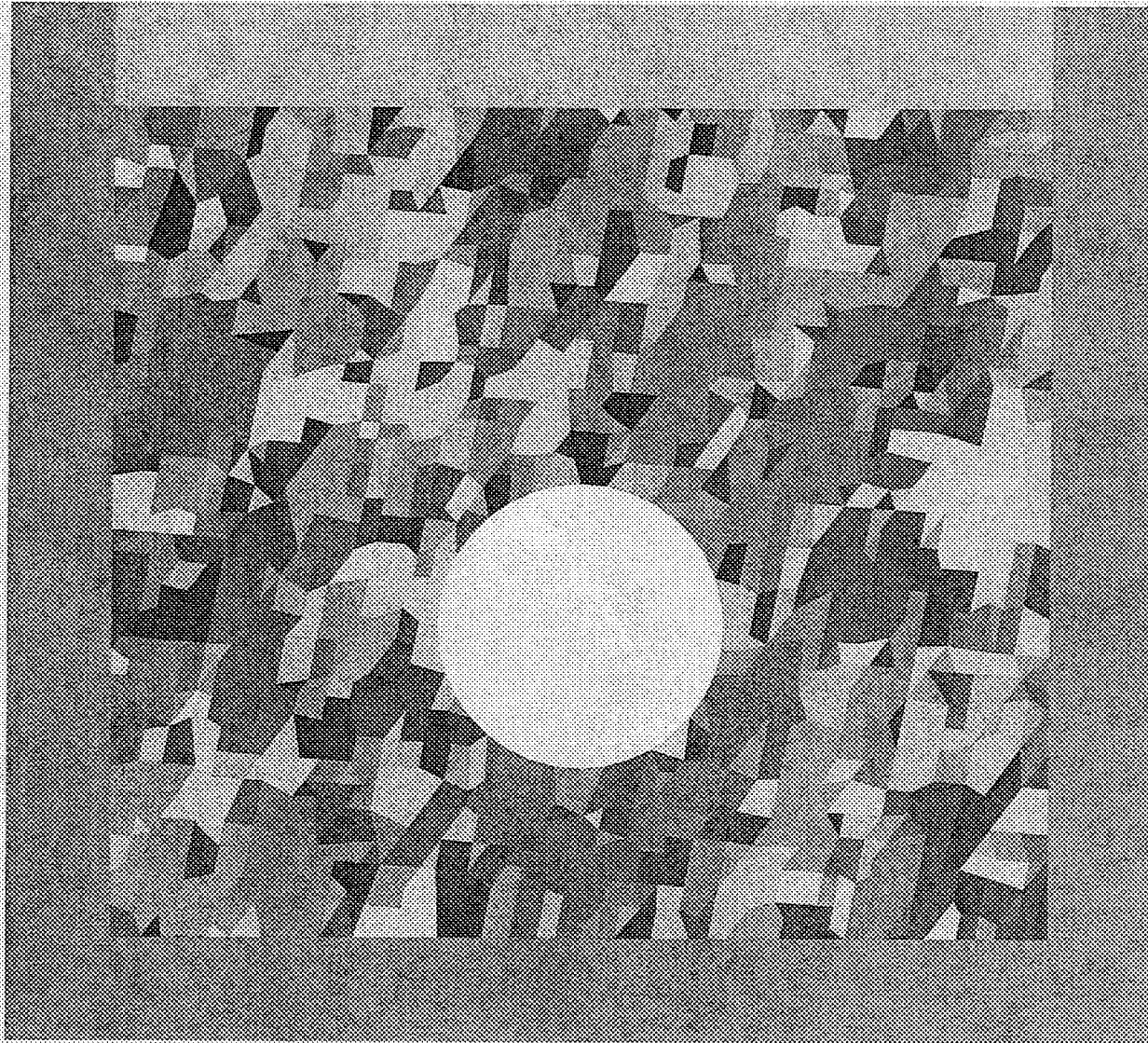


Figure 3-5. DDA block model 2

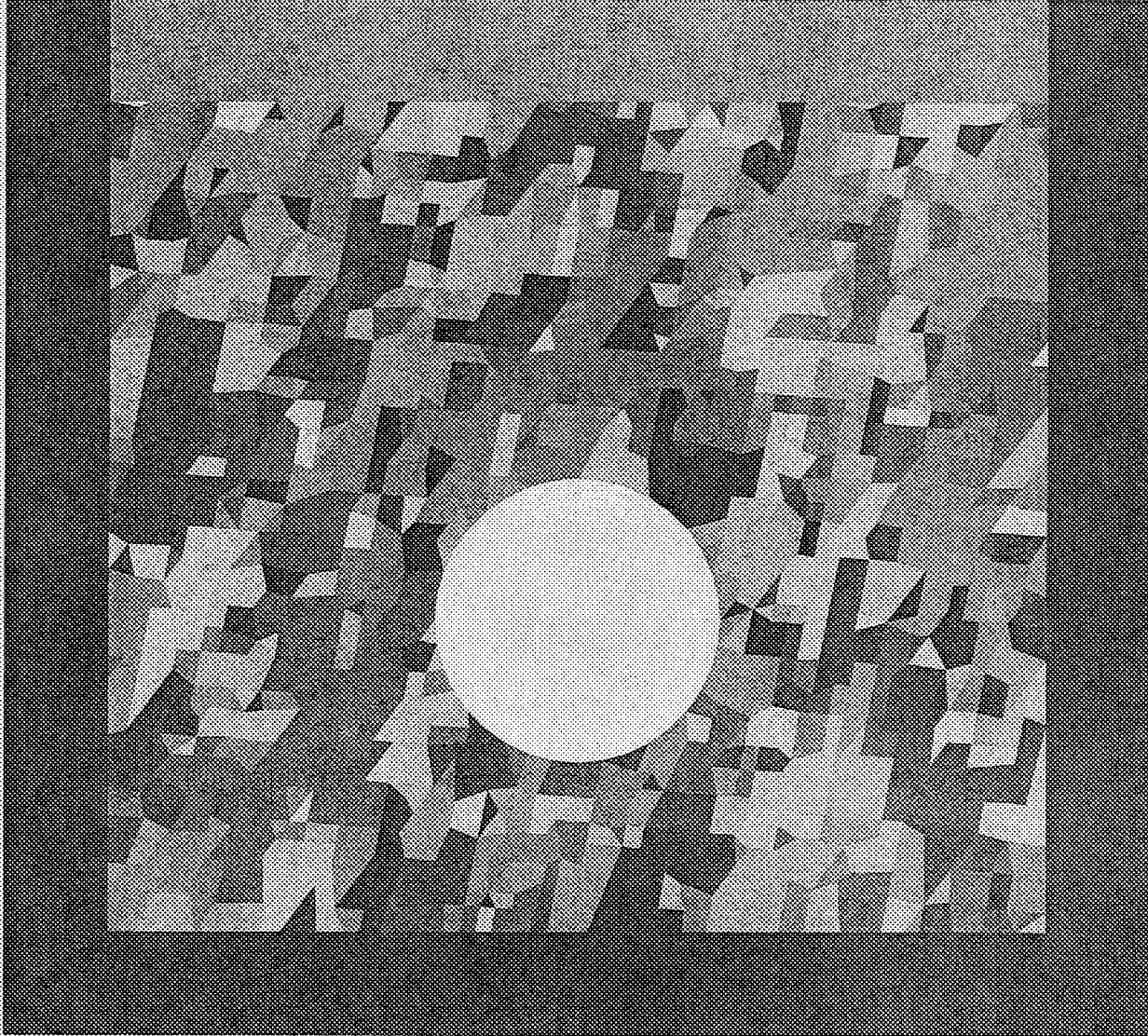
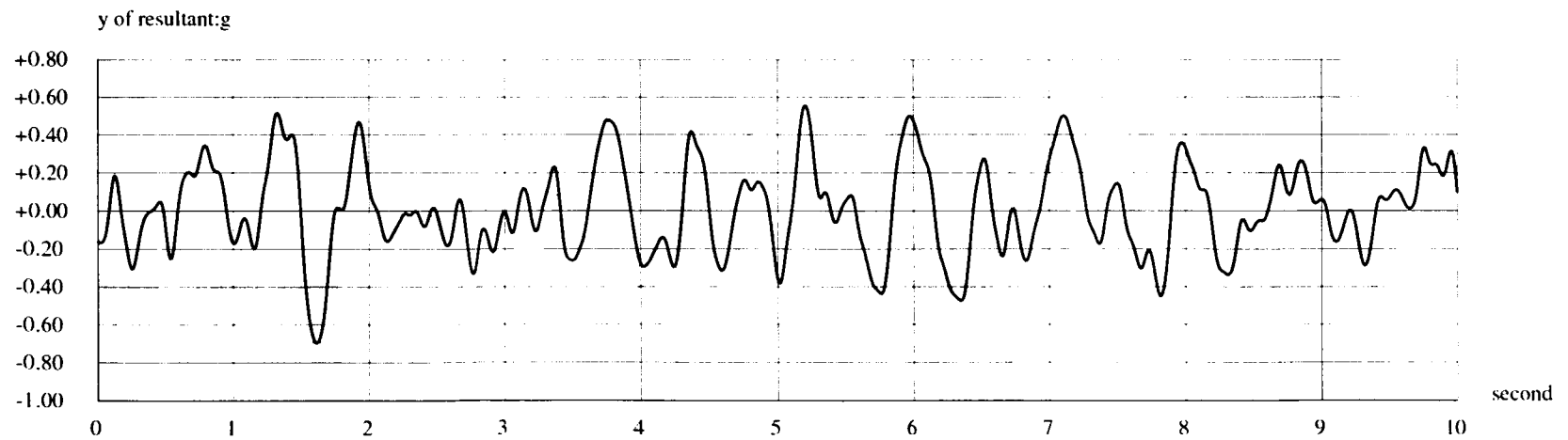
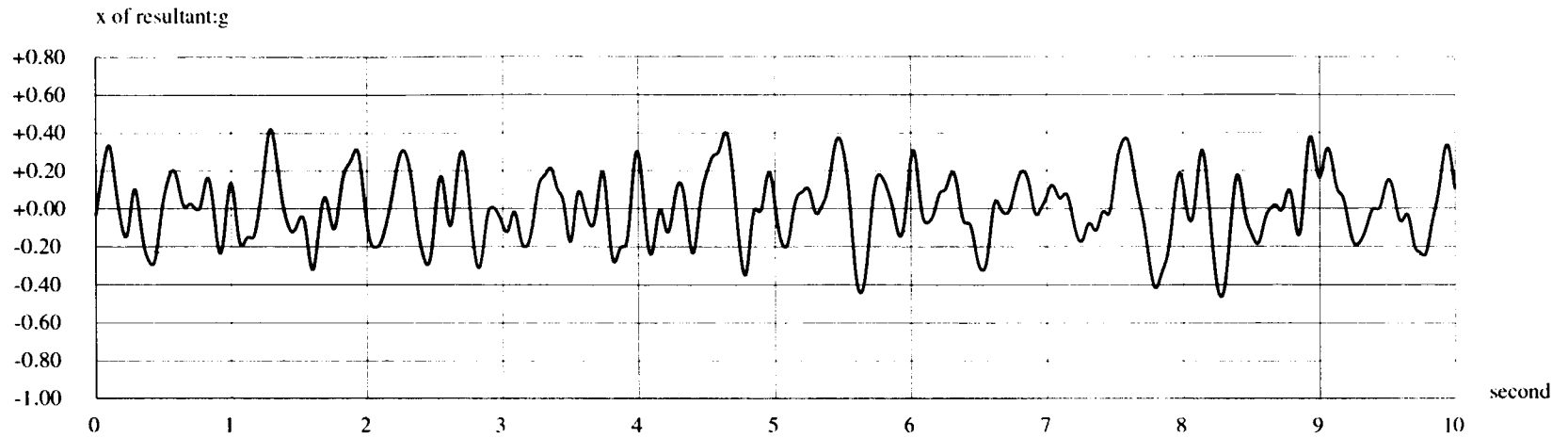


Figure 3-6. DDA block model 3



**Figure 3-7a. Components X and Y of earthquake accelerations**

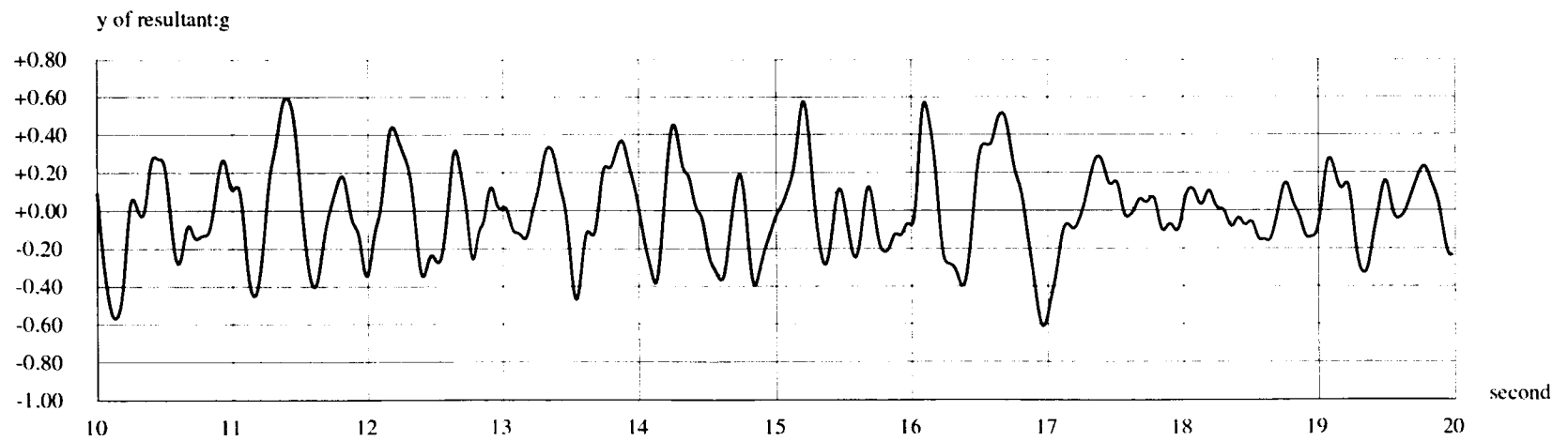
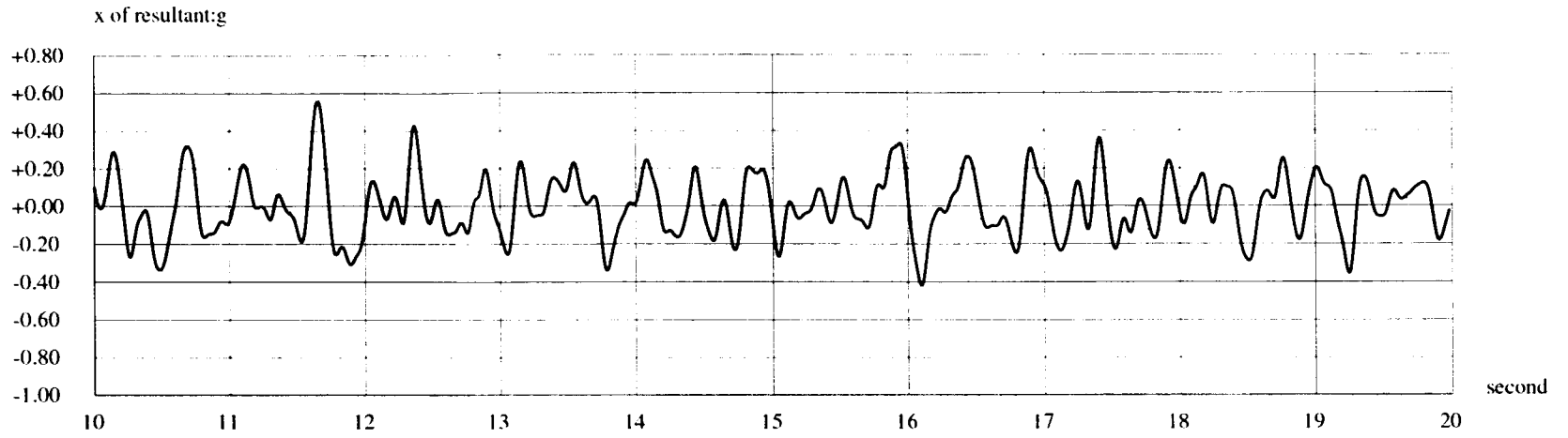


Figure 3-7b. Components X and Y of earthquake accelerations (cont'd)

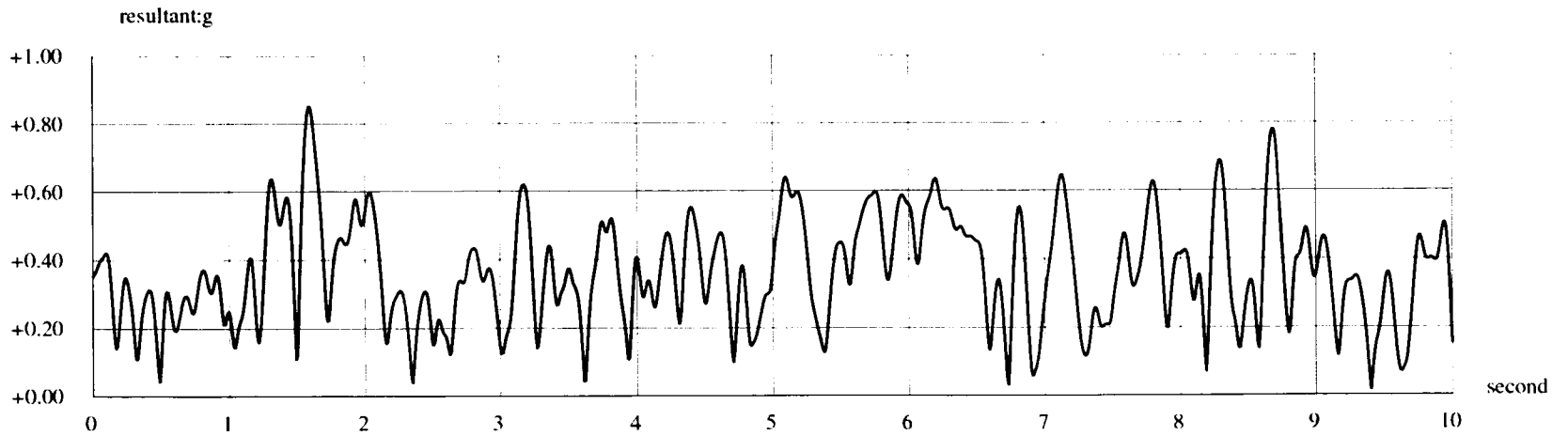
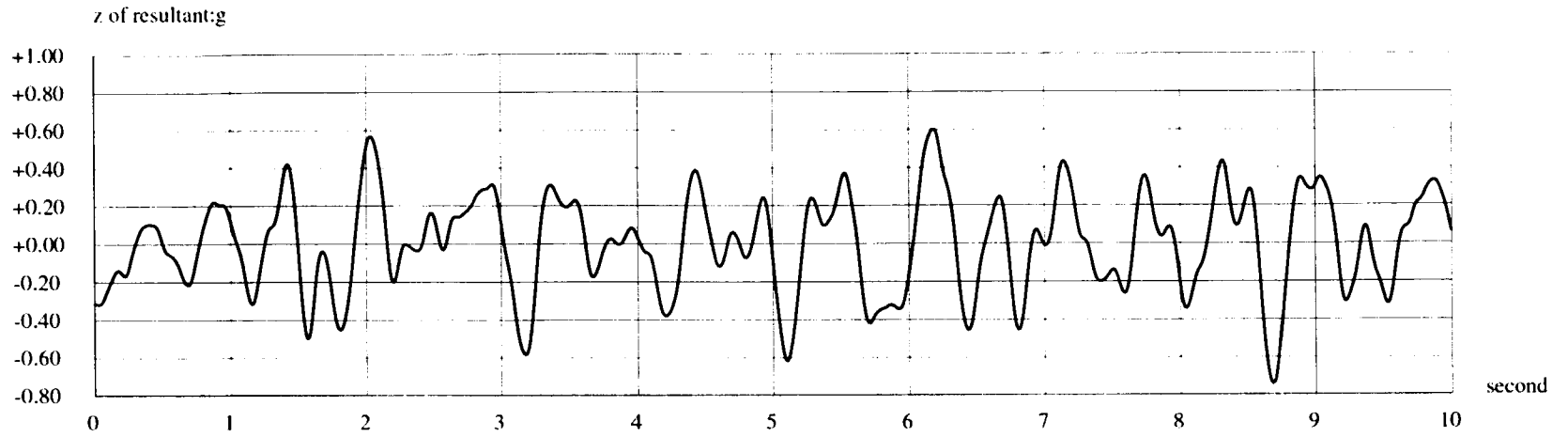


Figure 3-8a. Z component and resultant of earthquake accelerations

3-18

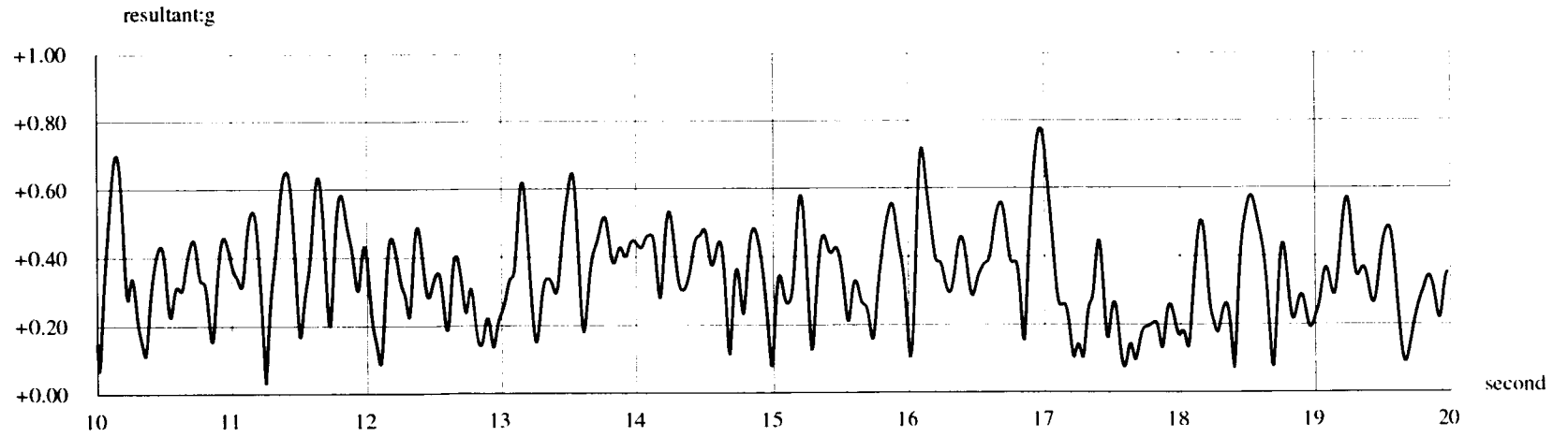
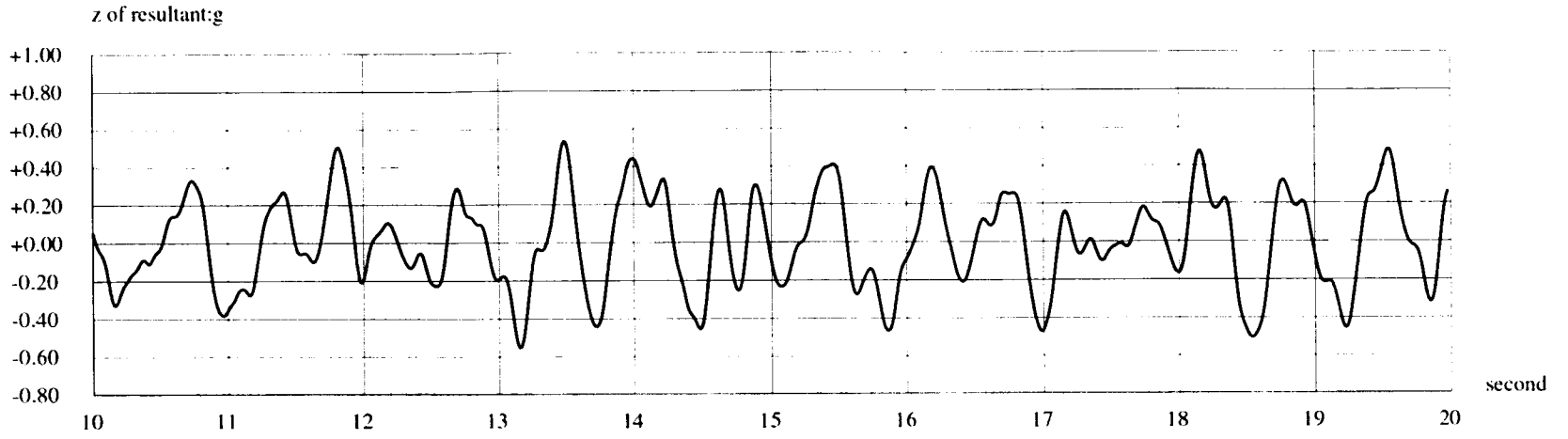


Figure 3-8b. Z component and resultant of earthquake accelerations (cont'd)

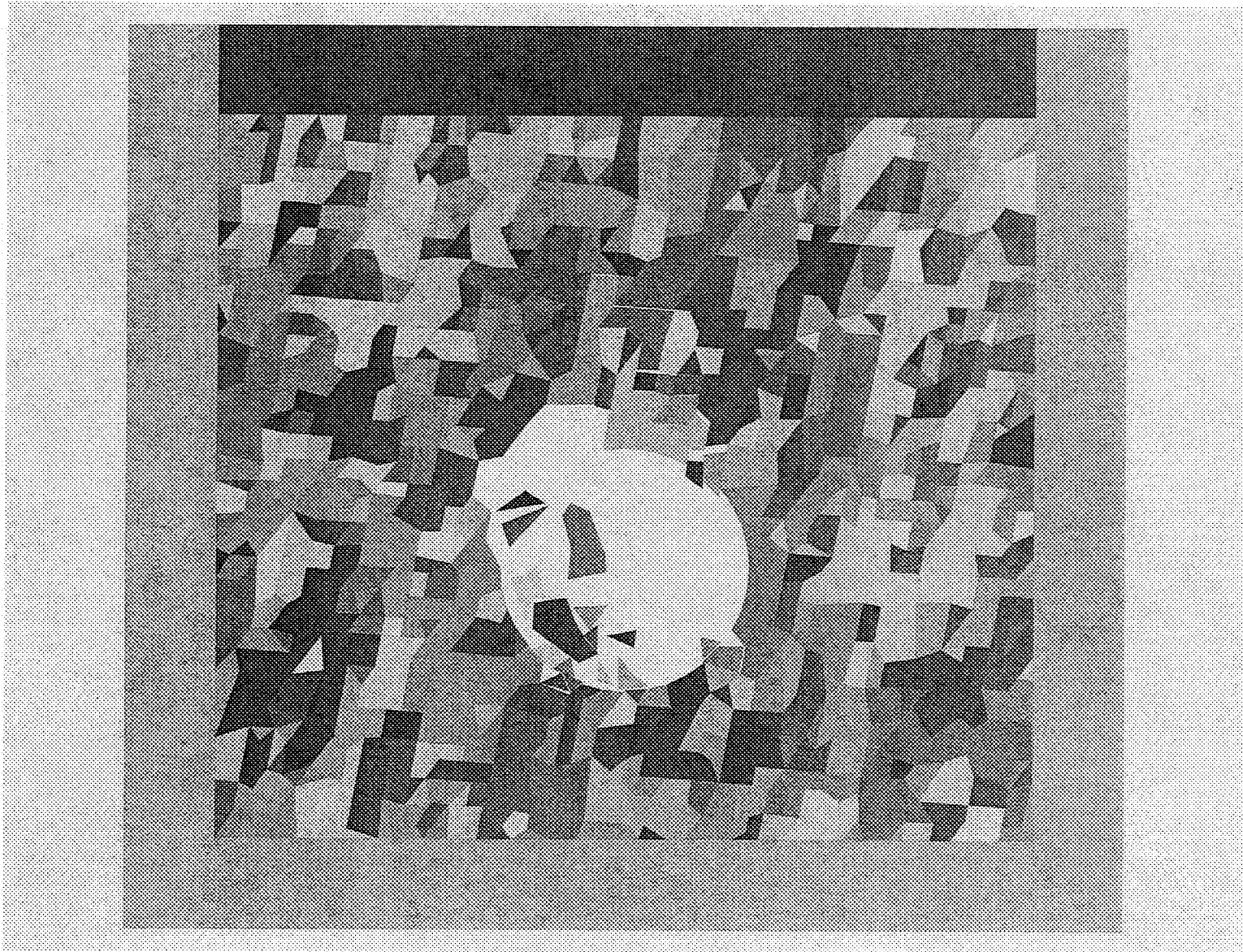


Figure 3-9. Effects of ground motion on rockfall after 1 s of shaking for DDA block model 1

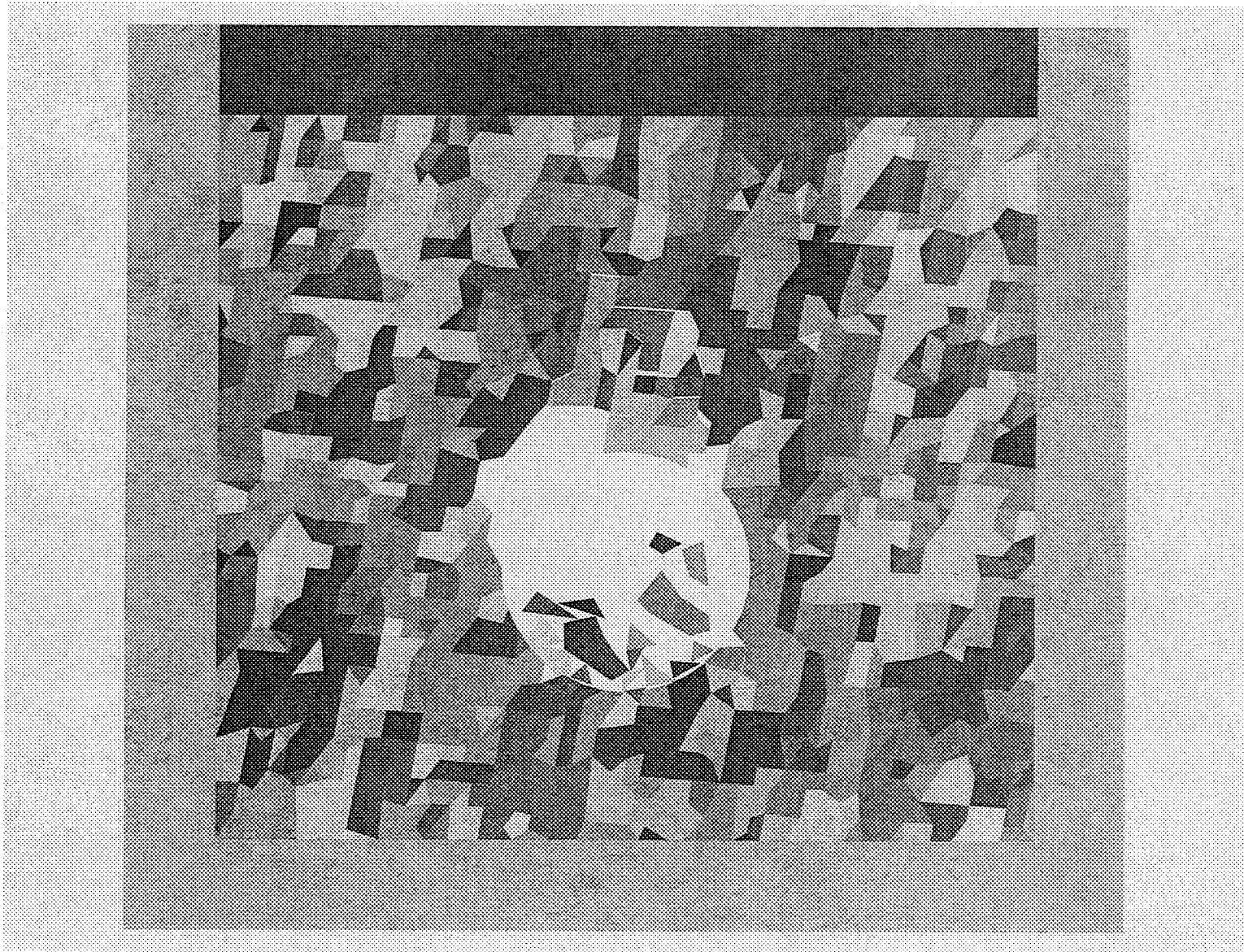


Figure 3-10. Effects of ground motion on rockfall after 2 s of shaking for DDA block model 1

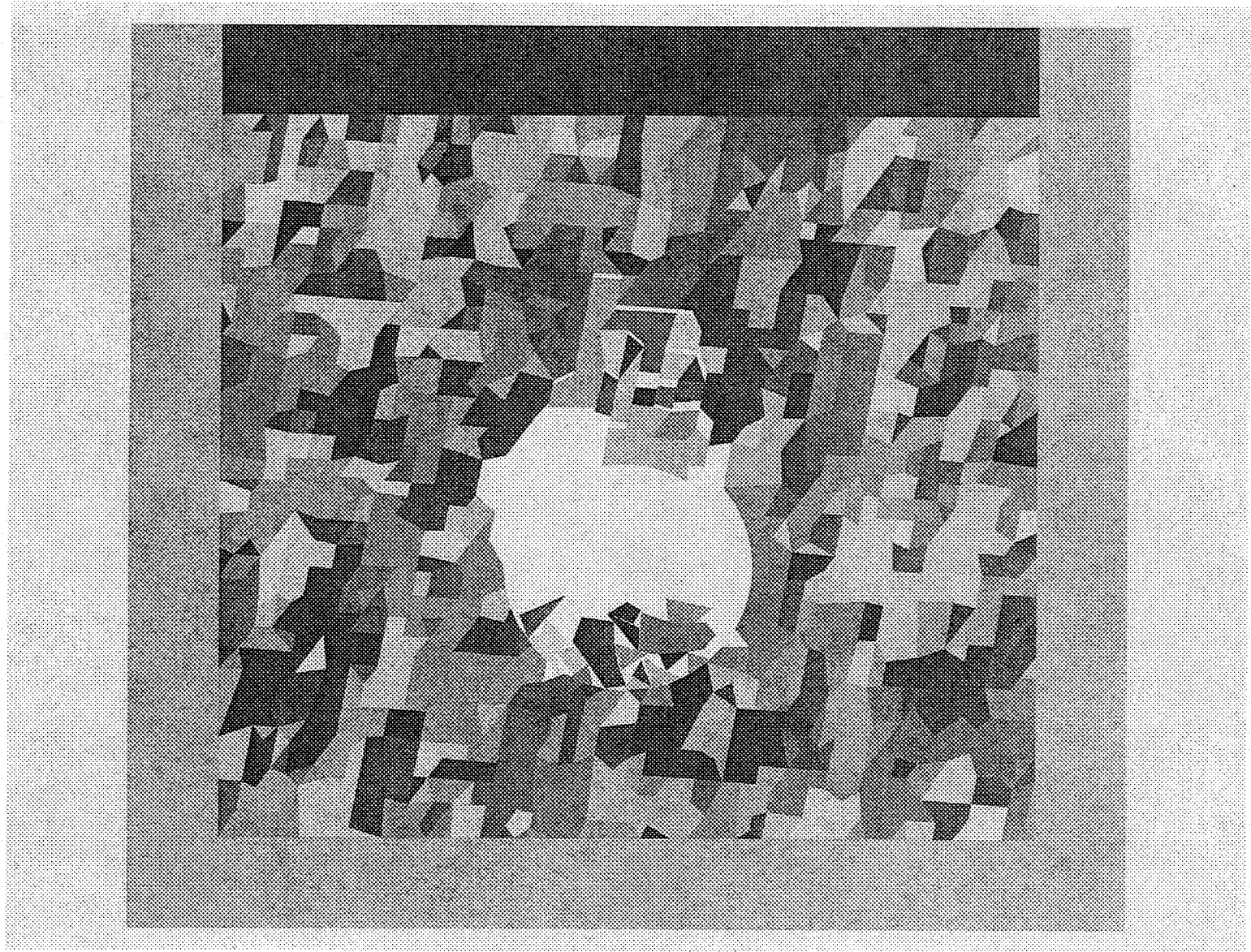


Figure 3-11. Effects of ground motion on rockfall after 5 s of shaking for DDA block model 1

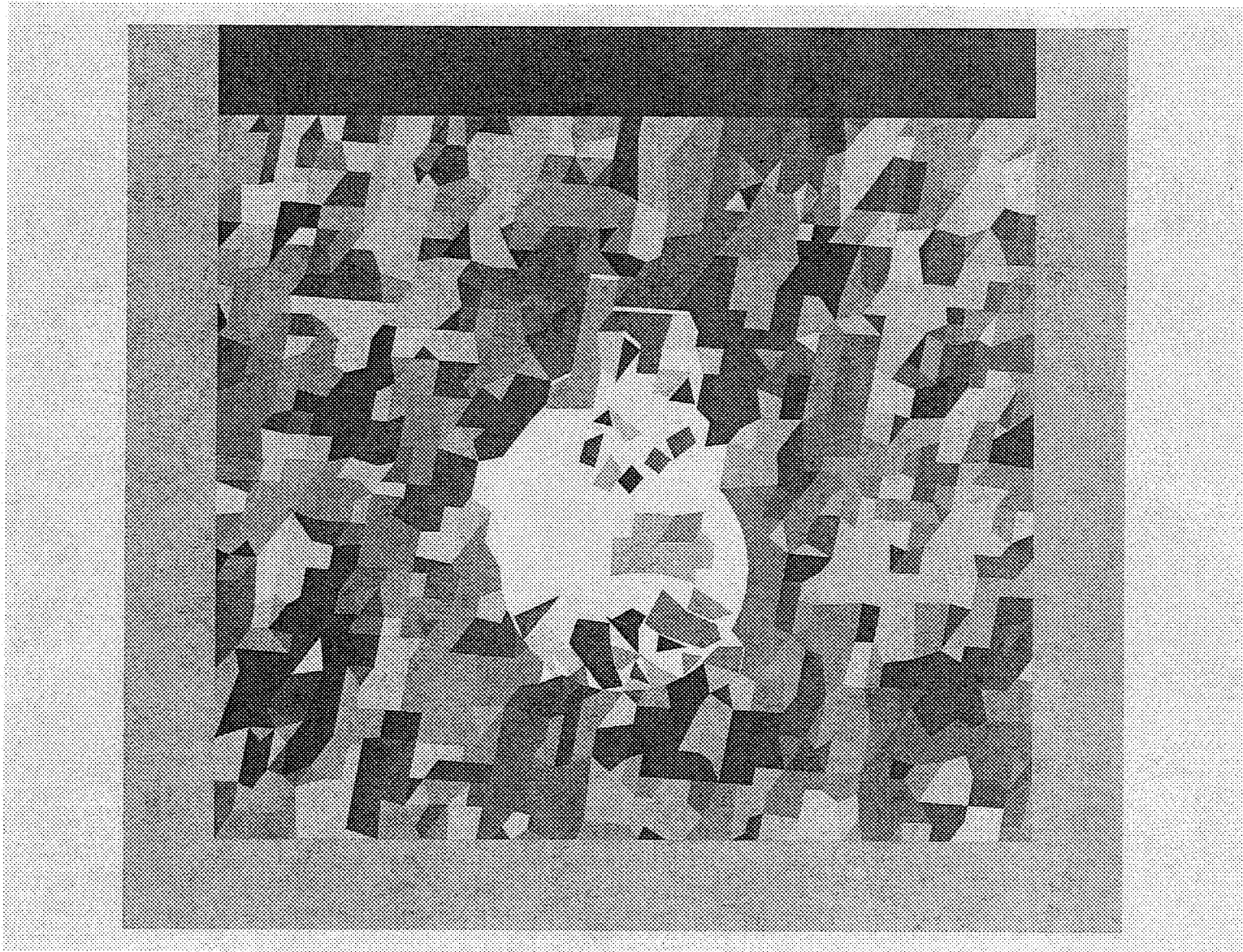


Figure 3-12. Effects of ground motion on rockfall after 6 s of shaking for DDA block model 1

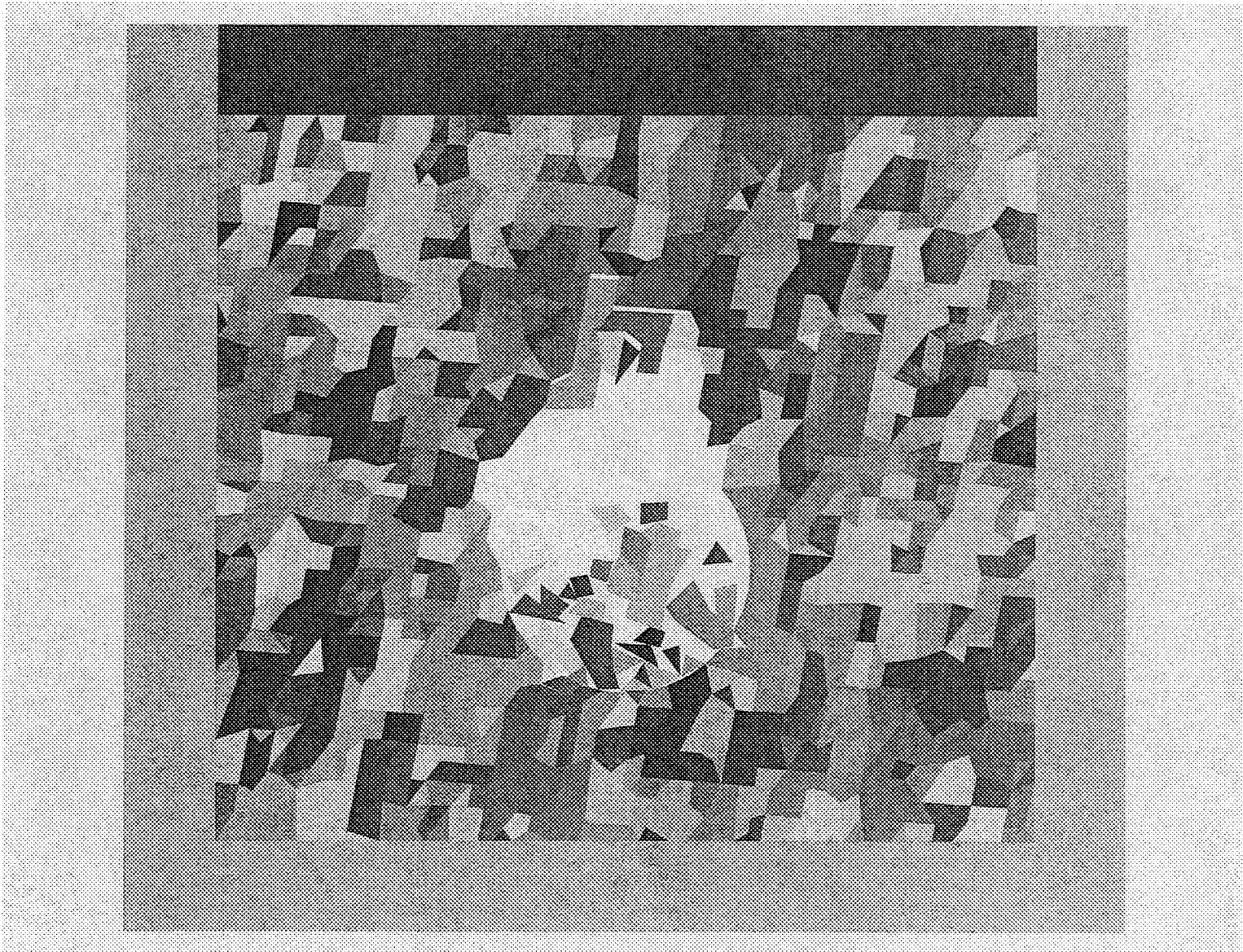


Figure 3-13. Effects of ground motion on rockfall after 7 s of shaking for DDA block model 1

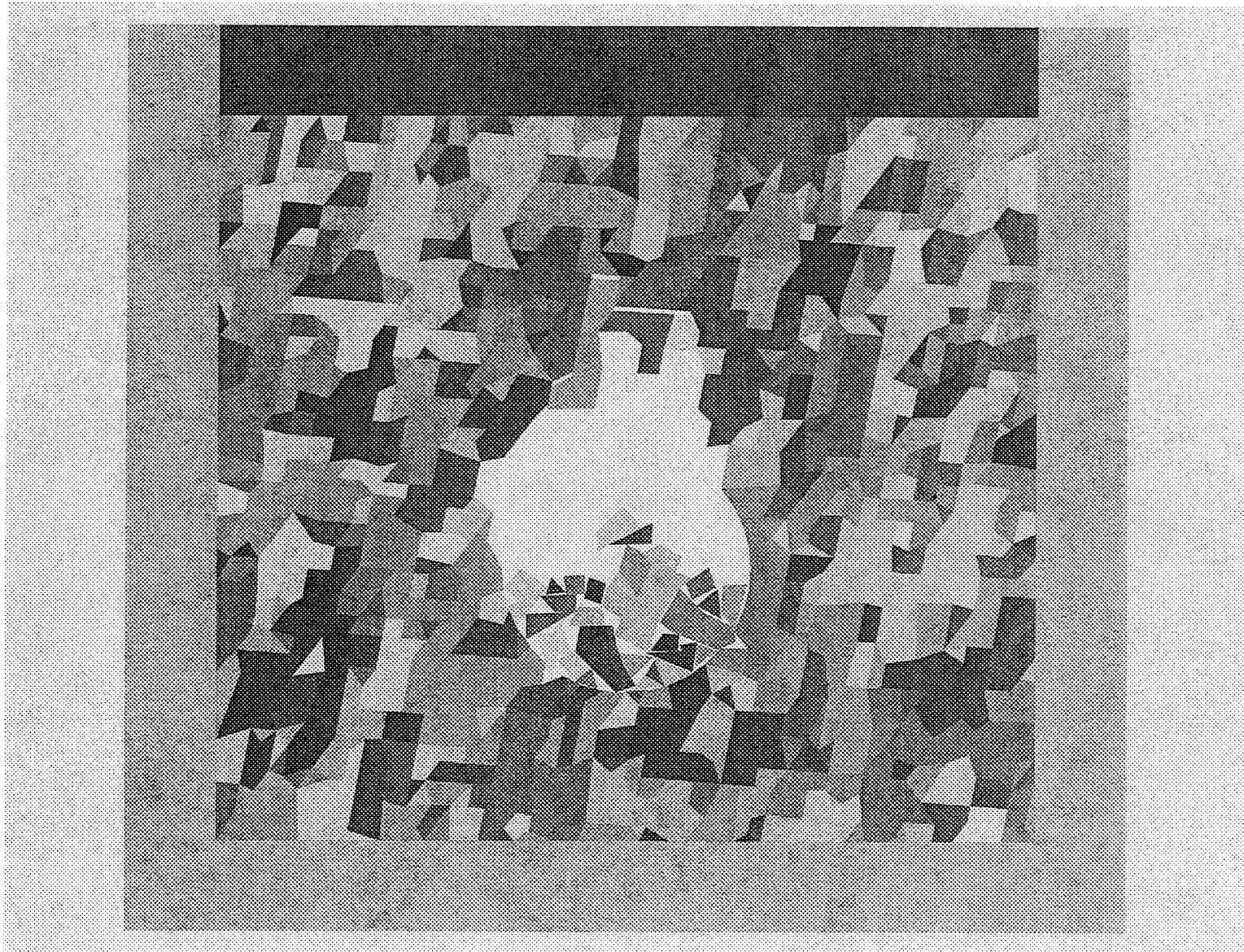


Figure 3-14. Effects of ground motion on rockfall after 16 s of shaking for DDA block model 1

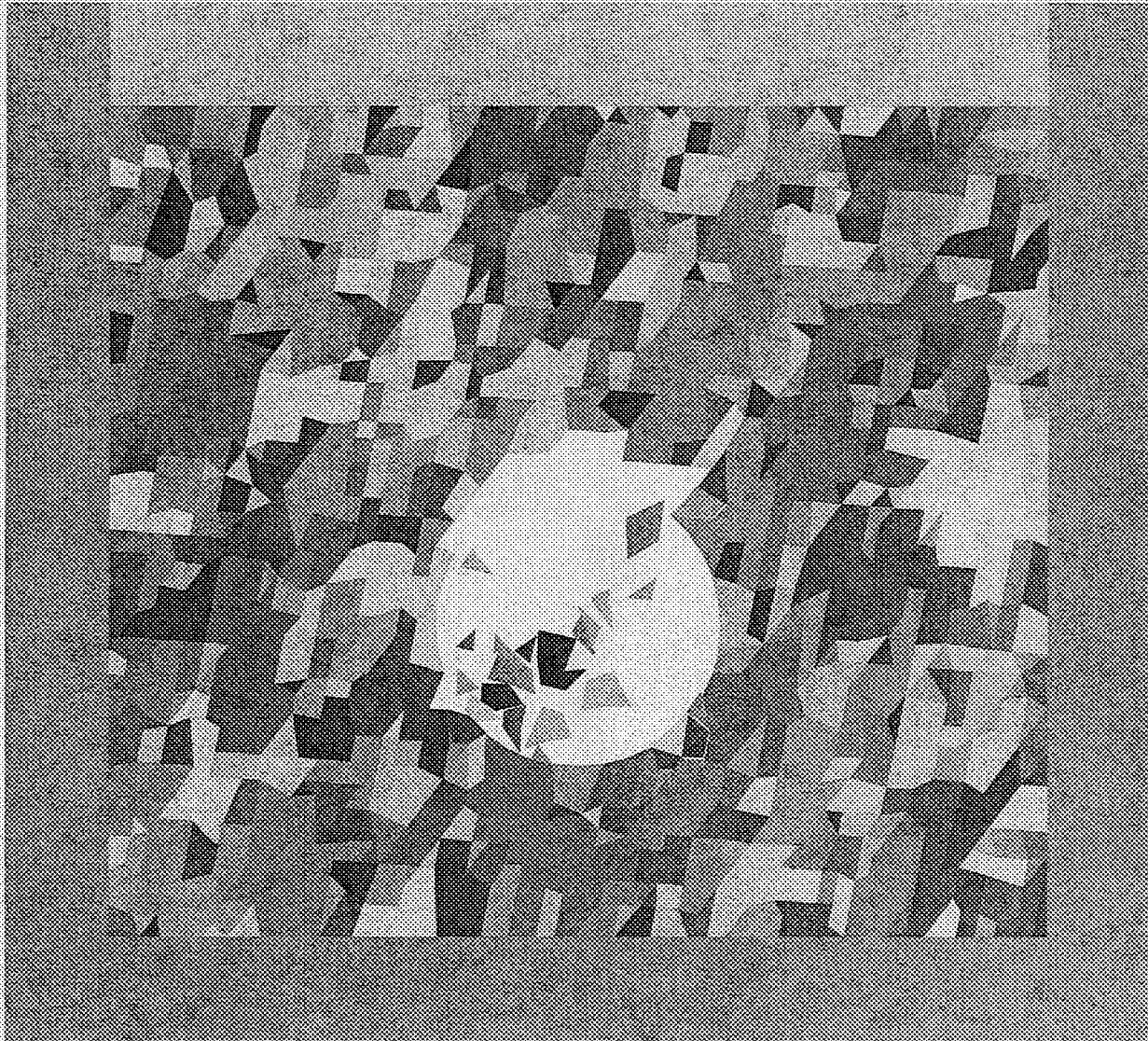


Figure 3-15. Effects of ground motion on rockfall after 1 s of shaking for DDA block model 2

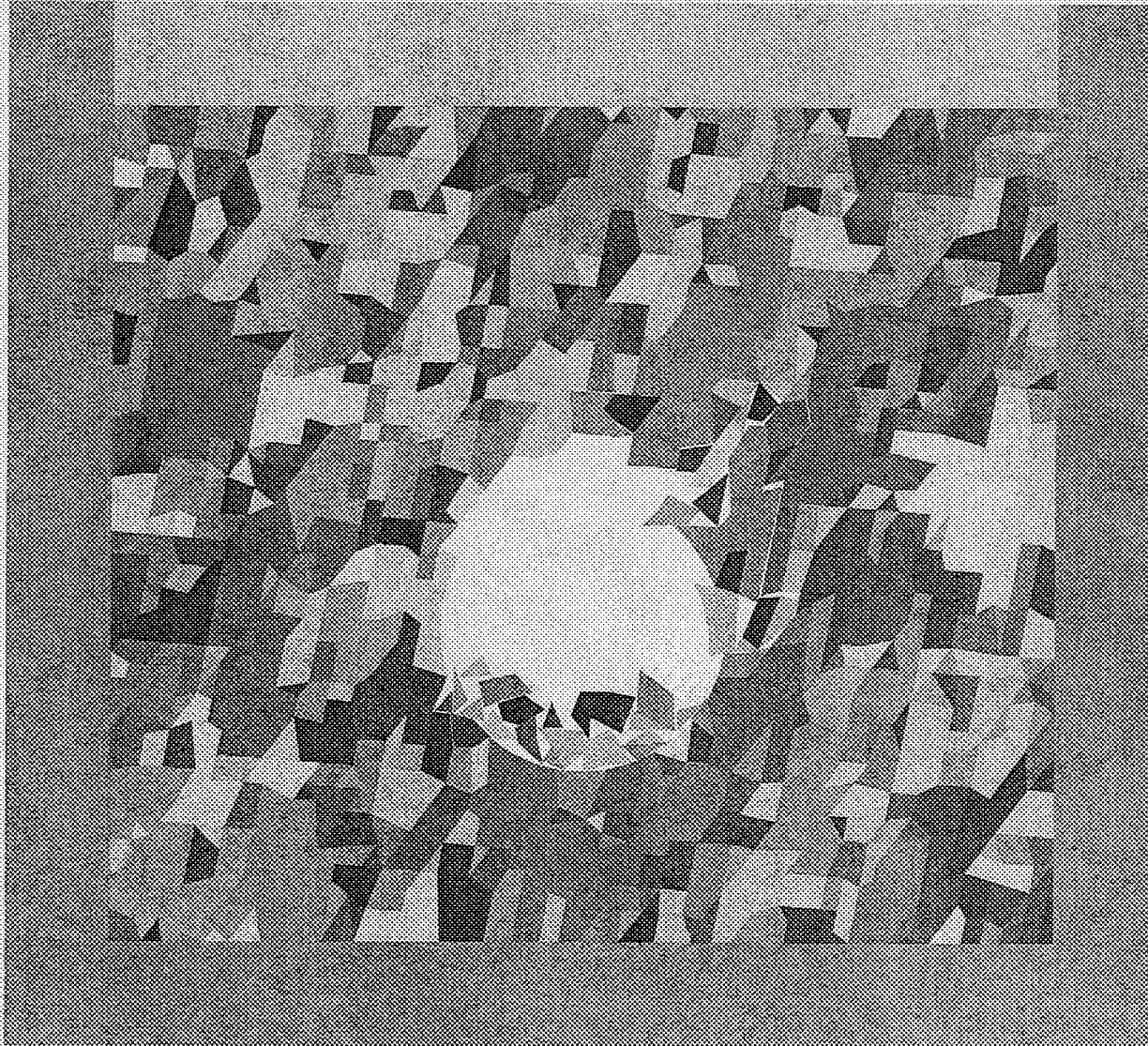


Figure 3-16. Effects of ground motion on rockfall after 4 s of shaking for DDA block model 2

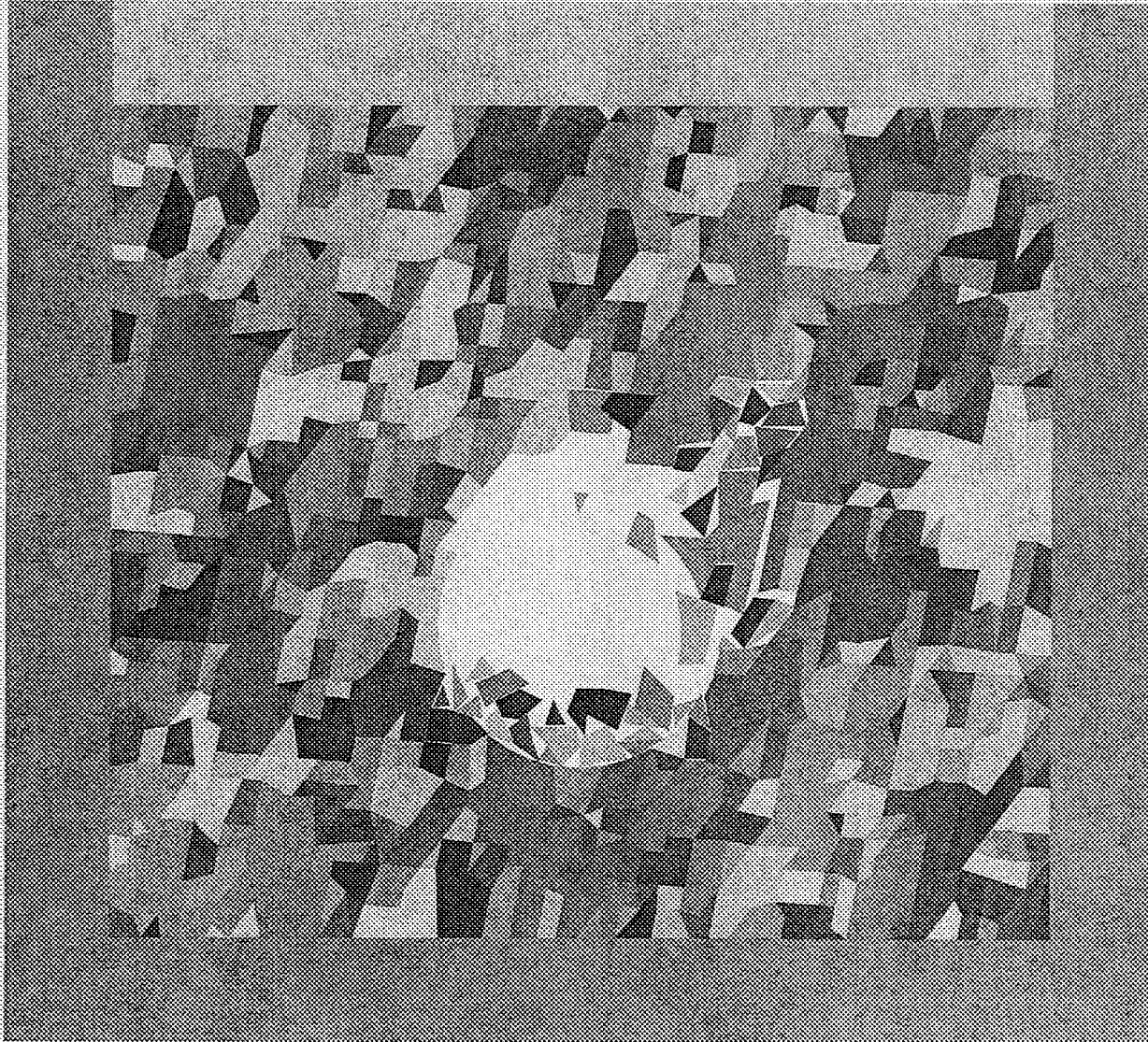


Figure 3-17. Effect of ground motion on rockfall after 5 s of shaking for DDA block model 2

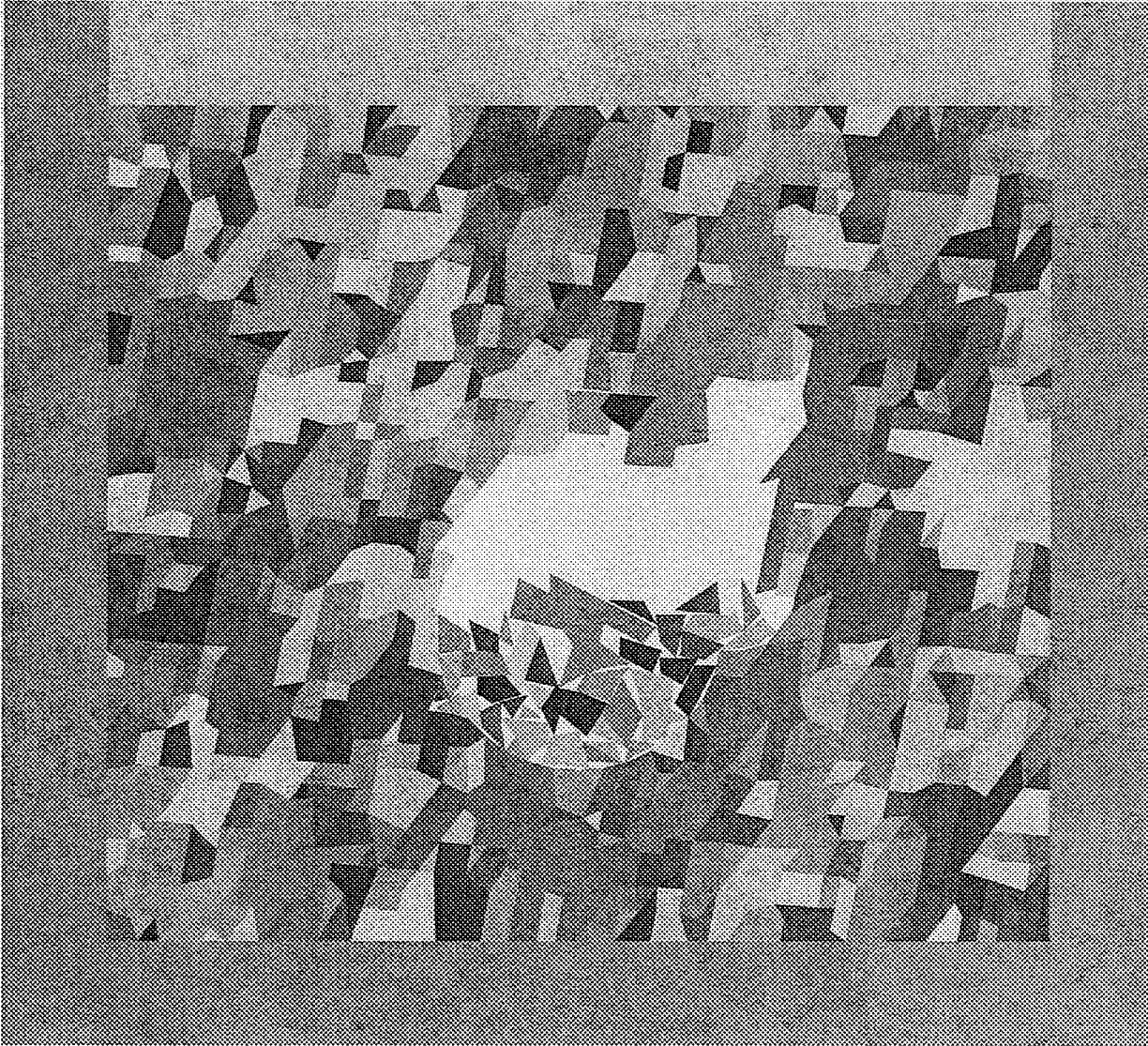


Figure 3-18. Emplacement drift condition after ground motion for DDA model 2

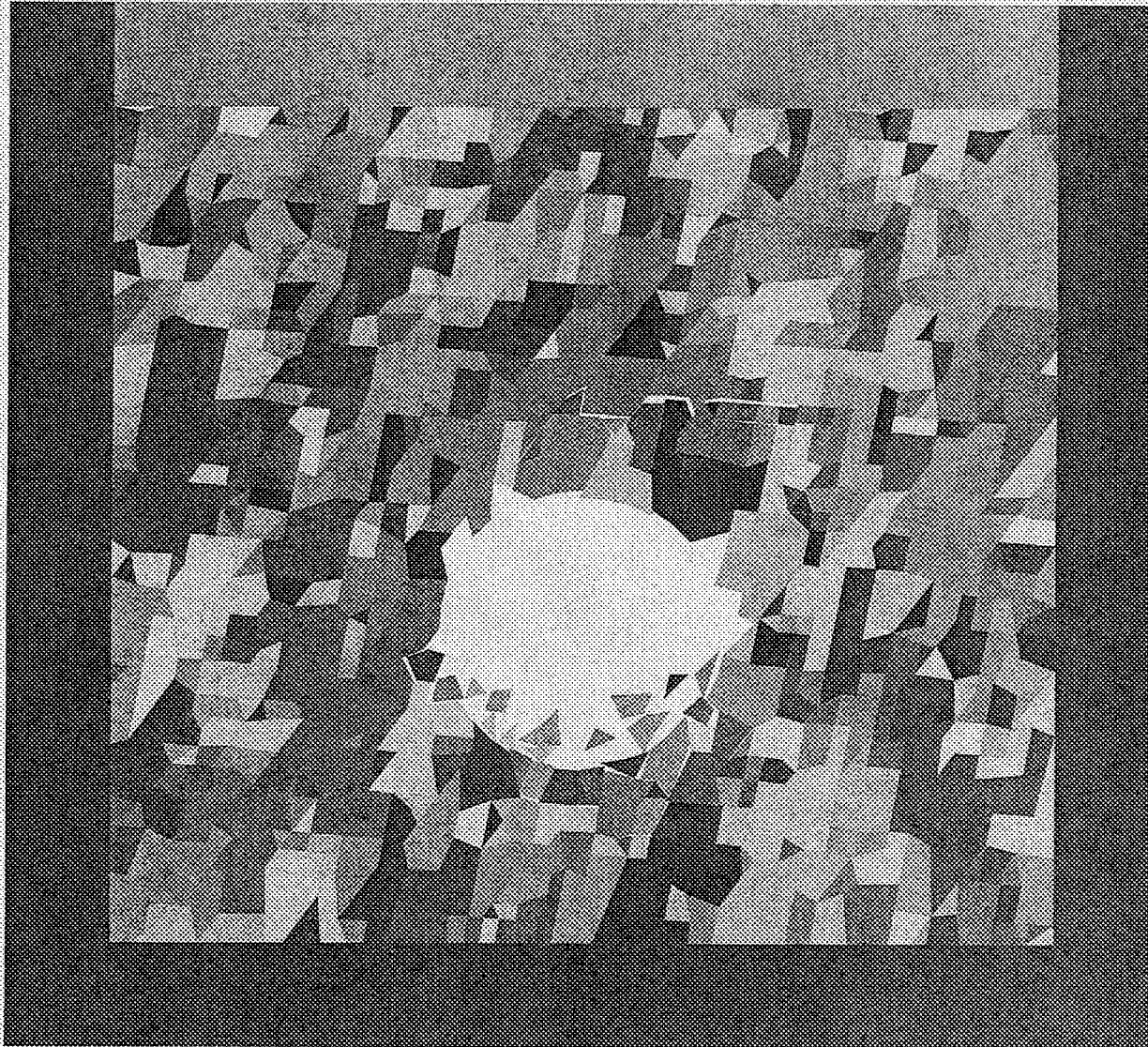


Figure 3-19. Effects of ground motion on rockfall after 1 s of shaking for DDA block model 3

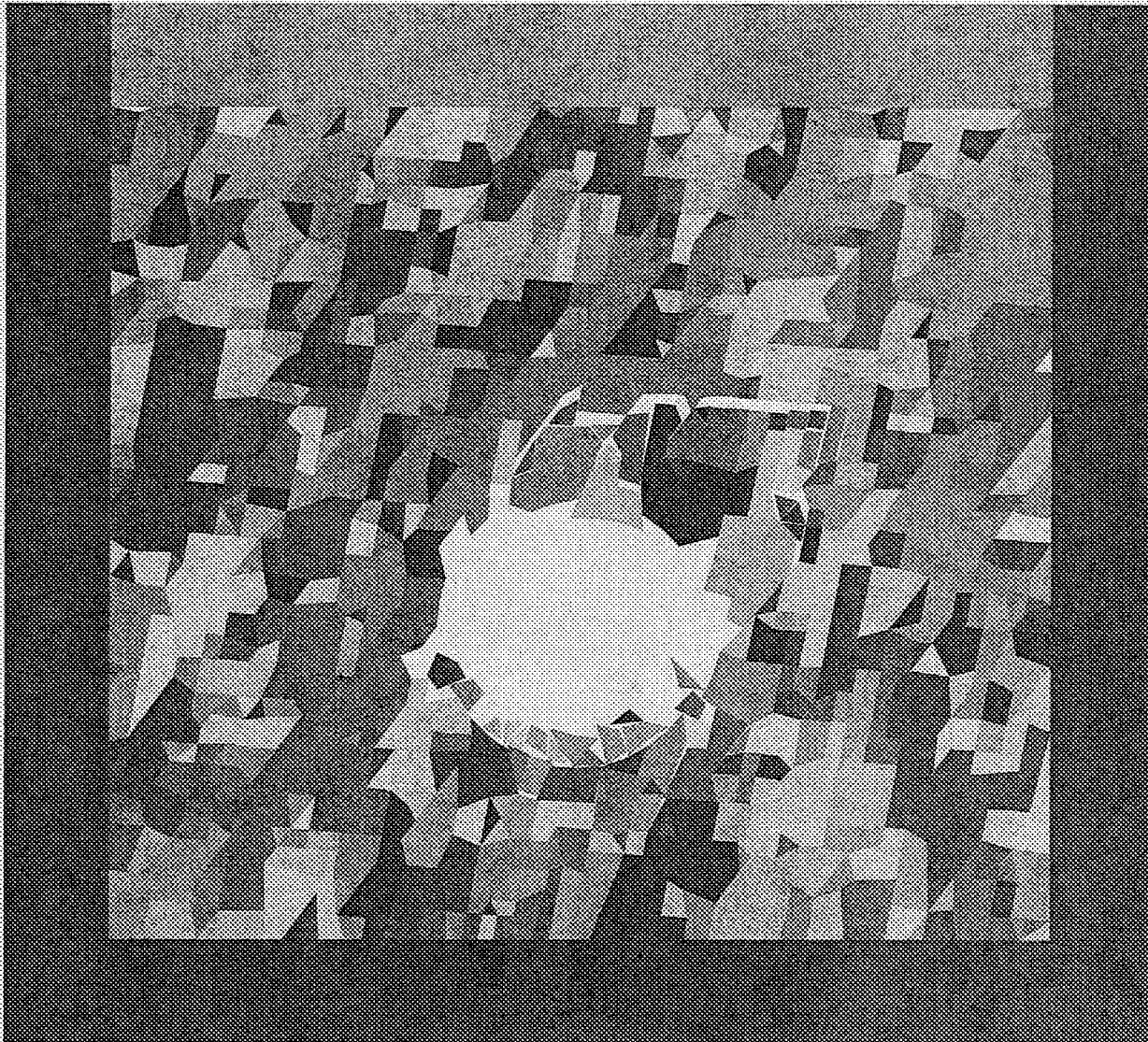


Figure 3-20. Effects of ground motion on rockfall after 2 s of shaking for DDA block model 3

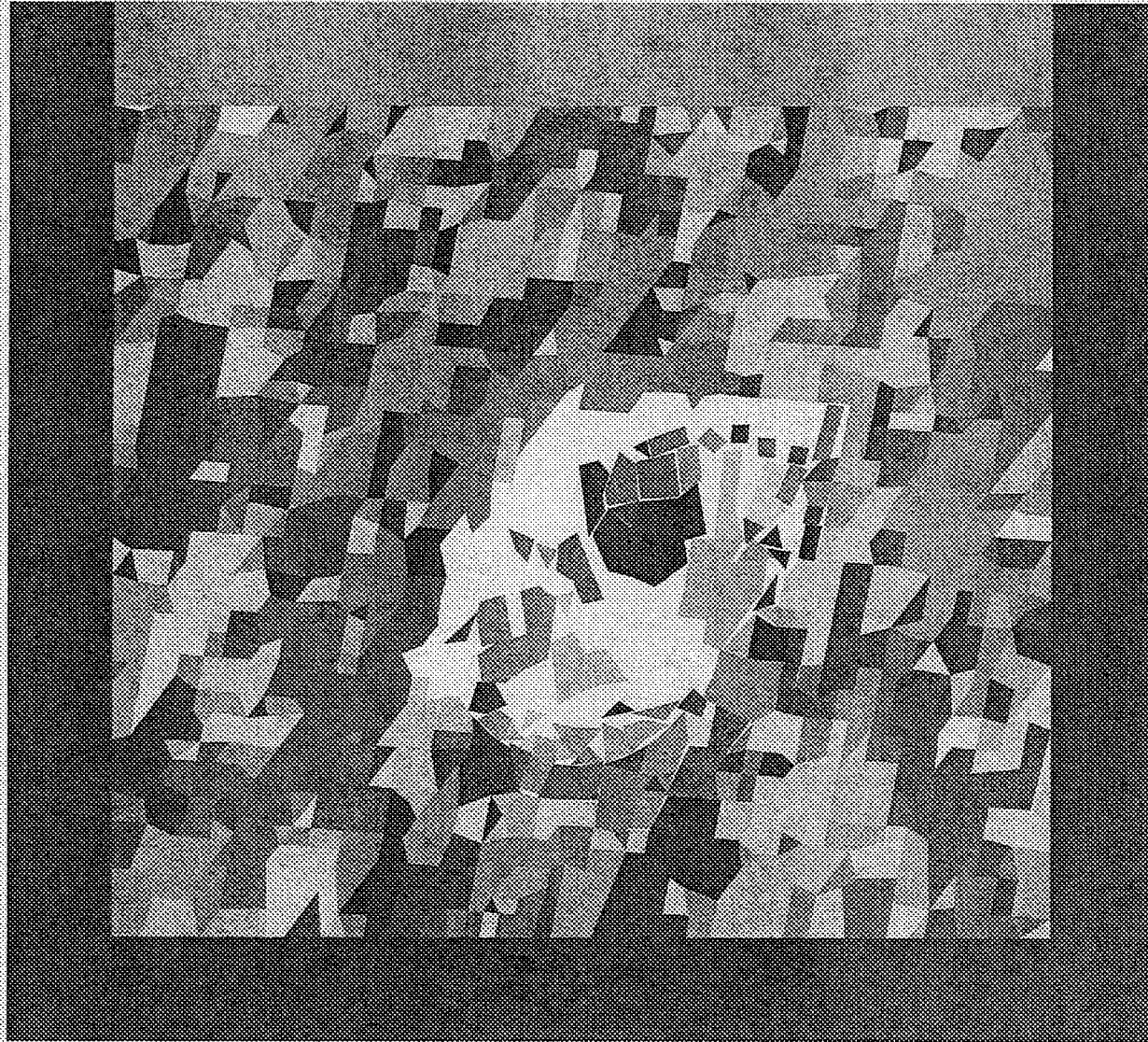


Figure 3-21. Effects of ground motion on rockfall after 3 s of shaking for DDA block model 3

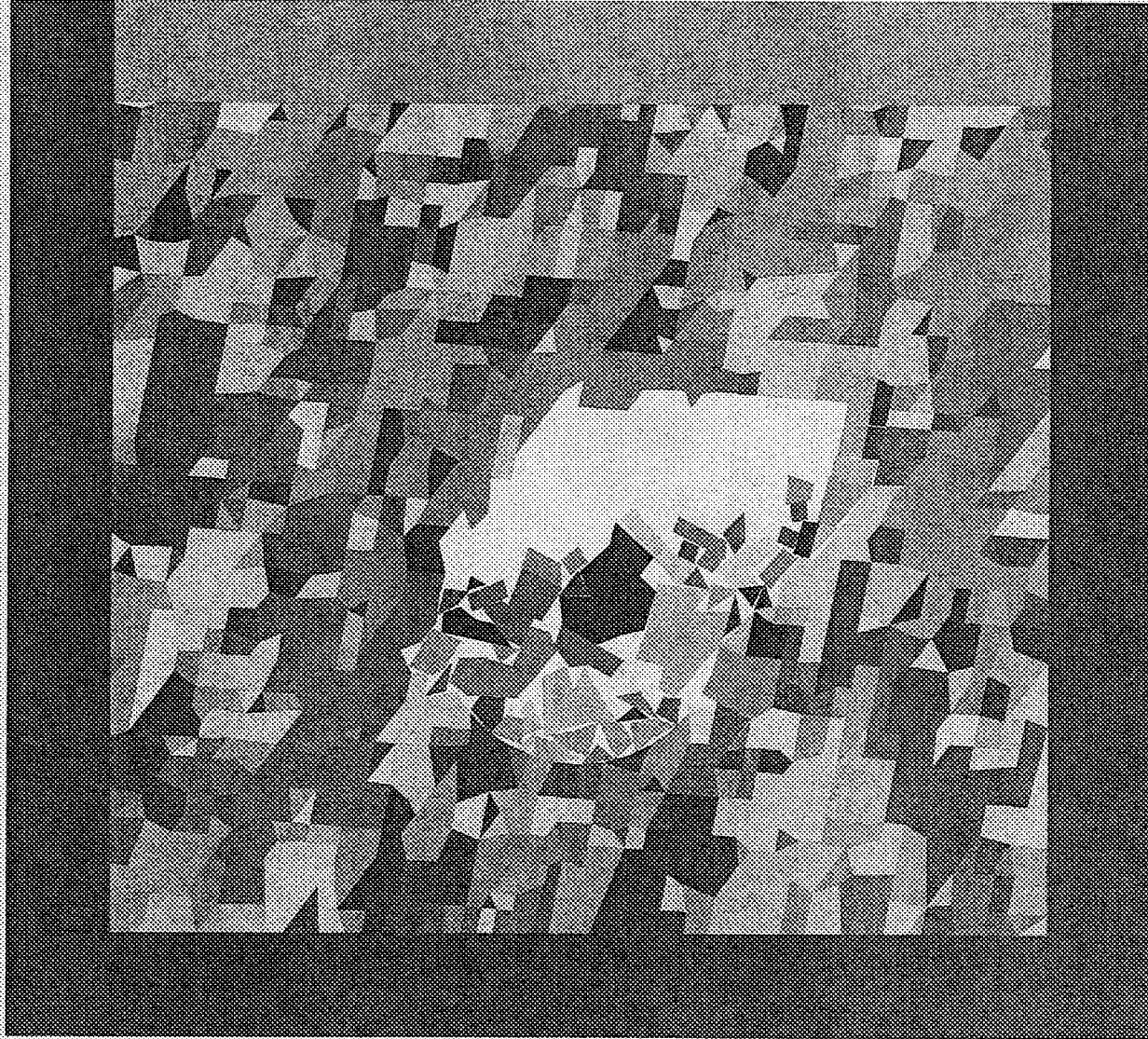


Figure 3-22. Effects of ground motion on rockfall after 6 s of shaking for DDA block model 3

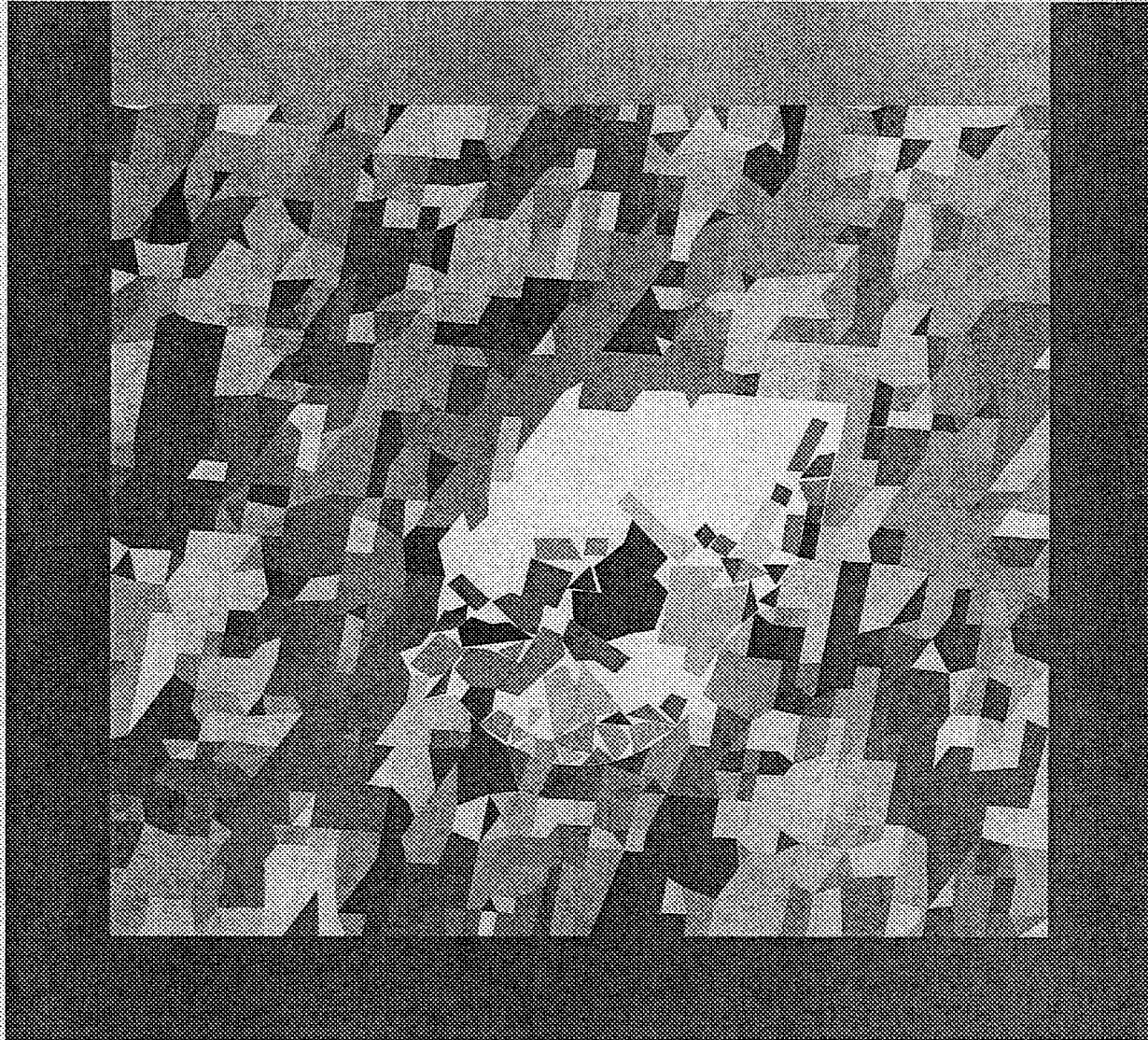


Figure 3-23. Effects of ground motion on rockfall after 4 s of shaking for DDA block model 3

## 4 SUMMARY

The seismically induced rockfall study attempts to develop relationships between the ground motions and rockfall potential and sizes, and assess how such rockfall may affect the emplacement drift geometry; this report documents the progress on addressing the two issues. The key block analysis was used to quantify unstable zones immediately after excavation. The study focused on TSw2 lower and upper lithophysal units. The 2D DDA computer code was used to evaluate rockfall induced by input ground motion for emplacement drifts located in TSw2 lower lithophysal unit. In both analyses, thermal load and long-term degradation of rock-mass including joint strength reduction and joint length growth are not included in this progress report. They will be considered in the future study.

Three major joint sets were used in the key block analysis for both TSw2 lower and upper lithophysal units. Eight JPs or zones of maximum key blocks were identified. All the key blocks of the same JP are in the same key block zone. Among the eight JPs for both TSw2 lower and upper lithophysal units, the key blocks located in JP=011 and JP=101 are liable to fall.

Based on the assumptions that the joint length for each joint set is sufficiently long and the joint spacing for each joint set is sufficiently small, the maximum possible key blocks for JP=011 and JP=101 were determined for both rock units. Any of the actual key blocks in a JP cannot be bigger than the maximum possible key block of that JP. The actual key blocks may be smaller if the joints have limited length and large spacing. The maximum possible key blocks sizes identified are relatively small. The largest size estimated is about 1.06 m<sup>3</sup>. The sliding surfaces for the JPs that are liable to fall are either along joint set 1 or 2. Given that joint sets 1 and 2 are near vertical for both rock units, relatively small resistance is available between joint interfaces to prevent rockfall.

Since the joint data are often developed based on joint trace mappings directly from the surface of an excavation, it is difficult to determine the persistency of a joint. The key block analysis assumed that the joints having traces on the surface of an excavation can extend sufficiently so that rock blocks can form through the intersections of these joints. Based on this assumption, the percentage of the key block traced areas to the emplacement drift surface area can be determined using the key block analysis. The combined key block areas for JP=011 and JP=101 on the emplacement drift wall are about 2.94 and 4.45 percent of the entire drift surface area for the TSw2 lower and upper lithophysal units, respectively. From the perspective of drift length affected, key blocks appear quite frequently on the top walls of both sides of the emplacement drift. Rockfall due to key blocks is a likely event throughout the entire emplacement drift. Most of these key blocks are expected to be small in size.

In analyzing seismically induced rockfall in the emplacement drifts, three DDA block models were constructed using the same joint information with a slight variation in joint spacing. The first rockfall took place at an early stage of the ground acceleration for all three models; before the first second of shaking for DDA block models 1 and 2, and between 1 and 2 s for DDA model 3. Compared to DDA block models 1 and 2, the rockfall with DDA block model 3 was massive. The second rockfall developed several seconds into the ground motion for DDA block models 1 and 2, and no further rockfall was observed for DDA block model 3.

The major rockfalls for DDA block models 1, 2, and 3 were completed before the first 6 s of ground motion. Within this time period, the maximum local peak ground acceleration was about 0.85 g. No further major rockfall occurred throughout the rest of the ground motion for any of the DDA block models, even if the models experienced several additional 0.6 and 0.7 g ground motions. The reason for no further rockfall may be because the remaining rock blocks are geometrically more stable. Further rockfall may still be possible if long-term deterioration of the associated joint and rock strength takes place or, perhaps, through repeated ground motions of similar magnitude to the one simulated in this analysis, or a ground motion with a

maximum acceleration greater than 0.85 g. After the massive rockfall, DDA block model 3 appears to be more stable compared to the other two.

The phenomenon of multiple rock blocks falling in unison appear to be possible, although these events may not be frequent. The limiting factor is the constraints associated with the block geometry that cause rock blocks to rotate and bump into each other. These situations tend to eliminate the potential for multiple rock blocks to fall in unison.

The final geometry of the emplacement drift after collapse appears to be quite different for the three models. However, it is not clear how these complex geometries will affect water dripping into the emplacement drifts.

## 5 FUTURE WORK

As discussed earlier, the main objectives of the rockfall study are to (i) develop relationships between the magnitude of ground motions and size of rockfall, and ground motions and areal coverage of rockfall in the emplacement drifts; and (ii) assessment of the potential change in drift geometry. The results from the first item will be used as input to the SEISMO module for the NRC TPA code and the results from the second item will be provided as input to investigate its effects on water seepage into emplacement drifts. The five activities identified in section 1.2 (also listed below) will continue in the next phase of the study using the approach described in section 3.

- Quantify sizes and areal coverage of key blocks in the emplacement drifts
- Determine size distribution of rockfalls subjected to various levels of ground motions
- Determine areal coverage of rockfalls subjected to various levels of ground motions
- Estimate the potential for multiple rock blocks to fall in unison
- Estimate changes in geometry under various levels of ground motions

Quantifying sizes and areal coverage of key blocks in the emplacement drifts is completed for the TSw2 lower and upper lithophysal units. The same work will be performed for the TSw2 middle non-lithophysal unit in the next phase.

Three cross-sectional areas with the joint data have been analyzed using DDA. For all three models, the same time history of ground acceleration was used as input. These models contain some potential key blocks (blocks held in place with frictions along joint interfaces) before earthquake shaking. Few additional models will be needed to permit quantification of rockfall sizes. Other models in areas where no potential key blocks exist will also be evaluated for potential of seismically induced rockfall. The total number of models will be determined through statistical treatment of rockfall sizes. The seismic signal used in the progress report represents a time history with a maximum magnitude of 0.85 g acceleration. This time history will be scaled upwards and downwards to generate various levels of ground motions for use as input to assess rockfall for the models mentioned above so that a relationship between the magnitude of ground motions and size of rockfall and a relationship between the magnitude of ground motions and areal coverage of rockfall in the emplacement drift can be developed for use in the SEISMO module. Long-term degradation of rock blocks and joint strength may be factored into consideration in the DDA analysis.

Multiple rock blocks falling in unison appear to be possible although would not be a frequent event. The time interval used in this progress report to generate graphic outputs for illustrating rock block movements during falling is not small enough to capture the interaction activities among falling rock blocks. A smaller time interval will be used in the future to permit investigation on the phenomenon of multiple rock blocks falling in unison.

The last proposed activity does not require special planning. The final shapes of the emplacement drift cross sections at the end of DDA modeling will address the changes in geometry in emplacement drifts due to seismicity.

## 6 REFERENCES

- Ahola, M.P., R. Chen., H. Karimi., S.M. Hsiung, and A.H. Chowdhury. *A Parametric Study of Drift Stability in Jointed Rock Mass. Phase I: Discrete Element Thermal-Mechanical Analysis of Unbackfilled Drifts*. San Antonio, TX: Center for Nuclear Waste Regulatory Analyses. 1996.
- Barrett, L.H. Letter to Jared L. Cohon and Enclosure: *Basis for Department of Energy Design Selection*. September 10, 1999.
- Barton, N., and H. Hansteen. Very large span openings at shallow depth: Deformation magnitudes from jointed models and finite element analysis. *Proceedings of the Fourth Rapid Excavation and Tunneling Conference*: Atlanta, GA. 2: 1,331–1,353. 1979.
- Brown, E.T., and J.A. Hudson. Fatigue failure characteristics of some models of jointed rock. *Earthquake Engineering and Structural Dynamics* 2: 379–386. 1974.
- Center for Nuclear Waste Regulatory Analyses. *Input to Structural Deformation and Seismicity Issue Resolution Status Report, Revision 2*. San Antonio, TX: Center for Nuclear Waste Regulatory Analyses. 1999a.
- Center for Nuclear Waste Regulatory Analyses. *Input to Igneous Activity Issue Resolution Status Report, Revision 2*. San Antonio, TX: Center for Nuclear Waste Regulatory Analyses. 1999b.
- Civilian Radioactive Waste Management System Management & Operating Contractor. *Yucca Mountain Site Geotechnical Report*. B00000000-01717-5705-00043 Rev 01. Vol 1. Las Vegas, NV: Civilian Radioactive Waste Management System Management & Operating Contractor. 1997.
- Civilian Radioactive Waste Management System Management & Operating Contractor. *Drift Degradation Analysis*. ANL-EBS-MD-000027 Rev 00. Las Vegas, NV: Civilian Radioactive Waste Management System Management & Operating Contractor. 1999.
- Civilian Radioactive Waste Management System Management & Operating Contractor. *License Application Design Report*. B00000000-01717-4600-00123 Rev. 01. Las Vegas, NV: Civilian Radioactive Waste Management System Management & Operating Contractor. 2000a.
- Civilian Radioactive Waste Management System Management & Operating Contractor. *Repository Safety Strategy: Plan to Prepare the Postclosure Safety Case to Support Yucca Mountain Site Recommendation and Licensing Considerations*. TDR-WIS-RL-000001 Rev 03. Las Vegas, NV: Civilian Radioactive Waste Management System Management & Operating Contractor. 2000b.
- Cruden, D.M.A Theory of brittle creep in rock under uniaxial compression. *Journal of Geophysical Research*. 75(17). 1970.
- Ghosh, A., J. Stamatakos, S. Hsiung, R. Chen, A.H. Chowdhury, and H.L. McKague. *Key Technical Issue Sensitivity Analysis with SEISMO and FAULTO Modules Within the TPA (Version 3.1.1) Code*. San Antonio, TX: Center for Nuclear Waste Regulatory Analyses. 1998.
- Goodman, R.E., and G.H. Shi. *Block Theory and its Application to Rock Engineering*. Englewood Cliffs, NJ: Prentice-Hall, Inc. 1985.

- Goodman, R.E., and W. Boyle. *Non-linear Analysis for Calculating the Support of a Rock Block with Dilatant Joint Faces*. Felsbau 4: 203-208. Englewood Cliffs, NJ: Prentice-Hall, Inc. 1986.
- Goodman, R.E. *Introduction to Rock Mechanics*. Second Edition. New York, NY: John Wiley & Sons. 1989.
- Griggs, D.T. The creep of rock. 47. *Journal of Geology*. 1939.
- Hardy, H.R. Time-Dependent Deformation and Failure of Geologic Materials. *Proceedings of the Tenth Symposium on Rock Mechanics*. Berkeley, CA: University of California. 137-175. 1969.
- Hill, B.E., and J.S. Trapp. *Sensitivity Analysis for Key Parameters in the VOLCANO and ASHPLUME Modules of the TPA Version 3.1 Code*. San Antonio, TX: Center for Nuclear Waste Regulatory Analyses. 1997.
- Hsiung, S.M., W. Blake, A.H. Chowdhury, and T.J. Williams. Effects of Mining-Induced Seismic Events on a Deep Underground Mine. *PAGEOPH* 139(3/4): 741-762. 1992.
- Hsiung, S.M., D.D. Kana, M.P. Ahola, A.H. Chowdhury, and A. Ghosh. *Laboratory Characterization of Rock Joints*. NUREG/CR-6178. Washington, DC: U.S. Nuclear Regulatory Commission. 1994.
- Hsiung, S.M., J.D. Fox, and A.H. Chowdhury. Effects of Repetitive Seismic Loads on Underground Excavations in Jointed Rock Mass. *Proceedings of the Seventh International Conference on Radioactive Waste Management and Environmental Remediation*. Nagoya: Japan. 1999.
- Hughson, D., and F. Dodge. The effect of cavity wall roughness on seepage into underground openings. *EOS Transactions. American Geophysical Union*. Supplement, H51B-02. 80(17). 1999.
- Kaiser, P.K., D.D. Tannant, D.R. McCreath, and P. Jesenak. *Rockburst Damage Assessment Procedure. Rock Support in Mining and Underground Construction*. P.K. Kaiser and D.R. McCreath, eds. A.A. Brookfield, VT: Balkema. 639-647. 1992.
- Ma, M.Y. Development of Discontinuous Deformation Analysis The First Ten Years (1986 to 1996). *Proceedings of the Third International Conference on Analysis of Discontinuous Deformation (ICADD-3) from Theory to Practice*. ed. B. Amadei. Alexandria, VA: American Rock Mechanics Association. 17-32. 1999.
- Mohanty, S., T.J. McCartin, and D.W. Esh. *Total-System Performance Assessment (TPA) Version 4.0-Code Module Descriptions and User's Guide*. San Antonio, TX: Center for Nuclear Waste Regulatory Analyses. 2000.
- Scholz, C.H. Mechanism of creep in brittle rock. *Journal of Geophysical Research*. 73: 3,295-3,302. 1968.
- Shi, G.H. Discontinuous Deformation Analysis Technical Note. *First International Forum on Discontinuous Deformation Analysis*: Berkeley, CA. 1996.
- Shi, G.H. Finding the Key Blocks of Unrolled Tunnel Joint Trace Maps User's Manual: Belmont, CA. 1998a.
- Shi, G.H. Discontinuous Deformation Analysis User's Manual: Belmont, CA. 1998b.
- U.S. Department of Energy. *Viability Assessment of a Repository at Yucca Mountain, Overview*. DOE/RW-0508. Las Vegas, NV: U.S. Department of Energy, Office of Civilian Radioactive Waste

Management. 1998a.

U.S. Department of Energy. *Viability Assessment of a Repository at Yucca Mountain, Preliminary Design Concept for the Repository*. DOE/RW-0508. Las Vegas, NV: U.S. Department of Energy, Office of Civilian Radioactive Waste Management. 1998b.

Wawersik, W.R. Time-Dependent Rock Behavior in Uniaxial Compression. *Proceedings of the Fourteenth Symposium on Rock Mechanics*. 85-106. PA: Pennsylvania State University. 1972.

Wilder, D.G., and J.L. Yow. *Geomechanics of the Spent Fuel Test—Climax*. UCRL-53767. Livermore, CA: Lawrence Livermore National Laboratory. 1987.